FROM GLUCOSE TO COLLAGEN: CHARACTERIZATION AND QUANTIFICATION OF BIOMOLECULES BY MASS SPECTROMETRY

by

Wei Jiang

A Thesis Submitted to the Faculty of the
DEPARTMENT OF CHEMISTRY

In Partial Fulfillment of the Requirements
For the Degree of

MASTER OF SCIENCE
In the Graduate College

THE UNIVERSITY OF ARIZONA

2008

STATEMENT BY AUTHOR

This thesis has been submitted in partial fulfillment of requirements for an advanced degree at the University of Arizona and is deposited in the University Library to be made available to borrowers under rules of the Library.

Brief quotations from this thesis are allowable without special permission, provided that accurate acknowledgement of source is made. Requests for permission for extended quotation from or reproduction of this manuscript in whole or in part may be granted by head of the major department or the Dead if the Graduate College when in his or her judgment the proposed use of the material is in the interests of permission must be obtained from the author.

SIGNED: Wei Jiang_____

APPROVAL BY THESIS DIRECTOR

This thesis has been approved on the date shown below:

_____ _____

Vicki H. Wysocki Date
Professor of Chemistry
Professor of Biochemistry and Molecular Biophysics

ACKNOWLEDGEMENT

I truly owe great thanks to my academic advisor Dr. Vicki Wysocki. There would be no thesis without her consistent guidance, help and patience in the past two and half years. She has turned me from inexperienced in mass spectrometry into a skilled mass spectrometrist, making it possible for me to start a career in industry now. She set up an example for me to be a professional and successful research scientist and a nice person, which will benefit me in the rest of my life. She is not only an "academic" advisor for me, but also she is very supportive to my career plans and provides very constructive suggestions.

I would also like to thank all the former and current members in the Wysocki research group, who made the past two and half years a joyful and unforgettable experience in my life. I can still remember the first time when Qingfen showed me how to use the old triple quad instrument; when Chris and I assembled the DESI source from a pile of "junk"; when Ashley taught me how to run an SDS-gel; when Sunghwan and Brittany showed me how to run the molecular simulations; and so many other "when"s. I especially need to thank Brittany, Ashley and Chris for reading the chapters of the thesis and make very useful comments. Our group coordinator Tanya is always very helpful during the preparation of the thesis.

Dr. Arpad Somogyi and Dr. Stephanie Shu taught and helped me a lot during my one-year internship in the Mass Spectrometry Facility. The skills I learned from them greatly benefited the present research and I believe they will continue benefiting my future work.

I need to say thanks to my collaborators too. Dr. Patricia Scaraffia worked with me on the mosquito project. Her passion for science and hardworking spirit really impressed me encouraged me when the experimental results were frustrating. Without Dr. Douglas Larson and his students, there wouldn't be such an interesting and wonderful research project on collagen cross-linking.

I appreciate that Dr. Dennis Evans and Dr. Bogdan Olenyuk were kindly willing to serve on my thesis committee, and they also read through my thesis and gave me very helpful feedbacks and comments.

Dr. George Tsaprailis, Dr. Linda Breci, Dr. Todd Mize and Yeleana Feistein in the Proteomics Facility of Bio5 institute gave me the opportunity to use the Q-trap instrument.

TABLE OF CONTENTS

LIST OF FIGURES …… 7

LIST OF SCHEMES &TABLES……..... 10

ABSTRACT…….. 11

CHAPTER 1 INTRODUCTION ...…… 12

1.1 Overview……..... 12

1.2 Introduction to Mass Spectrometry……..... 13

1.2.1 Soft Ionization Methods …….. 14

1.2.2 Mass Analyzers ……..…….. 18

1.2.3 Detectors in Mass Spectrometry…….. 24

1.2.4 Tandem Mass Spectrometry and Activation Methods…….. 25

1.3 Overview of Metabolomics…… 27

1.3.1 Origin of Metabolomics…… 27

1.3.2 Analytical Methods in Metabolomics…….. 28

REFERENCES …… 29

CHAPTER 2 DIFFERENTIATION AND QUANTIFICATION of C1 AND C2 ^{13}C-LABELED GLUCOSE BY TANDEM MASS SPECTROMETRY…… 36

2.1 Introduction…… 36

2.2 Experimental…….. 39

2.3 Results and Discussion …….. 40

2.3.1 Fragmentation Spectra of Underivatized and Derivatized Glucose …… 40

2.3.2 Possible Fragmentation Pathways……... 46

2.3.3 Differentiation and Quantification of C1 and C2 ^{13}C-Labeled Glucose by Multiple Reaction Monitoring Scans …….. 49

2.4 Conclusions and Future Directions……. 53

REFERENCES…… 54

CHAPTER 3 CHARACTERIZATION of CROSSED-LINKED COLLAGEN AND ITS CROSS-LINKS BY MASS SPECTROMETRY…… 56

3.1 Introduction…… 56

3.2 Experimental…….. 61

3.3 Results and Discussion …….. 64

3.3.1 Fragmentation Spectra of PYD and DPD …….. 64

3.3.2 Precursor Ion Scan MS Spectra of PYD and DPD…… 65

3.3.3 MS Spectrum and Precursor Ion Scan for Hydrolyzed Mouse Ventricle Collagen …… 69

3.3.4 LC-MS Analysis of Intact Type I Rat Tail Collagen……..... 72

3.4 Conclusions and Future Directions……. 76

REFERENCES……. 77

Chapter 4 CONSTRUCTION OF A DESI SOURCE AND ITS APPLICATION IN PEPTIDES AND PROTEIN ANALYSIS …… 81

4.1 Introduction…… 81

4.2 Experimental…….. 83

4.3 Results and Discussion …….. 86

4.3.1 Mass Spectra of Peptide and Proteins by DESI-MS…….. 86

4.3.2 Surface Effect on DESI-MS……..... 89

4.4 Conclusions and Future Directions……. 92

REFERENCES……. 93

REFERENCES (Chapters 1-4)……..... 96

LIST OF FIGURES

FIGURE 1.1. A schematic diagram of an electrospray ionization source (ESI) interface (figure from www.bris.ac.uk/nerclsmsf/techniques/hplcms.htmL) [6] ……. 14

FIGURE 1.2. A schematic diagram of matrix assisted laser desorption ionization (figure adapted fromhttp://www.chm.bris.ac.uk/ms/theory/maldi-ionisation.htmL) [21] …… 17

FIGURE 1.3. A schematic diagram of a quadrupole mass analyzer (figure from http://www.ivv.fraunhofer.de/ms/ms-analyzers.htmL) [27] ……. 19

FIGURE 1.4. A schematic diagram of a triple quadrupole mass spectrometer (figure from http://www.waters.com) [29] ……. 20

FIGURE 1.5. A schematic diagram of quadrupole ion trap mass analyzer (QIT) (figure from http://www.ivv.fraunhofer.de/ms/ms-analyzers.htmL) [33] ……. 22

FIGURE 1.6. A schematic diagram of a MALDI-TOF instrument (figure from http://edoc.hu-berlin.de/dissertationen/xie-jing-2003-12-15/HTML/chapter2.htmL)[35] …… 23

FIGURE 1.7. A schematic diagram of a MALDI-QTOF mass spectrometer (figure from http://edoc.hu-berlin.de/dissertationen/xie-jing-2003-12-15/HTML/chapter2.htmL) [39] ……. 23

FIGURE 1.8. A schematic diagram of a FT-ICR mass analyzer (figure from http://www.ivv.fraunhofer.de/ms/ms-analyzers.htmL) [41] ……... 24

FIGURE 2.1. Distribution of West Nile virus cases in the United States in 2003 [1] …… 40

FIGURE 2.2. Structure of glucose and the numbering of its carbon atoms …….. 37

FIGURE 2.3. MS/MS spectra of $[Glc+Li]^+$ (m/z = 187). The collision energy used was 35 eV …… 41

FIGURE 2.4. MS/MS spectra of ^{13}C-glucose. a) $[Glc\text{-}1\text{-}^{13}C+Li]^+$ (m/z = 187); b) $[Glc\text{-}2\text{-}^{13}C+Li]^+$ (m/z = 187); and c) $[Glc\text{-}1,2\text{-}^{13}C+Li]^+$ (m/z = 188). The collision energy used was 35 eV …… 44

FIGURE 2.5. Derivatization of glucose and the structure of the product methylglucosamine (Glc-MA) …… 44

FIGURE 2.6. MS/MS spectra of $[Glc\text{-}MA+H]^+$: a) $[Glc\text{-}MA+H]^+$ (m/z=196); b) $[Glc\text{-}1\text{-}^{13}C\text{-}MA+H]^+$ (m/z=197); c) $[Glc\text{-}2\text{-}^{13}C\text{-}MA+H]^+$ (m/z=197); d) $[Glc\text{-}1,2\text{-}^{13}C\text{-}MA+H]^+$ (m/z=198); e) $[Glc\text{-}D7\text{-}MA+H]^+$ (m/z=203); f) $[Glc\text{-}D2\text{-}MA+H]^+$ (m/z = 198) 45

FIGURE 2.7. Peak area ratio between the fragment ion $CH_2NHCH_3^+$ and its precursor ion for Glc-MA, Glc-1-^{13}C-MA, Glc-2-^{13}C-MA, Glc-C1-2-^{13}C-MA, Glc-D_7-MA and Glc-D_2-MA. ……..…… 51

FIGURE 2.8. a)The ratio between total fragment ion intensity and total ion abundance; b) the ratio between $CH_2NHCH_3^+$ ion intensity and the total ion abundance for Glc-MA, Glc-1-^{13}C-MA, Glc-2-^{13}C-MA, Glc-C1-2-^{13}C-MA, Glc-D_7-MA and Glc-D_2-MA.……... 52

FIGURE 3.1. A diagram of hydroxylysine cross-linking pathway. Hydroxylysine residues are the source of aldehydes formed by lysyl oxidase for intermolecular cross-linking reactions. (Figure adopted from Reference [14] with permission) ……. 58

FIGURE 3.2. Chemical Structures of pyridinoline (PYD) and deoxypyridinoline (DPD). They naturally exist as cations ……..... 63

FIGURE 3.3. MS/MS spectra of a) pyridinoline (PYD) and b) deoxypyridinoline (DPD). N_2 is used as collision gas, and the collision energy is set at 45 eV …… 64

FIGURE 3.4. The precursor ion scan MS spectrum of PYD and DPD standard. Q1 is scanning to transmit all the ions formed at the ESI source, and Q3 is fixed at m/z = 267. N_2 is used as the collision gas, and the collision energy is 45 eV …….. 66

FIGURE 3.5. The precursor ion scan spectra of PYD and DPD standard. a) Q3 is fixed at m/z = 84; b) Q3 is fixed at m/z = 82. N_2 is used as the collision gas, and the collision energy is 45 eV …… 68

FIGURE 3.6. a) MS spectrum of hydrolyzed mouse ventricle collagen. b) MSMS spectrum of the peak at m/z = 175 in Figure 3.6a. N_2 is used as the collision gas, and the collision energy is 25 eV …….. 69

FIGURE 3.7. The precursor ion scan spectrum of hydrolyzed mouse ventricle collagen. Q3 is fixed at m/z = 267. N_2 is used as the collision gas, and the collision energy is 45 eV …….. 70

FIGURE 3.8. The precursor ion scan spectrum of solvent. Q3 is fixed at m/z = 267. N_2 is used as the collision gas, and the collision energy is 45 eV ……. 71

FIGURE 3.9. a) Liquid Chromatogram of rat tail collagen protein; b) Mass spectrum of peak 1 in Figure 3.9a ……..... 73

FIGURE 3.10. a) Liquid Chromatogram of heated rat tail collagen protein; b) Mass spectrum of peak 1 in Figure 3.10a ……..... 74

FIGURE 3.11. 1D gel electrophoresis of collagen proteins. Lane1 Standard 2 μL; Lane2 Rat Tail Collagen (powder) 10 μL;Lane3 Rat Tail Collagen (powder) 20 μL; Lane4 Rat Tail Collagen (solution) 10 μL; Lane5 Rat Tail Collagen (solution) 20 μL; Lane6 Heated (60^0C 1h)Rat Tail Collagen (solution) 10 μL; Lane7 Heated (60^0C 1h) Rat Tail Collagen (solution) 20 μL; Lane8 Mouse Ventricle 10 μL; Lane9 Mouse Ventricle 20 μL. * powder means the sample was purchased as powder, and solution means the sample was purchased as solution.. 75

FIGURE 4.1. A diagram of desorption electrospray ionization source (figure adopted from reference [4] with permission) ……... 81

FIGURE 4.2. The set-up of DESI source used in the present study …….. 84

FIGURE 4.3. A diagram of DESI sprayer. (Picture taken from Reference [16] with permission) …….. 85

FIGURE 4.4. DESI mass spectra of intact peptide and protein standards under optimum conditions: a) bradykinin (1.06 kDa); b) cytochrome c (12.3 kDa); c) lysozyme (14.3 kDa) and BSA (66.4 kDa). The peptide and proteins (~ 1 μM) were deposited on a PMMA surface ……..... 86

FIGURE 4.5. DESI mass spectra of cytochrome c: a) The spectrum was collected under optimum condition; b) the spectrum was collected when the sprayer and sample surface are much closer to the mass spectrometer inlet …….. 87

FIGURE 4.6. a) DESI mass spectrum of cytochrome c; b) NanoESI mass spectrum of cytochrome c. All mass spectrometry parameters remain the same for those two measurements ……. 88

FIGURE 4.7. DESI-MS spectra of YGGFL, YGGFLR and angiotensin3 mixture: a) bare gold surface; b) PMMA surface; c) C16 self assembled monolayer surface; and d) CF12 self monolayer surface …….. 89

FIGURE 4.8. The peak intensity ratios between m/z = 712 (YGGFLR) and m/z = 631 for different surfaces used in DESI-MS ……..... 90

LIST OF SCHEMES & TABLES

SCHEME 2.1. Possible mechanism for the formation of ion m/z = 127 by fragmenting the ion m/z = 187 after a NL of 60 for glucose …….. 47

SCHEME 2.2. Possible mechanism for the formation of ion m/z = 44 by fragmenting the peak m/z = 196 after a NL of 152 for Glc-MA …… 48

TABLE 2.1. Precursor ion scan set-up of unlabeled and ^{13}C labeled Glc-MA ….. 50

TABLE 2.2. Calculated amounts of Glc-MA, Glc-1-^{13}C-MA, Glc-2-^{13}C-MA and Glc-C1-2-^{13}C-MA using MRM method, with and without correction ……... 52

ABSTRACT

In order to differentiate the C1- and C2-^{13}C labeled glucose isotopomers for metabolism studies in mosquitoes, a derivatization method is applied to chemically modify the glucose molecules. Then the derivatized C1 and C2 labeled glucose can be differentiated by tandem mass spectrometry, even though they have the same molecular weight. Based on the fragmentation mechanism of the derivatized glucose, a multiple reaction monitoring method is developed to quantify the C1- and C2-^{13}C labeled glucose, with deuterated glucose as the internal standard. Considering this "isotopic effect", a correction factor is introduced to make the quantification more accurate.

Based on the fragmentation of cross-linked amino acids (pyridinoline (PYD) and deoxypyridinoline (DPD)), a precursor ion scan method is developed to detect DPD and PYD from a complex matrix. DPD is detected in a hydrolyzed mouse ventricle collagen sample using the precursor ion scan method. The study shows the potential to investigate the relation between cross-linking in ventricle collagen and heart disease by using mass spectrometry.

A desorption electrospray ionization (DESI) source is constructed. A series of peptides and proteins are successfully ionized by it, although ionization is less efficient for large proteins. The charge distribution and peak width in a DESI mass spectrum is condition sensitive, and it is quite different from that in an ESI mass spectrum. The investigation of the sample surface effect shows that self assembled monolayer (SAM) surfaces produce the best signal, while bare gold surfaces produce the worst. It is proposed that this is due to the lower electron transfer on SAM film which allows more ions to survive.

Chapter 1

INTRODUCTION

1.1 Overview

The research presented in this thesis falls into the field of analyzing biomolecules by mass spectrometry (MS) and tandem mass spectrometry (MS/MS). Specifically, the research focuses on the following three areas: 1) Differentiation and quantification of ^{13}C-labeled glucose molecules for metabolism studies in mosquitoes; 2) Characterization of cross-linked collagen proteins by analysis of their cross-linked amino acids; 3) Analysis of peptides and proteins by desorption electrospray ionization (DESI) mass spectrometry.

How to differentiate and quantify the various ^{13}C-labeled carbohydrate molecules is an important and challenging problem in studies of biological metabolism pathways, because the metabolism studies of mosquitoes might be used develop a bio-rational method to control the mosquito populations. A mild chemical derivatization method is applied to modify the ^{13}C-labeled glucose in order to make C1 labeled glucose distinguishable from C2 labeled glucose by MS/MS. Based on the fragmentation patterns of derivatized glucose, a quantification method is developed to quantify those isotopomers by running multiple reaction monitoring scan mode (MRM) on a Q-trap mass spectrometer. Although C1 labeled glucose and C2 labeled glucose have the same molecular weight and molecular structure, derivatization at C1 yields a structure for which fragmentation distinguishes C1 labeled from C2 labeled glucose.

Collagen proteins are the most abundant proteins in the human body, and their most important function is to provide mechanical support for tissues and organs. The proper functioning of collagen proteins is strongly related to the extent and structure of cross-linking in the collagen protein. An HPLC-MS method on a Q-TOF mass spectrometer is applied to analyze the intact collagen protein. An MS/MS method on a Q-trap instrument is developed to characterize the cross-linked amino acids in the protein. Overall, the study shows an example of how mass spectrometry can be used to characterize protein cross-linking features and expands the understanding of collagen protein structures.

A Desorption electrospray ionization (DESI) source makes it possible to introduce biomolecules into gas phase under ambient pressure from a surface. A DESI source is designed and constructed in our lab. It is used to analyze several peptides and proteins deposited on different substrate surfaces. The initial results obtained from the experiments are valuable for further investigations of ionization mechanisms of DESI and coupling DESI to an electromigration separation technique based on the silica colloids.

1.2 Introduction to Mass Spectrometry

Because the research in the thesis uses mass spectrometry as the major analytical tool, a brief introduction to mass spectrometry is provided. Mass spectrometry has become one of the most widely used analytical tools in chemistry, biological sciences, medical sciences and related industries today since its invention by Joseph J Thomson in 1912, and especially since the introduction of soft ionization techniques two decades ago. Mass spectrometry is capable of providing critical information about molecular weight, chemical composition, molecular structure, quantitative composition of complex mixtures,

isotope ratios and more for both small and large molecules. Mass spectrometry also bears the advantages of high sensitivity and high speed analysis [1].

A single-stage mass spectrometer is composed of three parts: an ionization source that introduces the sample into the gas phase; a mass analyzer that separates the ions that form at the source based on their mass-to-charge (m/z) ratio; and a detector that counts the number of ions. The more advanced tandem mass spectrometer is more powerful for obtaining structural information about the sample. A tandem mass spectrometer has two mass analyzers, and a collision cell between the two mass analyzers where ions from the first mass analyzer collide with neutral gas molecules and get fragmented. The fragments are analyzed by the second mass analyzer, which can provide detailed structural information based on the mass-to-charge ratio of the fragment pieces.

1.2.1 Soft Ionization Methods

Electrospray ionization (ESI) and matrix-assisted laser desorption ionization (MALDI) are two of the most important soft ionization methods today in modern mass spectrometry. The invention of ESI and MALDI has brought mass spectrometry into a new era.

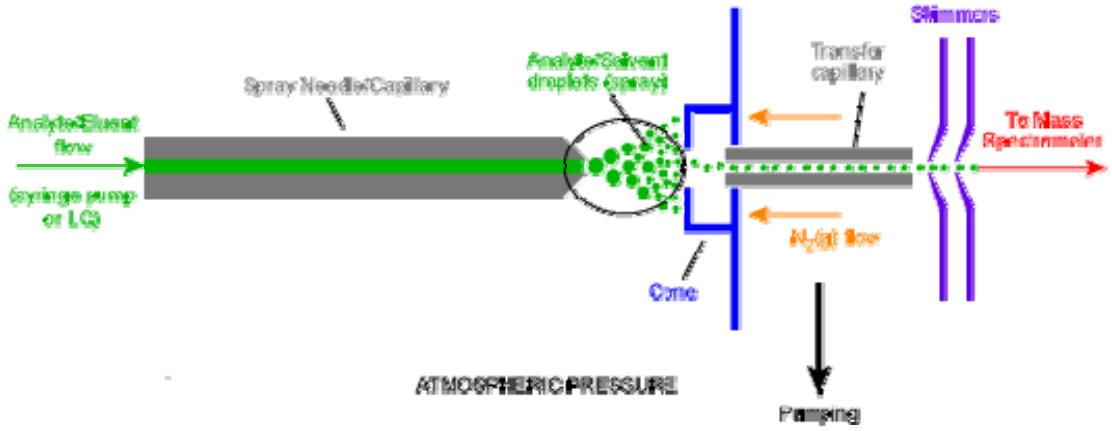

FIGURE 1.1. A schematic diagram of an electrospray ionization source (ESI) interface (figure from www.bris.ac.uk/nerclsmsf/techniques/hplcms.htmL) [6].

John Fenn, the co-recipient of the 2002 Nobel Prize in Chemistry, made significant contributions to the development of ESI [2]. At present, ESI is the most heavily applied atmospheric pressure ionization (API) method and the method of choice for liquid chromatography mass spectrometry (LCMS) coupling that has become a key analytical technology in chemistry, biology, medicine and industry [1, 3]. The mechanism of ESI has been widely studied [1, 4, 5]. The most critical question is how analytes are transformed from the solution phase to the gas phase in a mass spectrometer. In ESI, ions are formed directly from the sample solution to the mass spectrometer under atmospheric pressure through a capillary where a high voltage (2~5 kV) is applied relative to the sample inlet, as shown in Figure 1.1. It is accepted that highly charged droplets can be formed from the sample solution under a strong electric field. However, there are different models to describe what happens after the highly charged droplets have been formed. An early model called the charged-residue model (CRM), assumes that the successive loss of all solvent molecules under heat through evaporation would shrink the size of the droplet until the droplet is small enough to contain just one analyte molecule. The charges of the ultimate small droplet are then retained by the molecule, and the gas-phase ion is formed [7-9]. A later theory, ion evaporation model (IEM), describes the formation of ions as direct evaporation from the surface of highly charged microdroplets [10, 11]. In IEM model, the droplets keep shrinking through evaporation, resulting in increasing charge density on the droplet surface, which causes the ions to escape from the solution phase before the droplet breaks up into small ones [12].

One of characteristics of ESI is that ions formed from ESI can be multiply charged, which expands the mass range of analyte that can be detected by the analyzers with a low limit of mass-to-charge (m/z) ratio. This feature is especially useful for the analysis of large proteins [13]. ESI is also a "soft" ionization source, which means that the non-covalent interactions in complexes could be preserved, making ESI suitable to study protein complexes [14, 15]. Besides large proteins, ESI is widely used in the analysis of small molecules [16], metal complexes [17], DNA and RNA [18], oligosaccharides [19] and more. Because ESI is capable of ionizing the sample from the solution, it is often coupled with chromatographic separations such as high performance liquid chromatography (HPLC) or capillary electrophoresis (CE) [20]. ESI can be operated under either positive mode or negative mode. The presented research is done under positive mode.

Another commonly used ionization source without introducing extensive fragmentation is MALDI (Figure 1.2). In MALDI, the analyte is co-crystallized with organic matrix molecules, usually conjugated aromatic compounds, like sinapinic acid, dithranol, nicotinic acid and so on [22]. The matrix is believed to serves as the proton donor or acceptor to ionize the analyte under either positive or negative mode, respectively, as well as to absorb light of the wavelength which is used for the laser source [23], for example, 337 nm for nitrogen laser. The mechanism of MALDI is not completely clear yet. A recent model called the "cluster model" proposes that charged clusters containing analytes, matrix molecules and contaminants are formed upon laser desorption, and the clusters will evaporate in a short time by neutral loss of matrix molecules, hence analyte ions are formed through ion-ion or neutral-ion interactions in

the clusters [24]. MALDI usually generates singly charged ions, although doubly charged ions are formed occasionally. Because the matrix peaks also appear in the mass spectra, MALDI is not suitable to study molecules below ~ 800 Da due to the potential interference from the matrix peaks. It is worth noting that MALDI is especially useful for the analysis of synthetic polymers, because the repeated pattern in the mass spectrum can be used unambiguously to determine the mass of the repeating unit, ending group and the mass distribution of the polymer [25, 26].

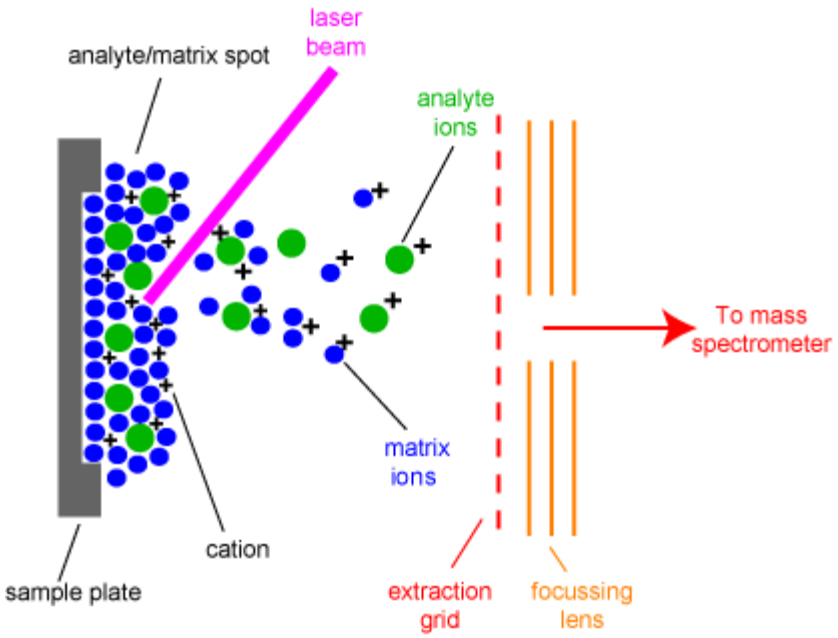

FIGURE 1.2. A schematic diagram of matrix assisted laser desorption ionization (figure from http://www.chm.bris.ac.uk/ms/theory/maldi-ionisation.htmL) [21].

A more recently developed ionization called "desorption electrospray ionization" (DESI) is able to desorb and ionize samples from a surface. And the DESI-MS spectrum has similar features to those of the ESI-MS spectrum. A more detailed introduction of DESI will be delivered in Chapter IV (Section 4.1).

1.2.2 Mass Analyzers

The mass analyzer is a key part of a mass spectrometer. There are numerous mass analyzers available to satisfy different purposes. In the present study, multiple mass spectrometers are used, so a brief introduction of the mass analyzers is included below.

Linear quadrupole mass analyzer and triple quadrupole mass spectrometer

A linear quadrupole mass analyzer (Figure 1.3) is composed of two parallel pairs of metal rods. Its capacity for filtering mass is achieved by applying both DC and RF on the rods. Positive DC is applied on one pair, and negative DC is applied on the other. RF is applied on all rods with the same amplitude but 180^{o} out of phase. The amplitude of DC and RF is gradually increasing in order to pass the ions at different m/z values, since the ion of a particular m/z value can be transmitted at a given DC and RF voltage. During the scan, the ratio of DC and RF is kept constant in order to keep the same resolution. Usually a linear quadrupole mass analyzer has an upper m/z limit of ~ 4000. Because a linear quadrupole mass analyzer is a continuous mass analyzer, it is very convenient to couple it with an ESI source and HPLC [28].

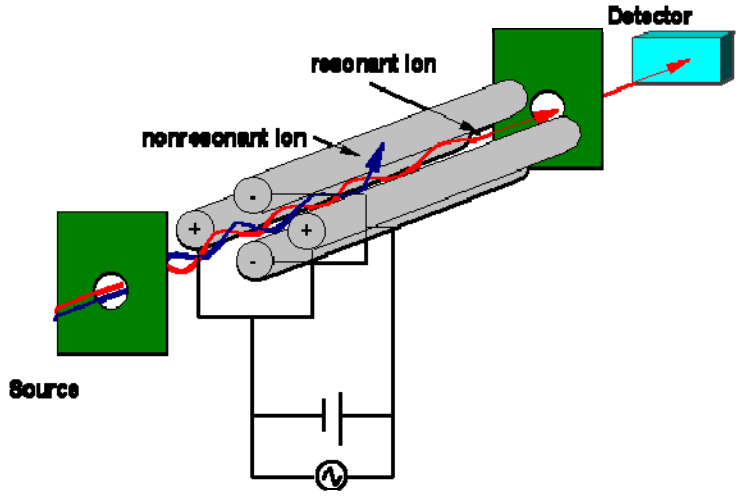

FIGURE 1.3. A schematic diagram of a quadrupole mass analyzer (figure from http://www.ivv.fraunhofer.de/ms/ms-analyzers.htmL) [27].

A tandem mode of linear quadrupole mass analyzers called triple quadrupole mass spectrometer (QqQ) is often used due to its versatile scan modes available for various purposes. A typical triple quadrupole mass spectrometer consists of three quadrupole mass analyzers, namely Q1, Q2 and Q3. Q1 and Q3 serve as normal quadrupole mass analyzers, while Q2 operates in RF only mode and can be filled with collision gas and acts as a collision cell to fragment the ions from Q1 (Figure 1.4). A QqQ instrument can perform the following scan modes: product ion scans (MS2), precursor ion scans, neutral loss scans and multiple reaction monitoring scans (MRM). The present research took advantage of all those scan modes.

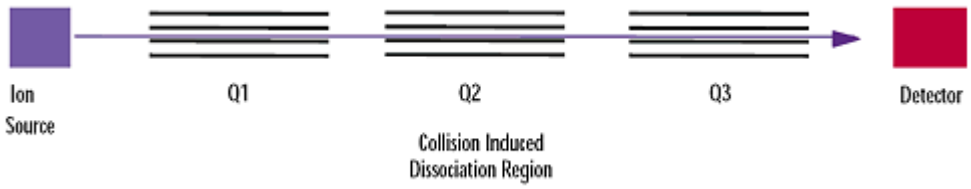

FIGURE 1.4. A schematic diagram of a triple quadrupole mass spectrometer (figure from http://www.waters.com) [29].

In a product ion scan, DC and RF are fixed for Q1 in order for an ion of a particular m/z value to pass through. The selected ion is then fragmented in the collision cell by colliding with neutral gas molecules, and Q3 scans to analyze the fragment ions. The resulting spectrum will be a typical MS/MS spectrum. This scan mode is very useful to study the fragmentation behavior of a certain ion of interest.

A precursor ion scan fixes the DC and RF of Q3 to ensure that only a fragment ion of a particular m/z value will be transmitted. Q1 scans to transmit ions with a range of m/z values into the collision cell. Only the ions that produce that specific fragment ion will show up in the resulting spectrum. This scan mode is usually employed to extract some targets from a complex matrix that can generate a specific fragment structure.

In a neutral loss scan, both Q1 and Q3 scan and transmit ions, however, the mass offset between Q1 and Q3 is fixed, hence only the ions that can produce a specific neutral loss will finally lead to a signal at the detector. This scan mode is especially useful to search a series of analytes that bear some identical structural features. For example, when phosphorylated peptides or proteins get fragmented, they tend to produce a neutral loss of the phosphate group (96 Da). The neutral loss scan is widely used in studies of post translational modification (PTM) of peptides or proteins [30].

In a multiple reaction monitoring (MRM) scan or selected reaction monitoring (SRM) scan, Q1 and Q3 are synchronized to transmit the specific ion pairs of interest. A signal is detected only when both precursor ion and fragment ion match the set m/z values. The advantage of MRM is that it is able to study multiple fragmentation pathways but largely exclude the interferences from the unwanted contaminant ions. The present study applied the MRM scan to quantify the ^{13}C-labeled glucose isotopomers.

Quadrupole ion trap (QIT) and linear ion trap mass analyzers (LTQ)

A quadrupole ion trap mass analyzer is made up of a hyperbolic ring electrode and two hyperbolic end-cap electrodes (Figure 1.5). Ions can be trapped in the central area by applying a three-dimensional electric field with the assistance of collisional cooling by helium gas. In MS mode, RF is applied on the ring electrode. Ions of different m/z values are ejected out sequentially from low m/z to high m/z by increasing the amplitude of the RF voltage. In collision-induced dissociation (CID), ions are activated resonantly by applying an additional RF voltage on the end-cap electrodes [31]. QIT mass analyzers are relatively small, cheap and easy to use, with unit resolution. However, the QIT has an intrinsic low mass cutoff so that ions below a certain m/z values cannot be trapped. And usually, QIT also has an upper m/z limit of ~ 2000 [32]. The linear ion trap (LIT) has much better sensitivity, resolution and mass accuracy compared with a QIT mass analyzer [34]. The replacement of Q3 in a QqQ instrument with a scanning LIT (QqLIT) enhances its sensitivity and offers new modes of operation such as MS^n. Many experiments in the present study were performed on an Applied Biosystem Q-Trap instrument.

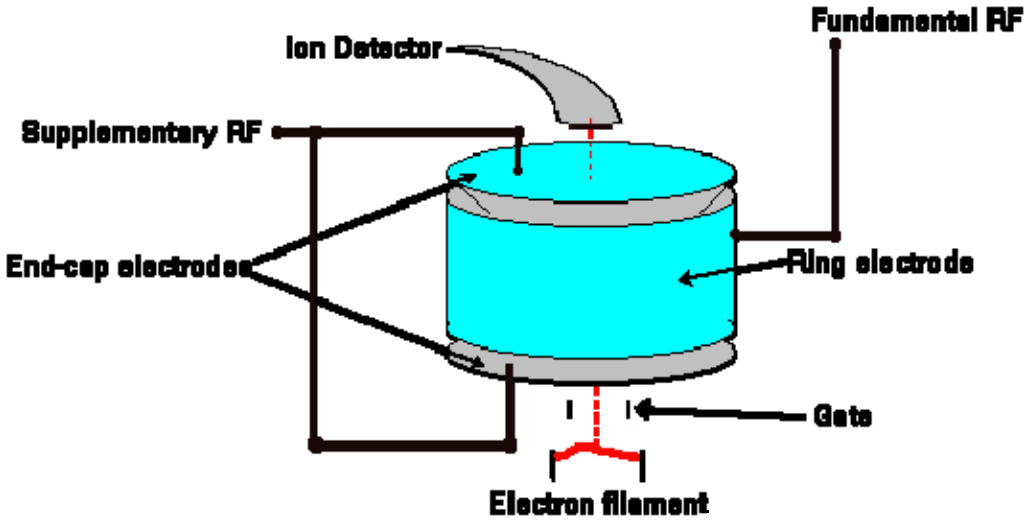

FIGURE 1.5. A schematic diagram of quadrupole ion trap mass analyzer (QIT) (figure from http://www.ivv.fraunhofer.de/ms/ms-analyzers.htmL) [33].

Time-of-flight (TOF) mass analyzer and quadrupole time-of-flight (QTOF) instrument

Time-of-flight (TOF) mass analyzers (Figure 1.6) have become popular since the availability of the pulsed ionization source. In a MALDI-TOF instrument, ions are formed at the source and get accelerated by an acceleration voltage (10-30 kV) to gain high kinetic energy (keV). Then the ions will enter a field-free drift tube, where ions with the same kinetic energy but different m/z are separated during flight time. The TOF analyzer has a theoretically unlimited dynamic range and a high resolution (up to 18,000) [36], which allow it to be used to perform exact mass measurements. However, the spatial distribution and kinetic energy distribution of the ions upon formation will decrease the resolution of the instrument. To solve this problem, delayed extraction and a reflectron are applied [37, 38]. Commercially available tandem mass spectrometers that use TOF analyzers include TOF-TOF and QTOF (Figure 1.7) with a collision cell placed between the two analyzers, where ions of interest are selected in the first analyzer and

fragments are analyzed by the second mass analyzer. In the present research, a QTOF instrument is employed to study the collagen proteins.

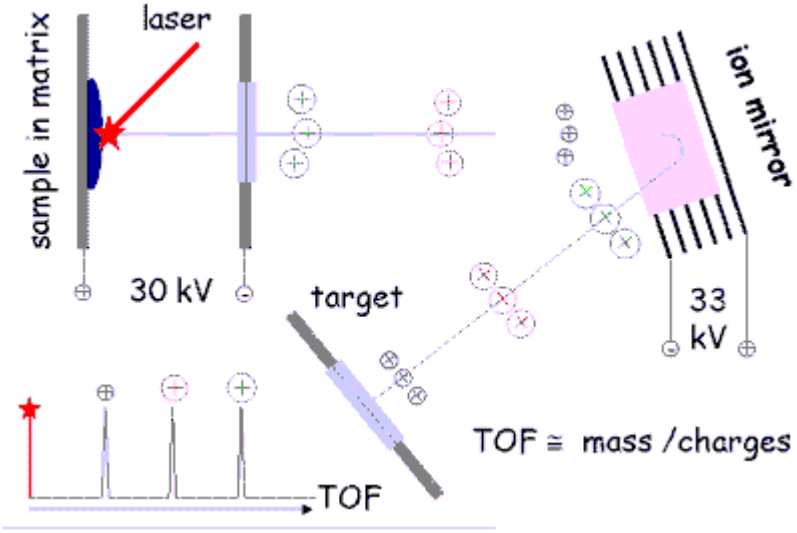

FIGURE 1.6. A schematic diagram of a MALDI-TOF instrument (figure from http://edoc.hu-berlin.de/dissertationen/xie-jing-2003-12-15/HTML/chapter2.htmL)[35]

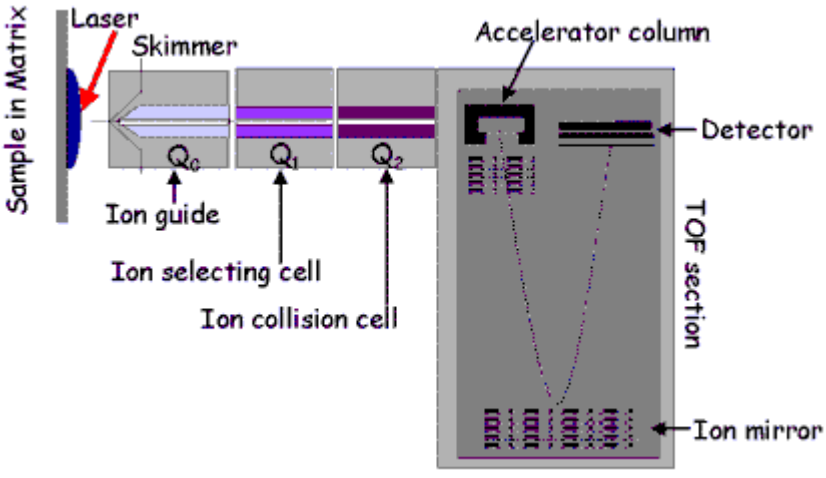

FIGURE 1.7. A schematic diagram of a MALDI-QTOF mass spectrometer (figure fromhttp://edoc.hu-berlin.de/dissertationen/xie-jing-2003-12-15/HTML/chapter2.htmL) [39].

Fourier transform ion cyclotron resonance (FT-ICR) mass analyzer

When ions enter a strong magnetic field, they will take circular motion perpendicular to the direction of the magnetic field. The cyclotron frequency is inversely proportional to the ions' m/z ratios. When the applied RF field matches a certain cyclotron frequency, the ion can absorb energy from the field resulting in an increasing velocity of the ion and increasing the radius of motion. The coherent motion of the ions can generate a capacitor current or image current. The image current is collected as a function of time, and the time-domain signal is converted into frequency-domain signal by Fourier transform. The frequency-domain signal carries the information about the m/z values of the ions. The FT-ICR mass analyzer is the analyzer with the highest resolution (hundreds of thousand to millions) and mass accuracy (ppm) [40]. The major disadvantages of FT-ICR are its large size, high expense, and low speed. A schematic diagram of one FT-ICR mass analyzer is shown in Figure 1.8 for a cubic cell; modern cells are typically cylindrical.

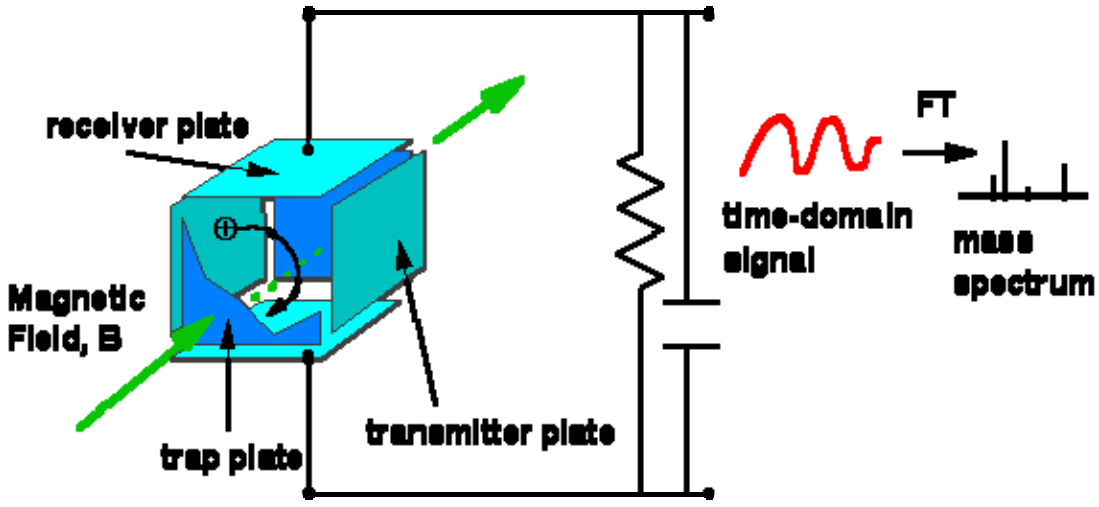

FIGURE 1.8. A schematic diagram of a FT-ICR mass analyzer (figure from http://www.ivv.fraunhofer.de/ms/ms-analyzers.htmL) [41].

1.2.3 Detectors in Mass Spectrometry

Although FTICR detection is based on measurement of an image current, most other mass spectrometers use impact of ions in an electron multiplier design. The common detectors include Faraday cup, discrete dynode electron multiplier, channel electron multiplier, microchannel plate, and focal plane detector. Channel electron multiplier (CEM) and microchannel plate (MCP) will be briefly discussed here.

The inner surface of the channel electron multiplier (CEM) tube is an emissive layer of silicon dioxide overlying a conductive layer of lead oxide on the supporting heavily lead-doped glass [42]. When an incident beam hits the inner surface of the tube, a number of secondary electrons will be generated, and all emitted electrons will be accelerated under the applied DC voltage (typically 1-2 kV) towards and hit the surface where they cause more secondary electrons. Straight CEMs can achieve a signal in the magnitude of 10^4, while curved CEMs can achieve up to 10^8. A CEM detector is present in the Q-trap, QTOF and LCQ instruments used for the present study.

The microchannel plate (MCP) is dedicated for a TOF analyzer. An MCP, typically a 2-5 cm diameter plate, consists of millions of channels with a diameter between 10 and 100 μm. It is analogous to a bundle of mini CEMs. The gain of an MCP is 10^3-10^4, much lower than that of a CEM, so two MCPs are often sandwiched together (Chevron plate) to obtain gains of 10^6-10^7. Occasionally, three MCPs are stacked together to get a gain up to 10^8 [43]. The reason MCP is an excellent detector for TOF analyzer is mainly because of its short response time (in the range of nanoseconds), and its fixed ion path length that is extremely important for time-of-flight measurement. However, MCP is not suitable for quantitative analysis, since the microchannel is very easily saturated.

1.2.4 Tandem Mass Spectrometry and Activation Methods

As discussed in Section 1.2.2, mass analyzers can be coupled together to form a tandem mass spectrometer. The purpose of doing so is to take advantage of different mass analyzers and combine them together in a single machine. A tandem mass spectrometer has a greater power for structural analysis, quantification and more [44]. The hybrid mass spectrometer started with the magnetic sector-quadrupole instrument, like BqQ [45], EBqQ or BEqQ [46, 47]. Now more tandem instruments are commercially available such as QqQ [48], QITTOF [49], QqLIT [50], and QqTOF [51]. There are two types of tandem mass spectrometers, "tandem-in-space" and "tandem-in-time". Tandem-in-space is performed in two discrete mass analyzers, like QqQ or QqTOF, while the latter is performed in the same mass analyzer, like quadrupole ion trap mass analyzer or linear ion trap mass analyzer.

The greatest advantage of tandem mass spectrometry over single-stage mass spectrometry is that ions of interest can be selected, activated and fragmented to provide critical structural information. Several activation methods have been applied in tandem mass spectrometry, including collision induced dissociation (CID), surface induced dissociation (SID), blackbody infrared radiative dissociation (BIRD), infrared multi-photon dissociation (IRMPD), electron capture dissociation (ECD) and electron transfer dissociation (ETD). Combination of spectra from different activation methods may provide complementary structural information. CID is most widely used nowadays and is applied for the present study. In CID, ions collide with the neutral gas molecules like helium, nitrogen, argon and more. During the multiple collision process, some of the kinetic energy of the ion is converted into internal vibrational energy. The distribution of

the internal energy results in the vibration of the chemical bonds in the ion, and then causes the dissociation of the ion [52].

1.3 Overview of Metabolomics

1.3.1 Origin of Metabolomics

Identification and elucidation of the structures of metabolites, as well as the quantification of the metabolites play major roles in understanding the functions of proteins and biochemical pathway regulation in cells, and in drug discovery and development of new pharmaceutical compounds.

Traditionally, radiolabeled parent compounds are used for identification of metabolites due to the highly selective detection of radioactivity. However, synthesis of radiolabeled compounds is expensive and time-consuming, and it is difficult to monitor hundreds of metabolites efficiently with a radioactive detector. In today's life science, it is becoming more and more desirable to have a fast and reliable method to handle hundreds or even thousands of metabolites to obtain a full picture of the entirety of the metabolites within a biological system. For example, 1,170 metabolites have been reported for *Escherichia coli* [53], and more than 200,000 metabolites are expected for plants [54]. The growing demands have made metabolomics develop into a valuable and fast-growing tool in life sciences. Simply speaking, metabolomics deals with the identification, qualitative and quantitative analysis of the metabolites acting in a biochemical network [55]. A detailed definition of metabolomics is described by Fiehn as a multi-functional tool, subdivided into 1) target analysis, quantitative analysis of the metabolites of a target protein; 2) metabolic profiling, quantitative analysis of a pre-

defined metabolite family; and 3) metabolomics, aiming at an unbiased overview of whole-cell metabolic patterns [56].

1.3.2. Analytical Methods in Metabolomics

Many analytical tools have been applied for metabolite analysis, for example, nuclear magnetic resonance (NMR) [57], gas chromatography (GC) [58], high performance liquid chromatography (HPLC) [59], direct infusion mass spectrometry (MS) [60] and more. But none of them alone is the perfect method for metabolomics studies. This is due to the challenges of metabolomics: First, most metabolites typically are in low concentrations, which can be down to picomolar range [61]; second, the metabolites cannot be concentrated by ultrafiltration which is a common method used in proteomics, because of the low molecular weight of the metabolites; and third, metabolites exist in a complex matrix that can surpress the metabolite signals [62]. Metabolomics thus needs a sensitive, selective, reliable method to handle a large number of compounds available small quantities.

Currently, MS serves as the central technique for metabolomics studies. Coupled with a chromatographic setup, like HPLC, GC or CE, it provides an even more powerful analytical system. To achieve higher resolution and sensitivity, tandem mass spectrometry or two-dimensional chromatography is applied, such as LC-MS/MS [63, 64], or GC-GC-MS [65]. Since MS has the great advantage of being able to distinguish isotopes, the ^{13}C metabolic flux analysis has become a popular method to determine ^{13}C-labeled proteinogenic amino acids after a feeding of a ^{13}C-labeled substrate (i.e. ^{13}C-glucose). With the development of LC-MS/MS methods, it is now possible to determine

labeling information of intra-cellular central metabolites, as reported for the first time using *E. coli* as a model system [66]. This MS-based isotope method can be applied to other biologically relevant isotopes, like ^{2}H, ^{18}O and ^{15}N. To perform quantification, an external standard (ES) or internal standard (IS) is usually added. An IS can correct for matrix effects and provide valid metabolite concentrations. One big challenge for metabolomics is the data processing, such as peak assignment and integration. The retention time may vary significantly after the matrix background is changed, which will cause false peak identifications. The data processing software supplied with MS is not powerful enough to analyze the metabolomic data, so the improvement of software has been put into progress [67, 68].

The present study aims to differentiate and quantify ^{13}C-labeled glucose isotopomers for the purpose of investigating metabolism in mosquitoes.

REFERENCES

(1) Fenn, J.B.; Mann, M.; Meng, C.K.; Wong, S.F.; Whitehouse, C.M.; ESI for MS of Large Biomolecules. *Science* **1989**, *246*, 64-71.

(2) *Modern Mass Spectrometry;* Schalley, C.A., editor; Springer: New York 2003.

(3) *Mass Spectrometry in Drug Discovery;* Rossi, D.T.; Sinz, M.W., editors; Marcel Dekker; New York, 2002.

(4) Fenn, J.B.; Mann, M.; Meng, C.K.; Wong, S.F.; Electrospray Ionization – Principles and Practice. *Mass Spectrom. Rev.* **1990**, *9*, 37-70.

(5) *Electrospray Ionization Mass Spectrometry – Fundamentals, Instrumentation and Applications;* 1st ed.; Dole, R.B., editor; John Wiley & Sons: Chiechester 1997.

(6) www.bris.ac.uk/nerclsmsf/techniques/hplcms.htmL Accessed on December

1st, 2007.

(7) Winger, B.E.; Light-Wahl, K.J.; Ogorzalek Loo, R.R.; Udseth, H.R.; Smith, R.D.; Observation and Implications of High Mass-to-Charge Ratio Ions From ESI-MS. *J. Am. Soc. Mass Spectrom.* **1993**, *4*, 536-545.

(8) Mack, L.L.; Kralik P., Rheude, A.; Dole, M., Molecular Beams of Macroions. II. *J. Chem. Phys.* **1970**, *52*, 4977-4986.

(9) Filitsyn, N., Peschke, M., Kebarle, P., Origin and Number of Charges Observed on Multiply-protonated Native Proteins Produced by ESI. *Int. J. Mass Spectrom.* **2002**, *219*, 39-62.

(10) Iribarne, J.V.; Thomson, B.A. On the Evaporation of Small Ions from Charged Droplets. *J. Chem. Phys.* **1976**, *64*, 2287-2294.

(11) Thomson, B.A.; Iribarne J.V.; Field-induced Ion Evaporation from Liquid Surfaces at Atmospheric Pressure. *J. Chem. Phys.* **1979**, *71*, 4451-4463.

(12) Labowsky, M.; Fenn, J.B.; de la Mora, J.F. A Continuum Model for Ion Evaporation from a Drop: Effect of Curvature and Charge on Ion Solvation Energy. *Anal. Chim. Acta* **2000**, *406*, 105-118.

(13) *Mass Spectrometry of Proteins and Peptides;* Chapman, J.R., editor; Humana Press: Totowa, 2000.

(14) Phillips, J.J.; Yao, Z.P.; Zhang, W.; McLaughlin, S.; Laue, E.D.; Robinson, C.V.; Jackson, S.E. Conformational dynamics of the molecular chaperone Hsp90 in complexes with a co-chaperone and anticancer drugs. *J. Mol. Biol.* **2007,** *372* 1189-1203.

(15) Justin, L. P.; Benesch, B.T.; Ruotolo, D.A.; Simmons; Robinson, C.V. Protein Complexes in the Gas Phase: Technology for Structural Genomics and Proteomics *Chem. Rev.* **2007,** *10*, 3544 – 3567.

(16) Ardrey, R.E. *Liquid Chromatography – Mass Spectrometry – An Introduction;* John Wiley & Sons: Chichester, 2003

(17) Traeger, J.C.; ESI-MS of Organometallic Compounds. *Int. J. Mass Spectrom. Rev.* **1995**, *14*, 79-104

(18) Little, D.P.; Chorush, R.A.; Speir, J.P.; Senko, M.W.; Kelleher, N.L.; McLafferty, F.W. Rapid Sequencing of Oligonucleotides by High-

Resolution-MS. *J. Am. Chem. Soc.* **1994**, 116,4893-4897.

(19) Karas, M.; Bahr, U.; Dulcks, T. Nano-ESI-MS: Addressing Analytical Problems Beyond Routine. *Fresenius J. Anal. Chem.* **2001**, 366, 669-676

(20) Smith, W.F.; Brooks, P. A critical evaluation of high performance liquid chromatography-electrospray ionization-mass spectrometry and capillary electrophoresis- electrospray-mass spectrometry for the detection and determination of small molecules of significance in clinical and forensic science. *Electrophoresis* **2004**, *25*, 1413-1446.

(21) http://www.chm.bris.ac.uk/ms/theory/maldi-ionisation.htmL Accessed on December 1st**,** 2007.

(22) *Mass Spectrometry;* Gross, J.H.; Springer: Berlin 2004

(23) Juhasz P.; Costello, C.E.; Biemann, K. MALDI-MS with 2-(4-Hydroxyphenylazo)benzoic Acid Matrix. *J. Am. Soc. Mass Spectrom.* **1993**, *4*, 399-409.

(24) Karas, M.; Gluckmann, M.; Schafer J. Ionization in MALDI: Singly Charged Molecular Ions Are the Lucky Survivors. *J. Mass Spectrom.* **2000**, *35*, 1-12.

(25) *Mass Spectrometry of Polymers;* 1st ed.; Montaudo, G.; Lattimer, R.P., editor; CRC Press: Boca Raton, 2001

(26) Murgasova, R.; Hercules, D.M. Quantitative Characterization of a Polystyrene/Poly(α-methylstyrene) Blend by MALDI-MS and Size-exclusion chromatography. *Anal. Chem.* **2003**, *75*, 3744-3750.

(27) http://www.ivv.fraunhofer.de/ms/ms-analyzers.htmL Accessed on December 2nd, 2007.

(28) Dawson, P.H. Quadrupole Mass Analyzers: Performance, Design, and Some Recent Applications. *Mass Spectrom. Rev.* **1986**, *5*, 1-37.

(29) http://www.waters.com/WatersDivision/ContentD.asp?watersit=EGOO-66MNYR#quads Accessed on December 2nd, 2007.

(30) Garcia, B.A.; Shabanowitz, J.; Hunt, D.F. Characterization of histones and their post-translational modifications by mass spectrometry. *Curr. Opini. Chem. Biol.* **2007**, *11*, 66-73.

(31) *Quadrupole Storage Mass Spectrometry.* March, R.E.; Hughes, R.J. John Wiley & Sons: Chichester, 1989.

(32) Griffiths, I.W. Recent Advances in Ion-Trap Technology. *Rapid Commun. Mass Spectrom.* **1990**, 69-73

(33) http://www.ivv.fraunhofer.de/ms/ms-analyzers.htmL Accessed on December 2nd, 2007.

(34) Mao, D.; Douglas, D.J. H/D Exchange of Gas Phase Bradykinin Ions in a Linear Quadrupole Ion Trap. *J. Am. Soc. Mass Spectrom.* **2003**, *14*, 85-94.

(35) http://edoc.hu-berlin.de/dissertationen/xie-jing-2003-12-15/HTML/chapter2.htmL Accessed on December 7th, 2007.

(36) Loboda, A.V.; Ackloo, S.; Chernushevich, I.V. A high-performance matrix-assisted laser desorption/ionization orthogonal time-of-flight mass spectrometer with collisional cooling. *Rapid Commun. Mass Spectrom.* **2003**, *17*, 2508-2516.

(37) Whittal, R.M.; Li. L. High-Resolution MALDI in linear TOF-MS. *Anal. Chem.* **1995**, *67*, 1950-1954.

(38) Mamyrin, B.A. Laser Assisted Reflectron Time-of-Flight Mass Spectrometry. *Int. J. Mass Spectrom. Ion Proc.* **1994**, *131*, 1-19.

(39) http://edoc.hu-berlin.de/dissertationen/xie-jing-2003-12-15/HTML/chapter2.htmL Accessed on December 7th, 2007.

(40) Amster, I. J. Fourier Transform Mass Spectrometry. *J. Mass. Spectrom.* **1996**, *31*, 1325-1337.

(41) http://www.ivv.fraunhofer.de/ms/ms-analyzers.htmL Accessed on December 7th, 2007.

(42) Busch, K.L. The Electron Multiplier. *Spectroscopy* **2000**, *15*, 28-33.

(43) Laprade, B.N.; Labich, L.J.; Microchannel Plate-Based Detectors in Mass Spectrometry. *Spectroscopy* **1994**, *9*, 26-30.

(44) Futrell, J.H.; Development of Tandem MS. One Perspective. *Int. J. Mass Spectrom.* **2000**, *200*, 495-508.

(45) Glish, G.L.; Mcluckey, S.A.; Ridley, T.Y.; Cooks, R.G. A New "hybrid" Sector/Quadrupole Mass Spectrometer for MS/MS. *Int. J. Mass Spectrom.*

Ion Phys. **1982**, *41*, 157-177.

(46) Bradley, C.D.; Curtis, J.M.; Derrick, P.J.; Wright, B. Tandem Mass Spectrometry of Peptides Using a Magnetic Sector/Quadrupole Hybrid-the Case for Higher Collision Energy and Higher Radio-Frequency Power. *Anal. Chem.* **1992**, *64*, 2628-2635.

(47) Schoen, A.E.; Amy, J.W.; Ciupek, J.D.; Cooks, R.G.; Dobberstein, P; Jung, G.A. Hybrid BEQQ Mass Spectrometer. *Int. J. Mass Spectrom. Ion Proc.* **1985**, *65*, 125-140.

(48) Yost, R.A.; Enke, C.G. Triple Quadrupole Mass Spectrometry for Direct Mixture Analysis and Structure Elucidation. *Anal. Chem.* **1979**, *51*, 1251-1261.

(49) Ehlers, M.; Schmidt, S.; Lee, B.J.; Grotemeyer, J. Design and Set-Up of an External Ion Source Coupled to a Quadrupol-Ion-Trap Reflectron-Time-of-Flight Hybrid Instrument. *Eur. J. Mass Spectrom.* **2000**, *6*, 377-385.

(50) Hager, J.W. A New Linear Ion Trap Mass Spectrometer. *Rapid Commun. Mass Spectrom.* **2002**, *16*, 512-526.

(51) Guilhaus, M.; Selby, D.; Miynski, V. Orthogonal Acceleration TOF-MS. *Mass Spectrom. Rev.* **2000**, *19*, 65-107.

(52) McLuckey, S.A. Principles of Collisonal Activation in Analytical MS. *J. Am. Soc. Mass Spectrom.* **1992**, *3*, 599-614.

(53) Keseler, I.M.; Collado-Vides, J.; Gama-Castro, S.; Ingraham, J.; Paley, S.; Paulsen, I.T.; Peralta-Gill, M.; Karp, P.D. Ecocyc: a Comprehensive Database Resource for *Escherichia coli*. *Nucleic Acids Res.* **2005**, *33*, D334-D337.

(54) Mungur, R.; Glass, A.D.M.; Goodenow, D.B.; Lightfoot, D.A. Metabolite fingerprinting in transgenic Nicotina tabacum altered by the *Escherichia coli* glutamate dehydrogenase gene. *J. Biomed. Biotechnol.* **2005**, *2*, 198-214.

(55) Oldiges, M.; Lutz, S.; Pflug, S.; Schroer, K.; Stein, N.; Wiendahl, C. Metabolomics: Current State and Evolving Methodologies and Tools. *Appl. Microbiol. Biotechnol.* **2007**, *76*, 495-511.

(56) Fiehn, O. Metabolomics-the Link between Genotypes and Phenotypes. *Plant Mol. Biol.* **2002**, *48*, 155-171.

(57) De Graaf, A.A.; Striegel, K.; Wittig, R.M.; Laufer, B.; Schmits, G.; Wiechert, W.; Sprenger, G.A.; Sahm, H. Metabolic State of Zymononas Mobilis in Glucose-, Fructose, and Xylose-fed Continuous Cultures as Analyzed by C-13- and P-31-NMR Spectroscopy. *Arch. Microbiol.* **1999**, *171*, 371-385.

(58) Womersley, C. A Micromethod for the Extraction and Quantitative Analysis of Free Carbohydrates in Nematode Tissue. *Anal. Biochem.* **1981**, *112*, 182-189.

(59) Meyer, S.; Noiseommit-Rizzi, N.; Reuss, M.; Neubauer, P. Optimized Analysis of Intracellular Adenosine and Guanosine Phosphates in *Escherichia coli*. *Anal. Biochem.* **1999**, *271*, 43-52.

(60) Castrillo, J.I.; Hayes, A.; Mohammed, S.; Gaskell, S.J.; Oliver, S.G. An Optimized Protocol for Metabolome Analysis in Yeast Using Direct Infusion Mass Spectrometry. *Phytochemistry* **2003**, *62*, 929-937.

(61) Dune, W.B.; Bailey, N.J.C.; Johnson, H.E. Measuring the Metabolome: Current Analytical Technologies. *Analyst* **2005**, *130*, 606-625.

(62) Annesley, T.M. Ion Suppression in Mass Spectrometry. *Clin. Chem.* **2003**, *49*, 1041-1044.

(63) Coulier, L.; Bas, R.; Jesperson, S.; Verheijm E.; van der Werf, M.J.; Hankemeier, T. Simultaneous Quantitative Analysis of Metabolites using Ion-pair Liquid Chromatography-Electrospray Ionization Mass Spectrometry. *Anal. Chem.* **2006**, *78*, 6573-6582.

(64) Luo, B.; Groenke, K.; Takors, R.; Wandrey, C.; Oldiges, M. Simultaneous Determination of Multiple Intracellular Metabolites in Glycolysis, Pentose Phosphate Pathway and Tricarboxylic Acid cycle by Liquid Chromatography-Mass Spectrometry. *J. Chromatogr. A* **2007**, *1147*, 153-264.

(65) Shellie, R.A.; Welthagen, W.; Zrostlikova, J.; Spranger, J.; Ristow, M.; Fiehn, O.; Zimmermann, R. Statistical Methods for Comparing

Comprehensive Two-dimensional Gas Chromatography-Time-of-Flight Mass Spectrometry Results: Metabolomic Analysis of Mouse Tissue Extracts. *J. Chromatogr. A* **2005**, *1086*, 83-90.

(66) Noh, K.; Gronk, K.; Luo, B.; Takors, R.; Oldiges, M.; Wiechert, W. Metabolic Flux Analysis at Ultra Short Time Scale: Isotopically Non-stationary ^{13}C Labeling Experiments. *J. Biotechnol.* **2007**, *129*, 249-267.

(67) Van den Berg, R.A.; Hoefsloot, H.C.J.; Westerhuis, J.A.; Smilde, A.K.; van der Werf, M.J. Centering, Scaling, and Transformations: Improving the Biological Information Content of Metabolomics Data. *Bmc. Genomics* **2006**, *7*, 142.

(68) Katajamaa, M.; Miettinen, J.; Oresic, M. MZmine: Toolbox for Processing and Visualization of Mass Spectrometry Based Molecular Profile Data. *Bioinformatics* **2006**, *22*, 634-636.

Chapter 2

DIFFERENTIATION AND QUANTIFICATION OF C1 AND C2 ^{13}C-LABELED GLUCOSE BY TANDEM MASS SPECTROMETRY

2.1 Introduction

The mosquito is one of the most common disease-transmitting insects, and it causes millions of deaths worldwide every year. Mosquitoes can transmit diseases like West Nile virus, yellow fever, malaria and more [1]. Figure 2.1 shows an example of the distribution of West Nile virus cases in the United States in 2003. The situation is much worse in many developing countries. However, the traditional control strategies have become more and more ineffective, so some bio-rational methods need be developed to control the populations of mosquitoes. In particular, bio-rational methods can be built on the basis of a clear understanding of the mosquito metabolism pathways. The present study is collaboration with Dr. Patricia Scaraffia and Dr. Roger Miesfield. The aim is to study the carbon metabolism in mosquitoes by feeding with isotope labeled compounds (Section 1.3).

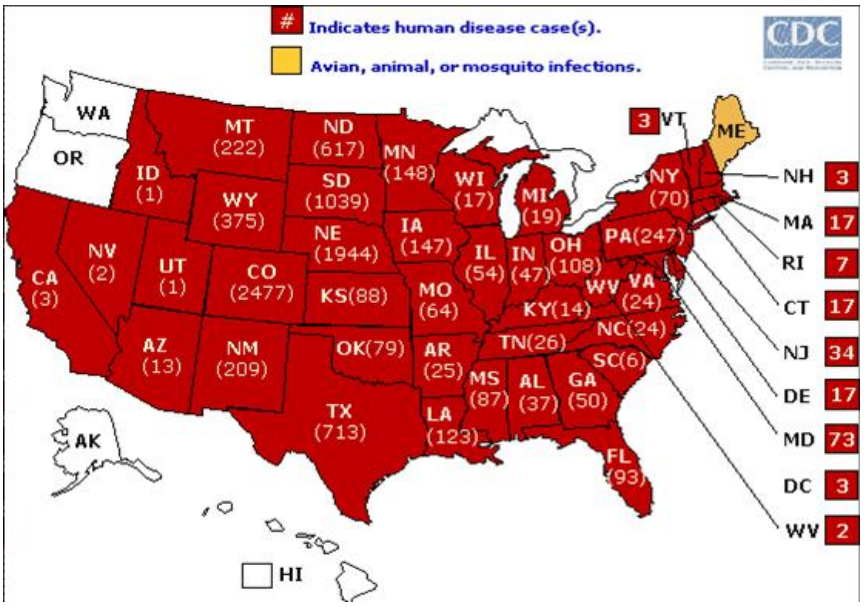

FIGURE 2.1. Distribution of West Nile virus cases in the United Stated in 2003 [1].(Figure from www.mosquito.org)

We first focus on glucose, the major fuel of most organisms, which is a core compound in carbohydrate metabolism studies. In order to understand and reveal in detail how glucose is metabolized into different metabolites or from different upstream metabolites, it is highly desirable to develop a sensitive, rapid and reliable method that allows identification of the individual carbon atoms in the D-glucose molecule (Figure 2.2).

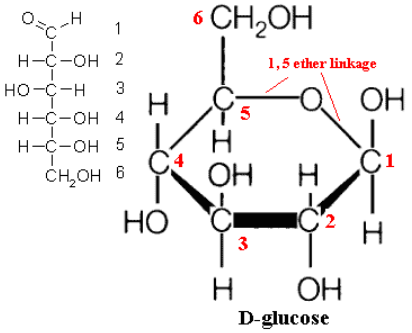

FIGURE 2.2. Structure of D-glucose and the numbering of its carbon atoms. Figure from reference [21].

Traditionally, gas chromatography coupled with mass spectrometry (GC-MS) has been widely used for carbohydrate analysis [2]. However, the major disadvantage of this method is that traditional chromatography cannot always distinguish between the labeled and unlabeled isotopes, or between isotopomers labeled by ^{13}C atoms at different positions. Moreover, these methods cannot perform accurate quantification of each isotopomer, although the intensities of the fragment peaks in EI-MS spectra can provide some relative ^{13}C enrichment information. Alternatively, nuclear magnetic resonance (^{13}C-NMR) is able to distinguish the compounds that are ^{13}C labeled at different positions, thus it has also been applied to study dynamic carbohydrate metabolism [3]. However, the low inherent signal-to-noise ratio weakens its sensitivity and increases the time for data collection. Therefore it is difficult to accurately quantify the amount of each metabolite rapidly, although ^{13}C NMR is able to follow the ^{13}C atom in the metabolic pathways.

Tandem mass spectrometry (MS/MS) has been used as a sensitive, rapid, reliable and effective method to perform metabolism studies, for example, identification and quantification of amino acids in blood for the detection of diseases [4-9], because the multiple reaction monitoring (MRM) scan mode in tandem mass spectrometry can identify and quantify multiple compounds in one measurement with high sensitivity but without previous purification (Section 1.2.2). This is a great advantage for studying complex biological samples, such as neonatal blood [10], whole body mosquitoes [11] and intracellular folates [12]. However, there is no established MS/MS method available to differentiate and quantify the glucose molecules that are ^{13}C labeled at different positions for metabolic study purposes.

This chapter will present results obtained for the differentiation and accurate quantification of C1 and C2 labeled glucose molecules based on a mild derivatization method [13] and the fragmentation patterns of those isotopomers in tandem mass spectrometry.

2.2 Experimental

Reagents

The labeled isotopes D-Glucose-1-^{13}C, D-Glucose-2-^{13}C, D-Glucose-1,2-$^{13}C_2$, , D-Glucose-D_7 (1,2,3,4,5,6,6-D7), and D-Glucose-D2 (6,6-D2) were purchased from Cambridge Isotope Laboratories (Andover, MA, USA). D-Glucose, methylamine solution (ca. 40w/v%), borane-dimethylamine complex (97%), boric acid, sodium tetraborate, methanol and toluene were obtained from Sigma-Aldrich (St. Louis, MO, USA).

Glucose Derivatization

The derivatization of glucose was performed according to a modification of a method previously developed by Honda et al. [13] for ultramicroanalysis of reducing carbohydrates by capillary electrophoresis with laser-induced fluorescence detection. Stock solutions were prepared by dissolving unlabeled or labeled ^{13}C-Glc or D7-Glc in 1 M methylamine solution containing 0.2 M dimethylamine–borane complex adjusted to pH 4.5 with acetic acid. Only 10 μL of the stock solutions (0.1 mM) were incubated at 40ºC for 30 minutes and the solvents evaporated to dryness under nitrogen atmosphere at 60ºC. The residue was treated with 100 μL of methanol and 100 μL of toluene and then the solvents were evaporated to dryness under nitrogen atmosphere at 60ºC. The last

operation was repeated twice more. The residue of methylglucosamine was stored at -20^{o}C until utilized.

Low-Energy Collision-Induced Dissociation (CID)

Low-energy CID experiments were performed on an Applied Biosystem Q-trap 4000 mass spectrometer (Foster City, CA) with a nanospray ionization source in the positive ion mode (Section 1.2.2). Underivatized and derivatized samples were dissolved in a solution of H_2O: MeOH (30:70, v/v) containing 1% acetic acid to reach a concentration of 20 μM. In some cases, an appropriate amount of Li_2CO_3 (100 μM final concentration) was added to the underivatized sample solution to improve the quality of the spectra. The solutions were then sprayed into the mass spectrometer with a flow rate of ca. 2.0 μL/min. The applied ionization voltage was between 2.2 kV and 2.5 kV, and the capillary temperature was maintained at 200^{o}C. Nitrogen served as the collision gas, and a laboratory collision energy of 25 to 35 eV was used to produce extensive fragments from the precursor ion, and the collision cell pressure was about 8 millitorr. Monoisotopic precursor ion was selected at unit mass resolution in order to avoid ambiguities from isotope contributions.

2.3 Results and Discussion

2.3.1 Fragmentation Spectra of Underivatized and Derivatized Glucose

The mass spectrum of underivatized glucose shows that the major ion formed is $[Glc+Na]^+$, for the base peak appears at m/z = 203 (data not shown). The Na^+ ion could be from chemical impurities or glass containers. When $[Glc+Na]^+$ ion is fragmented, the

quality of the MS/MS spectrum is poor (data not shown), it might be because the dominant fragment ion is Na^+, but we did not detect that low mass. It has been reported that addition of lithium ion improves the fragmentation of different carbohydrates such as disaccharides and oligosaccharides [14-17]. Thus, lithium carbonate was added to the spray solution, which exclusively produced the $[Glc+Li]^+$ ion (m/z = 187). The corresponding MS/MS spectrum of m/z = 187 shows a clear fragmentation pattern of high quality (Figure 2.3). Therefore Li_2CO_3 solution was added into all the other underivatized glucose samples.

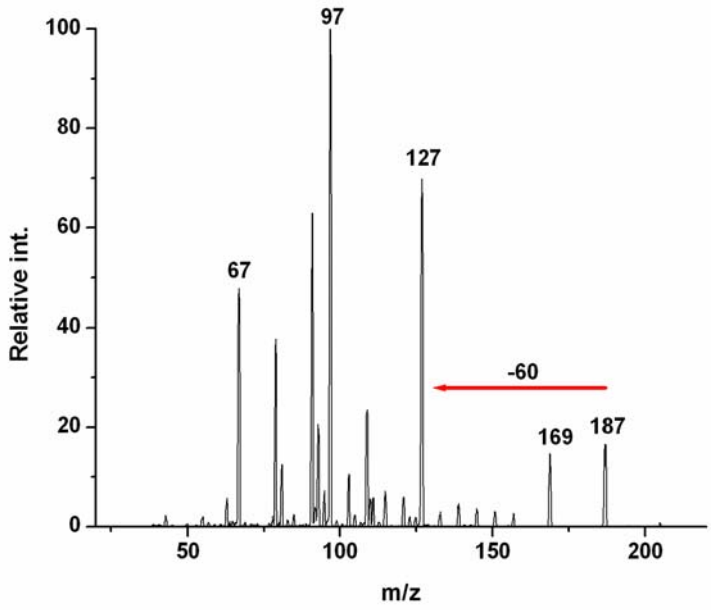

FIGURE 2.3. MS/MS spectra of $[Glc+Li]^+$ (m/z = 187). The collision used was 35 eV.

The spectrum shows a major mass loss of 60 Da from the molecular ion peak at m/z = 187; therefore, it is very likely to be a loss of $C_2H_4O_2$, because the elemental composition is consistent with it. However, the MS/MS spectrum of unlabeled glucose alone does not provide enough information to determine which two carbon atoms among the six carbons in glucose account for the carbon loss. Glucose, ^{13}C-labeled at C1 or C2,

as well as simultaneously at both C1 and C2, was also fragmented under the same conditions. The MS/MS spectra of those three compounds reveal that the two carbon atoms in the loss of $C_2H_4O_2$ must be C1 and C2, because C1 or C2 ^{13}C-labeled glucose lost 61 Da (188 → 127), while C1 and C2 ^{13}C-labeled glucose lost 62 Da (189 → 127) (Figure 2.4a-c), which indicates that the cleavage of the C-C bond between C1 and C2 is not a favored fragmentation pathway, and the loss of the C1 and C2 together is the major one in the pathway of $C_2H_4O_2$ loss. Therefore, C1 ^{13}C-labeled glucose cannot be distinguished from C2 ^{13}C-labeled glucose by tandem mass spectrometry without derivatization.

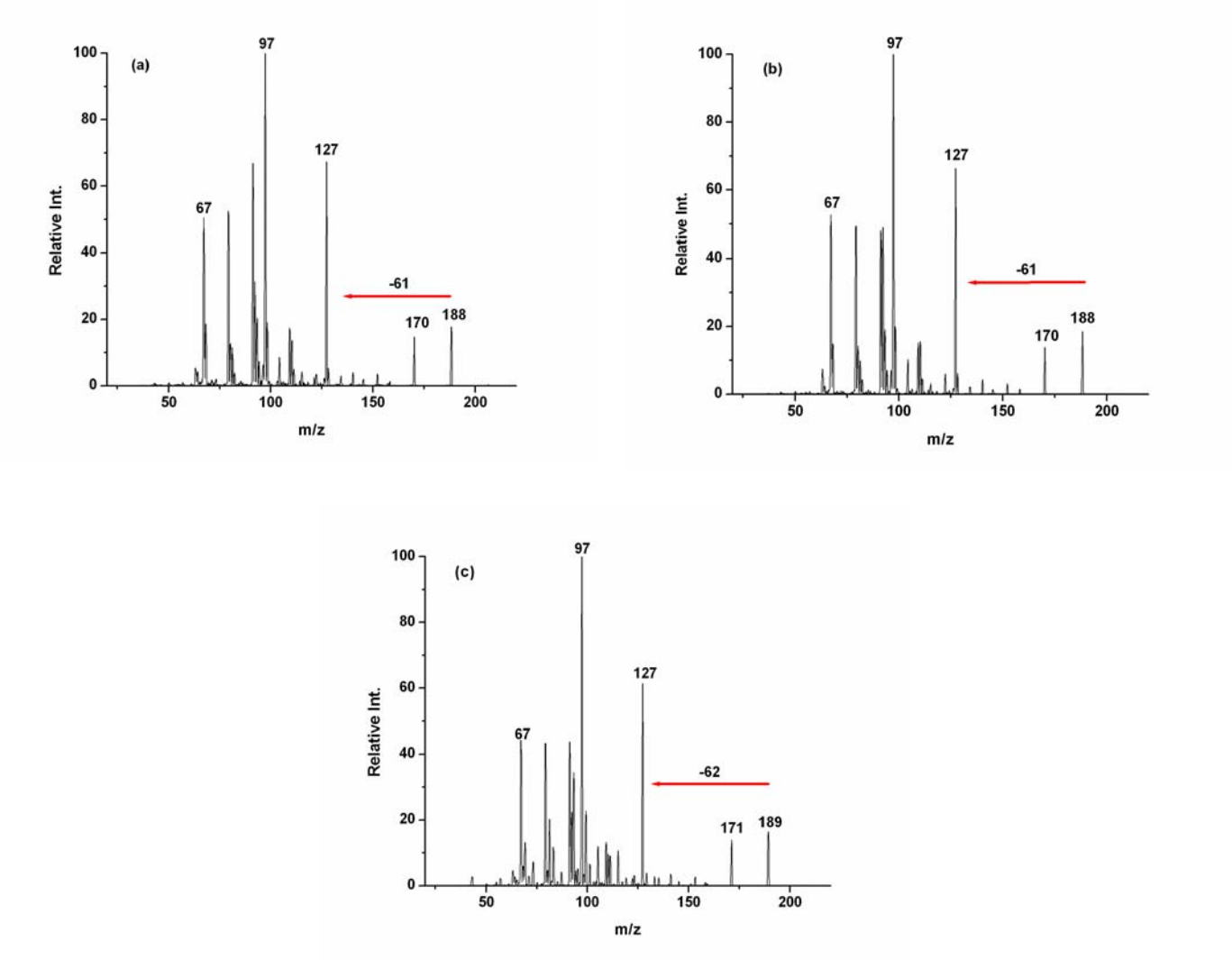

FIGURE 2.4. MS/MS spectra of ^{13}C-glucose. a) [Glc-1-^{13}C+Li]$^{+}$ (m/z = 187); b) [Glc-2-^{13}C+Li]$^{+}$ (m/z = 187); and c) [Glc-1, 2-^{13}C+Li]$^{+}$ (m/z = 188). The collision energy used was 35 eV.

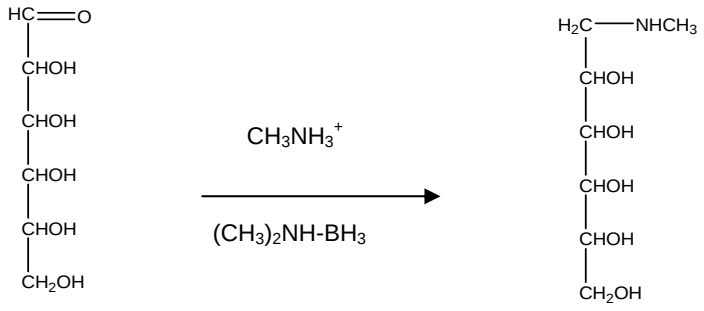

FIGURE 2.5. Derivatization of glucose and the structure of the product methylglucosamine (Glc-MA).

The structure of the methyglucosamine (Glc-MA), a derivatized product from the reaction of glucose with methylamine is shown in Figure 2.5. Compared with glucose, the C1 in the product is connected to a methylamine group. We speculated that bonding $NHCH_3$ to C1 might favor the cleavage of the C-C bond between C1 and C2 by forming a stable product ion $CH_2NHCH_3^+$ (m/z = 44) containing only C1. The MS/MS spectrum of unlabeled Glc-MA shows a huge product ion peak at m/z = 44 by loss of 152 Da ($C_5H_{12}O_5$) from the precursor ion m/z = 196 (Figure 2.6a), implying that the chemical modification turns the cleavage of C-C bond between C1 and C2 into the most favored fragmentation pathway. The MS/MS spectra of ^{13}C-labeled Glc-MA molecules further confirm that the major product ion $CH_2NHCH_3^+$ contains C1 only and that the C-C bond between C1 and C2 is cleaved (Figure 2.6b-d): C1 ^{13}C-labeled Glc-MA (Glc-1-^{13}C-MA) produces a fragment ion at m/z = 45 from its precursor ion at m/z = 197 upon activation (197 → 45). C2 ^{13}C-labeled Glc-MA (Glc-2-^{13}C-MA) generates a fragment ion at m/z = 44 from its precursor ion at m/z = 197 (197 → 44), whereas the Glc-MA labeled at C1 and C2 (Glc-1,2-^{13}C-MA) shows a fragment ion at m/z = 45 from its precursor ion at m/z = 198 (198 → 45). Therefore, the derivatized glucose molecules labeled at C1 or C2 and C1 plus C2 can be distinguished by tandem mass spectrometry. Glc-D_7-MA or Glc-D_2-MA can serve as an internal standard for quantification by MRM. When fragmented, Glc-D_7-MA produces a strong fragment ion at m/z = 45 from the precursor ion at m/z = 203 (203 → 45) (Figure 2.6e), while Glc-D_2-MA produces its counterpart at m/z = 44 from the precursor ion at m/z = 198 (198 → 44) (Figure 2.6f).

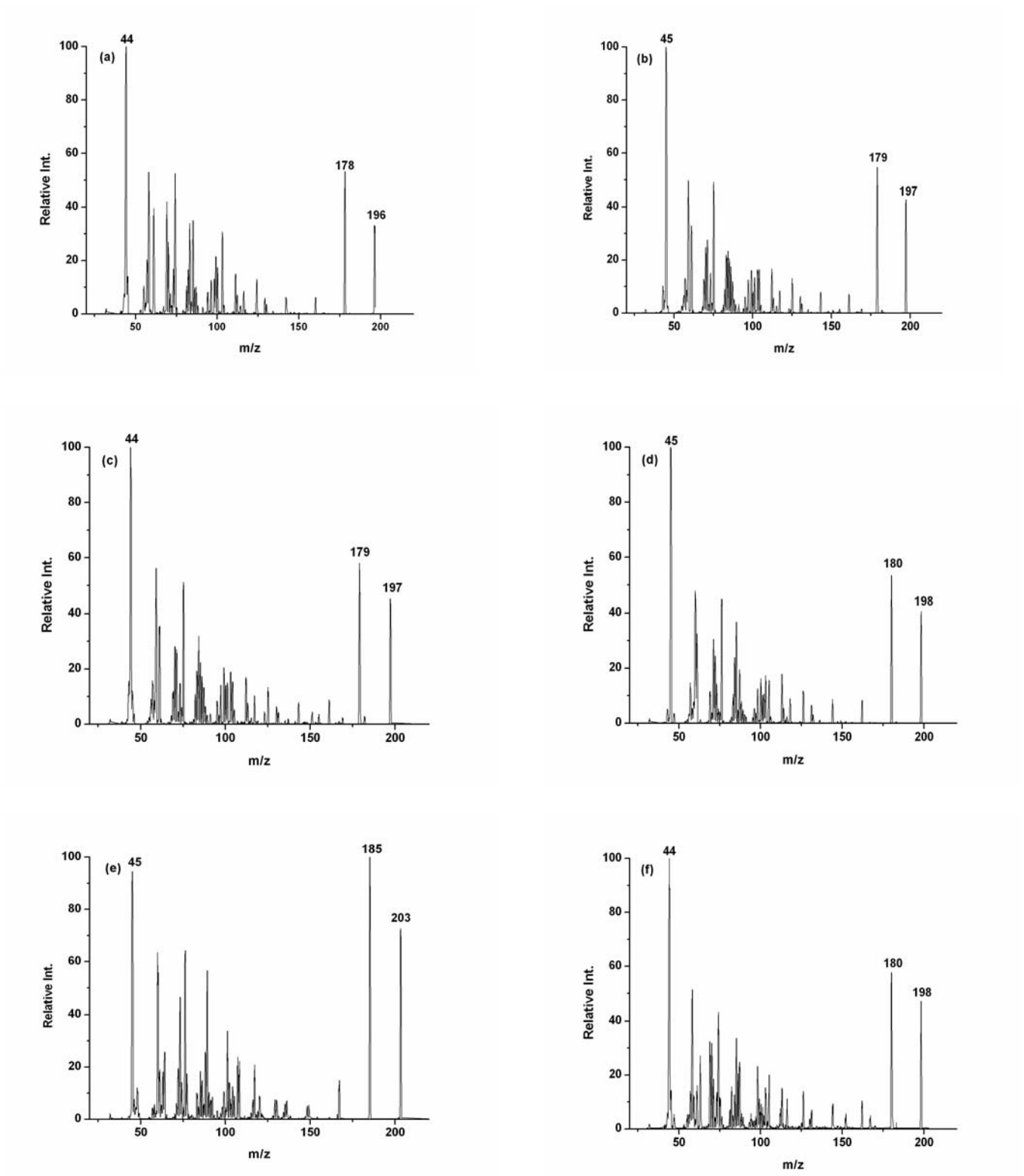

FIGURE 2.6. MS/MS spectra of $[Glc\text{-}MA+H]^+$: a) $[Glc\text{-}MA+H]^+$ (m/z=196); b) $[Glc\text{-}1\text{-}^{13}C\text{-}MA+H]^+$ (m/z=197); c) $[Glc\text{-}2\text{-}^{13}C\text{-}MA+H]^+$ (m/z=197); d) $[Glc\text{-}1,2\text{-}^{13}C\text{-}MA+H]^+$ (m/z=198); e) $[Glc\text{-}D7\text{-}MA+H]^+$ (m/z=203) f) [Glc-D2 (6, 6 D2)-$MA+H]^+$ (m/z = 198).

2.3.2 Possible Fragmentation Pathways

A possible mechanism for the neutral loss of 60 Da of underivatized glucose is shown in Scheme 2.1. There is an equilibrium between the cyclic glucose and its linear form. The carbonyl oxygen is more basic than the hydroxyl oxygen so if Li^+ affinities track proton affinities, the added lithium would first be located at the carbonyl oxygen. However, during collision induced dissociation, the lithium ion could be intra-molecularly transferred to the hydroxyl oxygen upon activation to initiate cleavage. Scheme 2.1 illustrates the possible processes for the neutral loss of 60 Da ($C_2H_4O_2$) and formation of the fragment ion at m/z = 127 ($C_4H_8O_4Li^+$): 1) the migration of hydrogen from the hydroxyl group to the carbonyl oxygen through a six-member ring structure forms a neutral $C_2H_4O_2$, and the charge is retained at the other fragment forming the fragment ion at m/z = 127; 2) the neutral $C_2H_4O_2$ is rearranged to a more stable form. This hydrogen migration process is similar to the McLafferty rearrangement, and occurs to metal adducts of peptide esters [18]. The proposed mechanism for the neutral loss of 60 Da results in the simultaneous loss of C1 and C2 in glucose, which is consistent with the experimental data (Figure 2.3b).

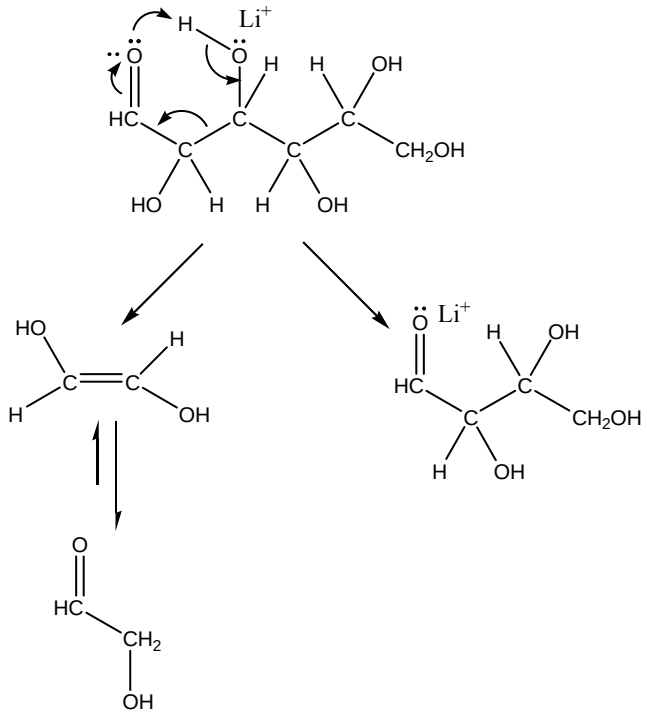

SCHEME 2.1. Possible mechanism for the formation of ion m/z = 127 by fragmenting the ion m/z = 187 after a NL of 60 for glucose.

Scheme 2.2 shows a possible fragmentation pathway to cleave the C-C bond between C1 and C2 in the derivatized glucose (Glc-MA) and to form a dominant fragment ion at m/z = 44: the added proton will be located on the amine group due to the high proton affinity of the amine group. The hydrogen on the amine would migrate to the hydroxyl oxygen upon activation on C3 via a six-member ring structure, causing a neutral loss of H_2O (18 Da). In the meantime, the C-C bond between C1 and C2 is cleaved and two new double bonds are formed between C2 and C3, and between C1 and the amine group. Thus, a stable fragment ion ($C_2H_6N^+$, m/z = 44) containing C1 is produced, and the neutral molecule containing C2 is rearranged to a more stable form (134 Da). Due to the stability of the product ion, the peak intensity is very strong, which will greatly benefit the quantification of glucose by the multiple reaction monitoring (MRM) scan in mass spectrometry.

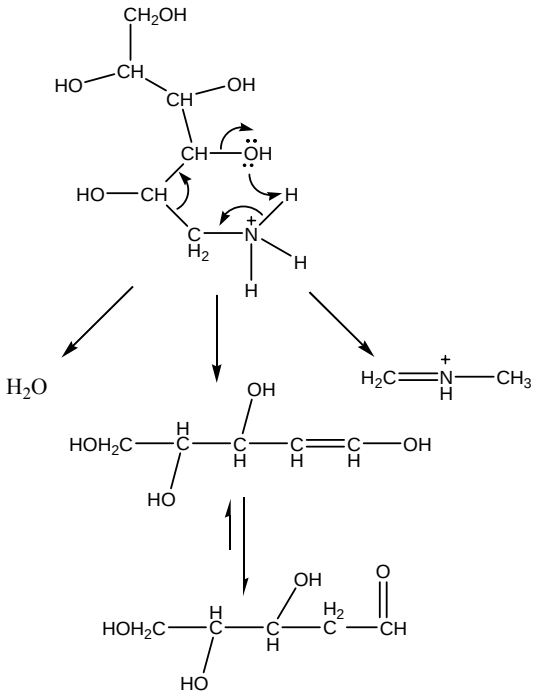

SCHEME 2.2. Possible mechanism for the formation of ion m/z = 44 by fragmenting the peak m/z = 196 after a NL of 152 for Glc-MA.

2.3.3Differentiation and Quantification of C1 and C2 ^{13}C-Labeled Glucose by Multiple Reaction Monitor Scans

The chemical modification performed to glucose makes the C-C bond between C1 and C2 more susceptible to cleavage, so Glc-1-^{13}C-MA and Glc-2-^{13}C-MA show different MS/MS spectra, even though they have the same molecular weight. The different product ion masses make it possible to differentiate those two compounds from a mixture without separation or purification, and quantify them with a known amount of Glc-D_7-MA or Glc-D_2-MA added into the sample as an internal standard. In the multiple reaction monitoring (MRM) scan mode, the first quadrupole mass analyzer is set to select the precursor ions, namely m/z = 197 for Glc-1-^{13}C-MA and Glc-2-^{13}C-MA, m/z = 203 for Glc-1,2,3,4,5,6,6-D_7-MA, and m/z=198 for Glc-C1-2-^{13}C-MA and Glc-6,6-D_2-MA; the third quadrupole mass analyzer transmits their corresponding neutral loss product

ions, namely m/z = 45 for Glc-1-^{13}C-MA, Glc-C1-2-^{13}C-MA and Glc-,2,3,4,5,6,6-D_7-MA, m/z = 44 for Glc-2-^{13}C-MA and Glc-6,6-D_2-MA (Table 2.1). In this way, the tandem mass spectrometry in the MRM scan mode identifies those two isotopic species, and provides a strategy to monitor each of those two carbon atoms separately. In addition, the result also provides important quantitative information, because the resulting peak intensity ratio between ^{13}C labeled Glc-MA and deuterium labeled Glc-MA is proportional to the original concentration ratio between them in the sample.

Table 2.1 Precursor ion and fragment ion pairs for methylglucosamine

Glc-MA	Precursor Ion	Neutral Loss	Precursor/Fragment Ion Pair
Glc-MA	196	152	196 → 44
Glc-1-^{13}C-MA	197	152	197 → 45
Glc-2-^{13}C-MA	197	153	197 → 44
Glc-C1-2-^{13}C-MA	198	153	198 → 45
Glc-1,2,3,4,5,6,6-D_7-MA	203	158	203 → 45
Glc-6,6-D_2-MA	198	154	198 → 44

Deuterium-labeled compounds are commonly used as internal standards for amino acid quantification [19], but usually the isotopic effect was not taken into account, because it is not significant if the deuteriums are not involved in reaction. However, it may affect the accuracy of the quantification if it exists [20], because isotopic substitution may greatly change the reaction rate, which is the rate of the fragmentation of CID in mass spectrometry. It is observed that when Glc-MA, Glc-1-^{13}C-MA, Glc-2-^{13}C-MA, Glc-1-2-^{13}C-MA, Glc-D_7-MA and Glc-D_2-MA with the same concentration were fragmented under the same conditions, the peak intensity ratios between the fragment ion $CH_2NHCH_3^+$ (its m/z value varies with the species accordingly, Table 2.1) and its precursor ion are slightly different (Figure 2.7). It means that the concentrations of ^{13}C

labeled species would be overestimated if Glc-D_2-MA is used as the internal standard but the peak ratio difference shown in Figure 2.7 is not considered. To make the quantification more accurate, a "correction factor" is introduced. We consider the correction factor for Glc-D_2-MA as 1, the correction factors for other species are 0.771 for Glc-MA, 0.805 for Glc-1-^{13}C-MA, 0.916 for Glc-2-^{13}C-MA, 0.783 for Glc-1-2-^{13}C-MA, and 1.556 for Glc-D_7-MA, which are calculated based on Figure 2.7.

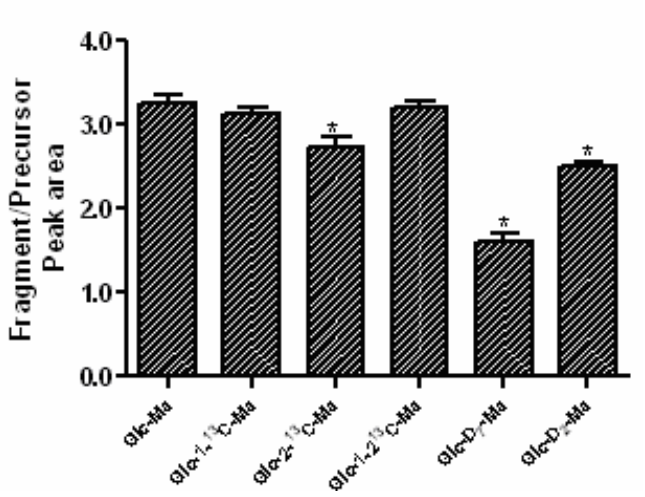

FIGURE 2.7. Peak area ratio between the fragment ion $CH_2NHCH_3^+$ and its precursor ion for Glc-MA, Glc-1-^{13}C-MA, Glc-2-^{13}C-MA, Glc-C1-2-^{13}C-MA, Glc-1,2,3,4,5,6,6-D_7-MA and Glc-6, 6-D_2-MA.

To test the performance of the MRM method and the correction factor, a mixture containing the same amount of Glc-1-^{13}C-MA, Glc-2-^{13}C-MA, Glc-C1-2-^{13}C-MA and Glc-D_2-MA was measured using the MRM method. Then the amount of, Glc-1-^{13}C-MA, Glc-2-^{13}C-MA and Glc-1-2-^{13}C-MA was calculated and corrected by the correction factor using Glc-D_2-MA as the internal standard. The results are listed in Table 2.2, showing that the introduction of the correction factor improves the accuracy of the quantification.

TABLE 2.2.
Calculated amounts of Glc-1-^{13}C-MA, Glc-2-^{13}C-MA and Glc-C1-2-^{13}C-MA using MRM method, with and without correction

	True Amount	Calculated Amount (without correction)	Error	Calculated Amount (with correction)	Error
Glc-1-^{13}C-MA	0.20 nmol	0.234 nmol	18.9 %	0.192 nmol	4.3 %
Glc-2-^{13}C-MA	0.20 nmol	0.215 nmol	7.4 %	0.197 nmol	1.6 %
Glc-1-2-^{13}C-MA	0.20 nmol	0.262 nmol	31.2 %	0.205 nmol	2.7 %
Glc-D_2-MA	0.20 nmol	--	--	--	--

It has to be pointed out that the correction factor is different from the general concept of "isotopic effect". The correction factor only considers the peak intensity ratio of two particular peaks of interest, but "isotopic effect" may affect the intensities of other peaks. To investigate the isotopic effect, the ratio between total fragment ion intensity and total ion abundance (Figure 2.8a) and the ratio between $CH_2NHCH_3^+$ ion intensity and the total ion abundance is obtained (Figure 2.8b). The peak ratio in Figure 2.8a is almost the same between all the derivatized glucose molecules, implying that there is no significant isotopic effect among those species overall. However, the peak ratio pattern in Figure 2.8b is very similar to that in Figure 2.7. Combining the information from Figure 2.7 and Figure 2.8b, it can be concluded that the fragmentation pathways to form the $CH_2NHCH_3^+$ ion from derivatized glucose is affected by the ^{13}C or deuterium labeling. Glc-2-^{13}C-MA, Glc-D_7-MA and Glc-D_2-MA have more significant isotopic effect than Glc-1-^{13}C-MA and Glc-1-2-^{13}C-MA.

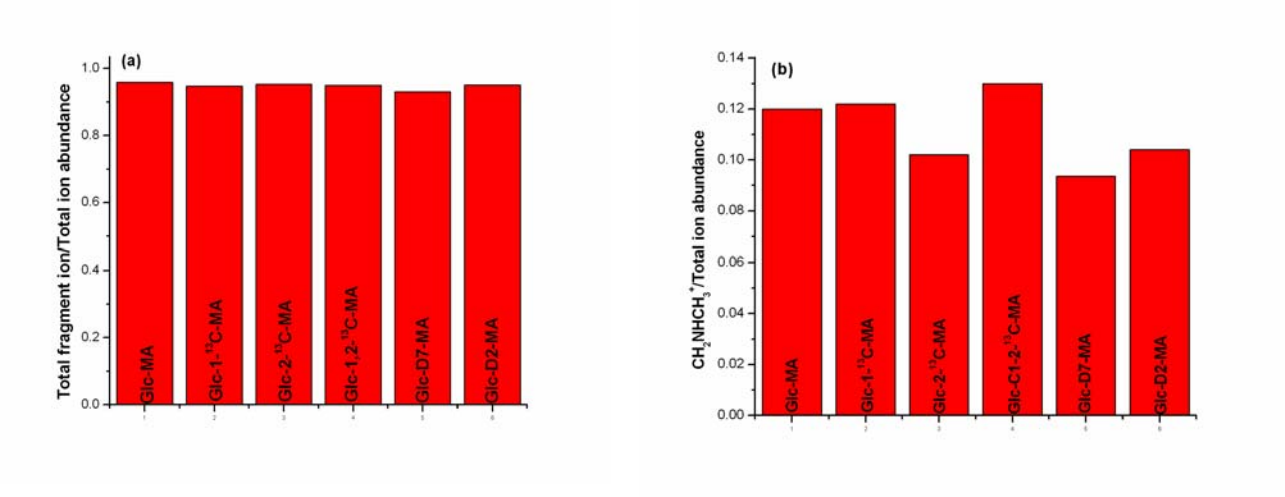

FIGURE 2.8. a)The ratio between total fragment ion intensity and total ion abundance; b) the ratio between $CH_2NHCH_3^+$ ion intensity and the total ion abundance for Glc-MA, Glc-1-^{13}C-MA, Glc-2-^{13}C-MA, Glc-C1-2-^{13}C-MA, Glc-D_7-MA and Glc-D_2-MA.

2.4 Conclusions and Future Directions

It is observed in this study that adding lithium ions into the spray solution improves the quality of MS/MS spectra of underivatized glucose in CID. However, C-C bond between C1 and C2 atoms in glucose is not cleaved, and C1 and C2 tend to be lost together in CID, so the fragmentation cannot differentiate C1 ^{13}C-labeled glucose from C2 ^{13}C-labeled glucose. To resolve this problem, we chemically modified the glucose molecule into methyglucosamine, which makes the C-C bond between C1 and C2 in glucose the most favored bond cleavage site with CID by forming a stable product ion containing only C1. Therefore, the chemical derivatization makes it possible to distinguish the C1 and C2 ^{13}C-labeled glucose molecules by tandem mass spectrometry, which allows following each of them separately in different metabolic pathways. Based on the fragmentation patterns of derivatized glucose, we developed a MRM method to identify C1 and C2 labeled glucose molecules and quantify each isotopomer using Glc-D_2-MA or Glc-D_7-MA as the internal standard. The "isotopic effect" is considered in the

study and a correction factor is introduced in order to make the quantification more accurate. The high speed, high sensitivity and reliability of tandem mass spectrometry make this novel method a promising one to follow the metabolic pathways of carbon atoms in glucose and quantitatively study the kinetics of the transformations of the isotopomers in biological systems.

In future studies, we plan to apply the developed quantitative method to the analysis of mosquito samples. We will be able to identify and quantify the isotopomers individually in mosquito bodies as a function of time. We will combine this method with other quantitative MRM method to monitor the metabolism pathways and kinetics between glucose and other metabolites (i.e. alanine, arginine etc.). Once we figure out the critical metabolism pathways and the involved enzymes, a bio-rational method may be developed to control the mosquito populations.

REFERENCES

(1) http://www.mosquito.org Accessed on December 10, 2007.

(2) Price, N.P. Acylic sugar derivatives for GC/MS analysis of ^{13}C-enrichment during carbohydrate metabolism. *Anal Chem*. **2004**, *76*, 6566-6574.

(3) Ross, B.; Lin, A.; Harris, K.; Bhattacharya, P.; Schweinsburg, B. Clinical experience with ^{13}C MRS in vivo. *NMR Biomed.* **2003,** *16*, 358-369.

(4) Chace, D. H.; Millington, D. S.; Terada, N.; Kahler, S. G.; Roe, C. R.; Hofman, L. F. Rapid Diagnosis of Phenylketonuria by Quantitative Analysis for Phenylalanine and Tyrosine in Neonatal Blood Spots by Tandem Mass Spectrometry. *Clin. Chem.* **1993**, *39*, 66–71.

(5) Chace, D. H.; Hillman, S. L.; Millington, D. S.; Kahler, S. G.; Roe, C. R.; Naylor,

E. W. Rapid Diagnosis of Maple Syrup Urine Disease in Blood Spots from Newborns by Tandem Mass Spectrometry. *Clin. Chem.* **1995**, *41*, 62–68.

(6) Chace, D. H.; Hillman, S. L.; Millington, D. S.; Kahler, S. G.; Adam, B. W.; Levy, H. L. Rapid Diagnosis of Homocystinuria and Other Hypermethioninemias from Newborns' Blood Spots by Tandem Mass Spectrometry. *Clin. Chem.* **1996**, *42*, 349–355.

(7) Chace, D. H.; Sherwin, J. E.; Hillman, S. L.; Lorey, F.; Cunningham, G. C. Use of Phenylalanine-to-tyrosine Ratio Determined by Tandem Mass Spectrometry to Improve Newborn Screening for Phenylketonuria of Early Discharge Sspecimens Collected in the First 24 Hours. *Clin. Chem.* **1998**, *44*, 2405–2409.

(8) Chace, D. H.; Kalas, T. A.; Naylor, W. The Application of Tandem Mass Spectrometry to Neonatal Screening for Inherited Disorders of Intermediary Metabolism. *Annu. Rev. GenomicsHum. Genet.* **2002,** *3,* 17–45.

(9) Chace, D. H.; Kalas, T. A.; Naylor, E. W. Use of Tandem Mass Spectrometry for Multianalyte Screening of Dried Blood Specimens from Newborns. *Clin. Chem.* **2003**, *49*, 1797–1817.

(10) Nagy, K.; Takats, Z.; Pollreisz, F.; Szabo, T.; Vekey, K. Direct tandem mass spectrometric analysis of amino acids in dried blood spots without chemical derivatization for neonatal screening. *Rapid Commun. Mass Spectrom.* **2003**, *17*, 983–990.

(11) Scaraffia, P.Y.; Zhang, Q.; Wysocki, V.H.; Isoe, J.; Wells, M.A. Analysis of whole body ammonia metabolism in Aedes aegypti using [15N]-labeled compounds and mass spectrometry. *Insect Biochem Mol Biol*. **2006,** *36*, 614-22

(12) Luo, W.Y.; Kwon, Y.K.; Rabinowitz, J.D. Isotope Ratio-Based Profiling of Microbial Folates. *J. Am. Soc. Mass Spectrom*. **2007**, *18*, 898-909

(13) Honda, S.; Oked, J.; Iwanaga, H.; Kawakami, S.; Taga, A.; Suzuki, S.; Imai, K. Ultramicroanalysis of reducing carbohydrates by capillary electrophoresis with laser-induced fluorescence detection as 7-nitro-2,1,3-benzoxadiazole-tagged N-methylglycamine derivatives. *Anal Biochem.* **2000**, *286*, 99-111.

(14) Zhou, Z.R.; Ogden, S.; Leary, J.A. Linkage position determination in oligosaccharides - MS/MS study of lithium-cationized carbohydrates *J. Org. Chem.*

1990, *55*, 5444-5446

(15) Staempfli, A.; Zhou, Z.R.; Leary, J.A. Gas-Phase dissociation mechanisms of dilithiated disaccharides- Tandem mass-spectrometry and semiempirical calculations. *J. Org. Chem.* **1992,** *57*, 3590-3594

(16) Hofmeister, G.E.; Zhou, Z.; Leary, J.A. Linkage position determination in lithium – cationized disaccharides- tandem mass-spectrometry and semiempirical calculations *J. Am. Chem. Soc.* **1991,** *113*, 5964-5970

(17) Harvey, D.J. Collision-induced fragmentation of underivatized N-linked carbohydrates ionized by electrospray *J. Mass Spectrom.* **2000**, *35*, 1178-1190

(18) Anbalagan, V.; Patel, J.N.; Niyakorn, G.; Stipdonk, M.J.V. Mclafferty-type Rearrangement on the collision-induced Dissociate of Li^+, Na^+ and Ag^+ Cationed Ester of N-Actetylated Peptides. *Rapid Commun. Mass Spectrom.* **2003**, *17*, 291-330

(19) Trinh, M.B.J.; Harrison, RJ.; Gerace, R.; Ranieri, E.; Fletcher, J.; Johnson, D.W. Quantification of Glutamine in Dried Blood Spots and Plasma by Tandem Mass Spectrometry for the Biochemical Diagnosis and Monitoring of Ornithine Transcabamylase Deficiency. *Clin. Chem.* **2003**, 481-683.

(20) Zhang, Q.; Wysocki, V.H.; Scaraffia, P.Y.; Wells, M.A. Fragmentation pathway for glutamine identification: loss of 73 Da from dimethylformamidine isobutyl glutamine. *J. Am. Soc. Mass Spectrom*. **2005**, *16*, 1192–1203.

Chapter 3

CHARACTERIZATION OF CROSS-LINKED COLLAGEN AND ITS CROSS-LINKS BY MASS SPECTROMETRY

3.1 Introduction

Collagen is the most abundant protein in mammals, accounting for 30% of all proteins; it serves as the major source of extracellular support for multicellular animals [1]. Collagen is localized primarily in the extracellular matrix and it usually forms fibril structures (type I, II, III, V, or XI). Fibril-forming collagens of type I, III, and V are found in human tissue and are made up of three linear α-chains of approximately 100 kDa each (approximately 1,000 amino acid residues each) in molecular weight, which forms a closely coiled left-handed triple helices structure (γ), stabilized by hydrogen bonding involving hydroxyproline residues in different chains [2, 3]. The arrangement of amino acids in collagen molecule follows the repeating sequence pattern of Gly-X-Y, where X and Y can be proline, hydroxy-proline, alanine, arginine, lysine and other amino acid residues.

Type I collagen was the only mammalian collagen identified prior to 1969. It is composed of three chains, two identical, termed α1 chains or α1(I); and one different from the other two, termed α2 chain or α2(I). Type I collagen is the most abundant in skin, tendons, ligaments, bone, and the cornea, where it comprises between 80% and 99% of the total collagen [4]. Type II collagen usually exists in a variety of cartilages, which is made up of three identical α chains, called α1(II). Cartilage can be found in many places in the body including joints, ear and the nose. The most significant features of type II

collagen are its high hydroxylysine content and the presence of glycosidically bound carbohydrates. It can contain up to fivefold more of hydroxylysine than those α chains from skin [5]. Type III collagen is very similar to Type I collagen, but it contains a relatively high content of hydroxyproline and glycine, and it can form intramolecular disulfide bonds involving two cysteine residues close to the C-terminal region of the triple helix. The ratio of Type I and III collagens in skin can vary with age [6, 7]. The ability to isolate and distinguish different types of collagen involves the use of solvents of different ionic strength and pH followed by differential salting out [8]. The precipitated fraction of collagen is usually analyzed by identification of its intact α chains or CNBr digested peptides by polyacrylamide gel electrophoresis [9].

Collagen fibrils provide the mechanical support that enabled large multicellular animals to evolve on earth [10]. The mechanical strength of collagen depends on the formation of covalent intermolecular cross-links between the individual protein subunits, for crosslinking renders the collagen fibers stable and provides them with an adequate degree of tensile strength and viscoelasticity to perform their structural role. The degree of crosslinking, the number and density of the fibers, including their orientation and diameter, dictate the function and the type of collagen [11]. Almost all fibril-forming collagens are cross-lined through a mechanism based on the reaction where aldehydes are generated from lysine or hydroxylysine side-chains by lysyl oxidase (Figure 3.1). Crosslinking starts with the conversion of specific lysine or hydroxylysine residues in collagen to peptide-bound aldehydes, which involves the oxidative deamination of ε-carbon of lysine or hydroxylysine [12]. Incubation of purified enzyme-bound collagen at 37^0C, neutral pH and physiologic ionic strength can cause additional aldehyde formation

in vitro. The enzymatic activities can be inhibited by β-aminopropionitrile, EDTA, D-penicillamine and other carbonyl reagents. If the crosslinking occurs between two residue side chains, it is called divalent crosslinking, while if three side chains are involved, it is called trivalent or mature crosslinking. It is also worth noting that different collagen types can crosslink with each other heterotypically in the assembly of multi-component fibrils [13]. Other mechanisms of collagen crosslinking include the cysteine disulfide mechanism, gamma-glutamyl lysine cross-links, and tyrosine-derived cross-links. [14].

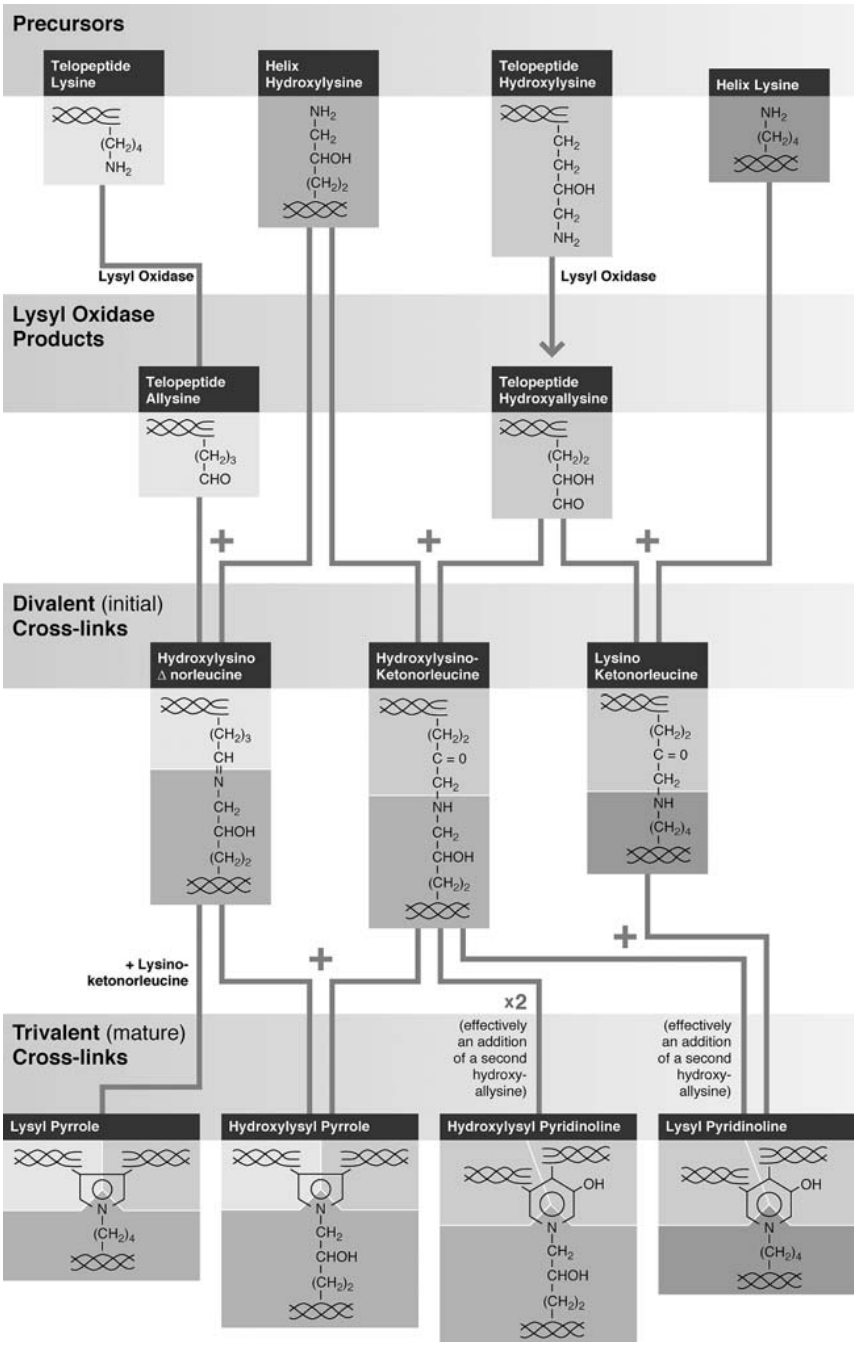

FIGURE 3.1. Diagram of hydroxylysine cross-linking pathway. Hydroxylysine residues are the source of aldehydes formed by lysyl oxidase for intermolecular cross-linking reactions. (Figure from Reference [14] with permission)

In the past decade, significant attention has been paid to the clinical importance of collagen cross-linking by measuring pyridinolines or cross-linked telopeptides in body

fluids as molecular markers [15-17]. For example, higher level of pyridinolines cross-links and hydroxylysine than normal in bone has been used as an indicator of osteogenesis imperfecta [18]. Specific fragments from cartilage type II collagen have been identified and targeted for immunoassay as a biomarker of cartilage breakdown [19]. It has also been found that extracellular matrix (ECM) fibrillar collagen synthesis and degradation and collagen cross-linking by lysyl oxidase (LOX) may lead to heart failure when ECM composition undergoes remodeling as a response to hypertension [20, 21]. In a more recent mouse study conducted by the Larson group at the University of Arizona, the total cardiac fibrillar collagen, the percentage of fibrillar collagen cross-linking, and the activity of cross-linking enzyme lysyl oxidase varied significantly in response to increasing blood pressure. Additionally, it was revealed that gene expression, enzymatic activity, and LOX mediated collagen cross-linking, are associated with ventricular stiffness [22].

Statistics show that hypertension causes five million premature deaths worldwide each year and accounts for 13% of global fatalities. 19,250 people died from hypertension in the United States in 2001 [23]. So study of the relationships among heart collagen cross-linking, stiffness of heart ventricle, enzyme activity and gene regulations has great scientific significance with high application potential. In the present study, we aim to develop a reliable method to identify and quantify some of the important cross-linked amino acids in collagen protein using mass spectrometry. Then it allows us to compare the difference in the speciation and extent of cross-linking between the collagen proteins from hearts in different states – for example, it would let a healthy heart be differentiated from a diseased heart. Once an observed relationship between cross-linking

and diseased states is understood, the long-term focus would be to take advantage of that knowledge in order to control and cure the heart disease by chemically or biologically regulating the enzyme activities that are responsible for the cross-linking processes. This thesis will mostly focus on the development of a tandem mass spectrometry method for identification of pyridinoline (PYD) and deoxypyridinoline (DPD), two common cross-linked amino acids in collagen proteins.

Pyridinoline (PYD) has been known as the major trivalent cross-link in mature cartilage. Deoxypyridinoline (DPD) has been found almost exclusively in bone collagen [24]. Most literature focuses on their use as biomarkers in collagen metabolism; specifically their detection in urine has been used to monitor bone diseases [25]. However, the role of PYD and DPD in heart collagen is not well understood; the initial motivation for the present research is to determine this role. This is a collaborative research project with Dr. Larson's group at the University of Arizona Saver Heart Center. All collagen samples extracted from mouse are provided by the Larson group. The author is responsible for the majority of method development and sample analysis.

3.2 Experimental

Reagents

Pyridinoline (PYD) and deoxypyridinoline (DPD) were purchased from Quidel (San Diego, CA). Collagen Type I rat tail was purchased from BD Biosciences (Bedford, MA). HPLC grade methanol, H_2O, acetonitrile, acetic acid, Trifluoacetic acid (TFA) were purchased from Sigma-Aldrich (St. Louis, MO).

Sample Preparation

Extraction, purification and hydrolysis of mouse ventricle collagen is performed by Larson group. The procedure is described briefly below.

Isolation of Collagen

Mice were anesthetized with isoflurane and sacrificed using cervical dislocation. Hearts were dissected out and a dissecting microscope was used to remove atria, valves, right ventricle, and papillary muscles. The hearts were weighed and immediately the left ventricles were put into a 1.5 mL tube of cold 0.1M NaOH in a 2 mL tube. Left ventricles were minced with scissors as thoroughly as possible. The mixture was pipeted into a larger tube and 10 volumes of cold NaOH was added. After 24 hours at 4 ^{0}C, collagen was removed from mixer and was ultracentrifuged for 20 minutes at 10,000 RPM. Supernatant was removed and collagen was put into a 20 mL tube with 10 volumes of cold 0.1 M NaOH. The mixer was put in the cold room (4 °C) for another 24 hours. After the final wash, the supernatant was poured off and the collagen was transferred to a 2 mL tube, and 1 mL cold nanopure water was added. Then it was vortexed and spined for 10 minutes at 10,000 RPM, 4° C in a microcentrifuge and washed with water for three more times. The collagen sample was stored at -20 ^{0}C.

Borohydride Reduction of Collagen

The collagen sample was weighed. A weight of $NaBH_4$ equal to 1% of the sample weight was dissolved in 0.0001 M NaOH. The $NaBH_4$/NaOH mixture was added to sample and let it sit out at room temperature for 3 hours with mixing occasionally. Glacial acetic acid was added to the sample (only a couple of drops until it begins to bubble) until pH reached about 2. Then it was spined for 10 minutes at 10,000 RPM, 4° C,

and the supernatant was removed. 1 mL nanopure H_2O was added, and then it was vortexed, spined again and washed for two more times. Samples were transferred to scintillation vials and lyophilized with speedvac.

Acid Hydrolysis of Collagen

1 mL of 6 N HCl was added to 5 mg of sample. The mixture was put in oven at 110° C for 24 hours. Then the hydrolyzed sample was put in a -20° C freezer.

Low-Energy Collision-Induced Dissociation (CID)

Low-energy CID experiments were performed on an Applied Biosystem Q-trap 4000 mass spectrometer (Foster City, CA) with a nanospray ionization source using the positive ion mode (Section 1.2.2). PYD and DPD standard were diluted 10 times using MeOH:H_2O (70:30 v/v). Two hundred microliters of MeOH:H_2O (70:30 v/v) was added into hydrolyzed collagen samples, and the mixture was then sonicated and centrifuged, and the supernatant was taken out for dilution and further analysis. The sample solutions were then sprayed into the mass spectrometer with a flow rate of approximately 2.0 μL/min. The applied ionization voltage was between 2.0 kV and 2.2 kV, and the capillary temperature was maintained at 200^{o}C. Nitrogen served as the collision gas, and a laboratory collision energy of 25 to 45 eV was used. The pressure in collision cell is maintained about 8 millitorr in MS/MS experiments. Unit mass of the monoisotopic precursor ion was selected in order to avoid ambiguities from isotope contributions.

The intact collagen protein analysis was performed with a LC-MS system based on a micro Q-TOF mass spectrometer (Manchester, UK). The LC column is a C4 revered

phase column (Micro-Tech Scientific, Vista, CA). The mobile phases in HPLC used were water and acetonitrile, both of which contain 0.05 % of TFA.

3.3 Results and Discussion

3.3.1 Fragmentation Spectra of PYD and DPD

PYD and PDP have very similar chemical structure (Figure 3.2), and their molecular ion peaks appear at m/z = 429 and m/z = 413 in a MS spectrum (data not shown).

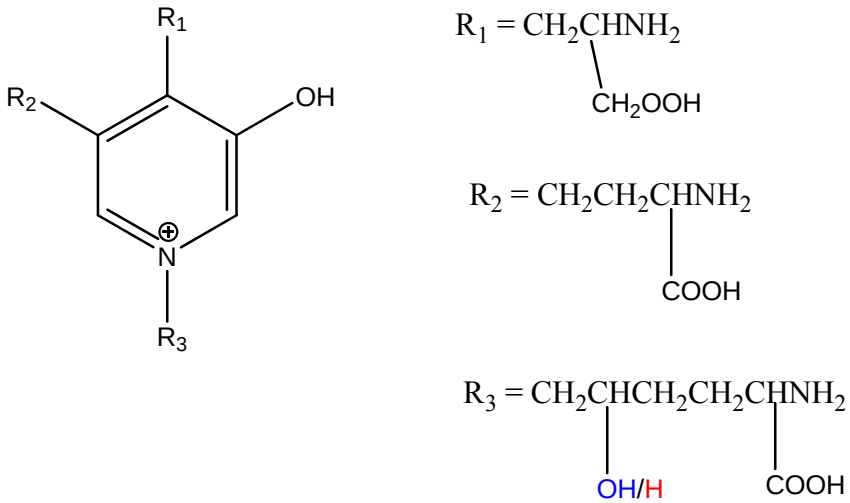

FIGURE 3.2. Chemical Structures of pyridinoline (PYD) and deoxypyridinoline (DPD). They naturally exist as cations.

The MS/MS spectrum of PYD cation is shown in Figure 3.3a. The molecular ion shows up at m/z = 429. Upon activation, several fragmentation pathways have been observed. First, a neutral loss of ammonia (17 Da) leads to a fragment ion at m/z = 412. The cleavage of N-alkylated R_3 side chain (R_3 + 16 Da) forms the fragment ion at m/z = 267. A water loss of m/z = 267 ion produces the fragment ion at m/z = 249. The fragment ion at m/z = 146 is the R_3^+ ion. The m/z = 128 ion is the product of water loss (18 Da) of R_3^+ ion, and the m/z = 100 is the product of HCOOH (46 Da) loss of R_3^+ ion, and finally the m/z = 82 is the [H_2O+HCOOH] neutral loss of R_3^+ ion.

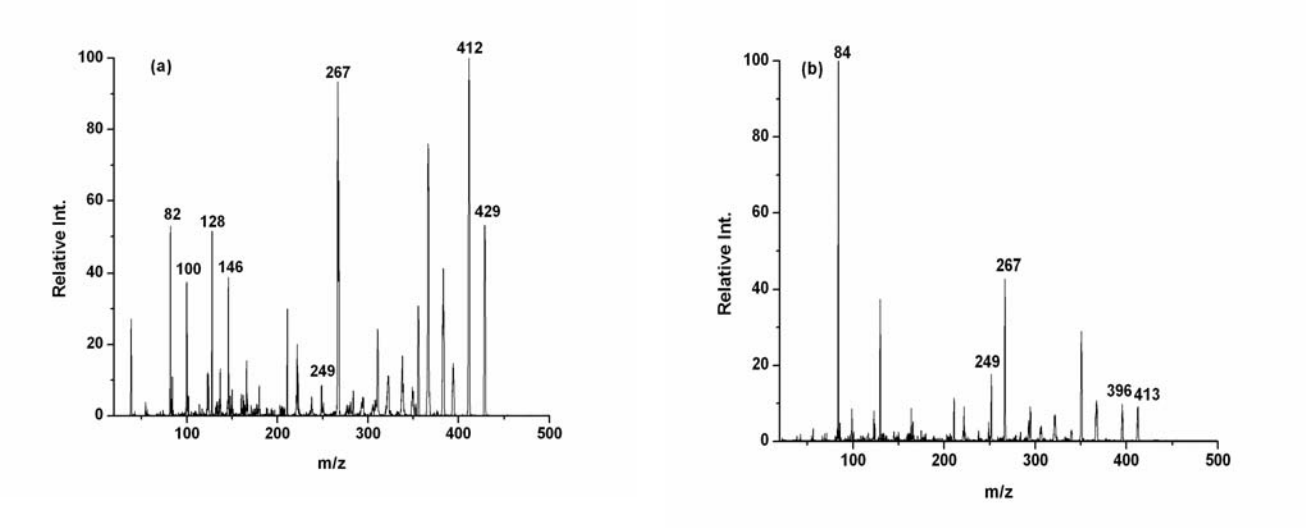

FIGURE 3.3. MS/MS spectra of a) pyridinoline (PYD) and b) deoxypyridinoline (DPD). N_2 is used as collision gas, and the collision energy is 45 eV.

The MS/MS spectrum of DPD cation is shown in Figure 3.3b, whose molecular ion appears at m/z = 413. DPD undergoes the similar fragmentation pathways to PYD. Briefly, an ammonia (17 Da) neutral loss leads to the product ion at m/z = 396. There is also an R_3^+ fragment ion (m/z = 146) formed, followed by a HCOOH (46 Da) loss to form a product ion at m/z = 84. It is very worth noting that DPD also shows the N-alkylated R_3 side chain cleavage and the following water loss, leading to the formation of m/z = 267 and m/z = 249 ions, which is identical to that in PYD.

Comparing the fragmentation spectra of PYD and DPD, we can see that PYD and DPD undergo similar fragmentation pathways. The fragmentation pathway of DPD is simpler, because DPD does not have an OH group on R_3 side chain (Figure 3.2), and thus it cannot perform as many H_2O losses as PYD.

3.3.2 Precursor Ion Scan MS Spectra of PYD and DPD

Precursor ion scan mode of a triple quadrupole mass spectrometer is a very powerful tool when used to identify a target molecule from a complex mixture. Precursor ion scan fixes the DC and RF of Q3 to ensure that only a fragment ion of a particular m/z value will be detected. Q1 scans to transmit the ions with a range of m/z values into the collision cell. Eventually, only the ions that produce that specific fragment ion will show up in the resulting spectrum (Section 1.2.2). In the present study, the hydrolyzed collagen samples contain a mixture of amino acids and cross-linked amino acids. Since it is very difficult to purify PYD and DPD from the mixture by normal HPLC or other separation techniques, precursor ion scan mode is suitable to identify PYD and DPD in the mixture if there are any present.

The fragmentation behaviors of PYD and DPD are similar, and more importantly, they both generate the fragment ion at m/z = 267. This peak can be used as the fingerprint peak for either the PYD or DPD cross-links in precursor ion scan experiments, because the formation of this peak involves the opening of the ring structure, which is more unique than other fragmentation pathways like H_2O or NH_3 neutral loss. And another advantage of choosing this peak instead of others is that it allows for the identification of PYD and DPD in one measurement. The precursor ion scan MS spectrum of the PYD and DPD standard is shown in Figure 3.4. Two peaks at m/z = 429 and 413 rise up in the spectrum almost exclusively, corresponding to PYD and DPD respectively. The exclusiveness of those two peaks indicates that the selectivity of the precursor ion scan of m/z = 267 is very high, and the interference from other ions is small. However, it is noticeable that there are still signals although very weak from other precursor ions, such as m/z = 423 and 388, implying that it could be a potential problem for the hydrolyzed

mouse ventricle collagen, because the concentration of PYD and DPD is expected to be significantly lower than that in the PYD and DPD standard, thus the contaminant effect could be greater, which will lower the selectivity of the method.

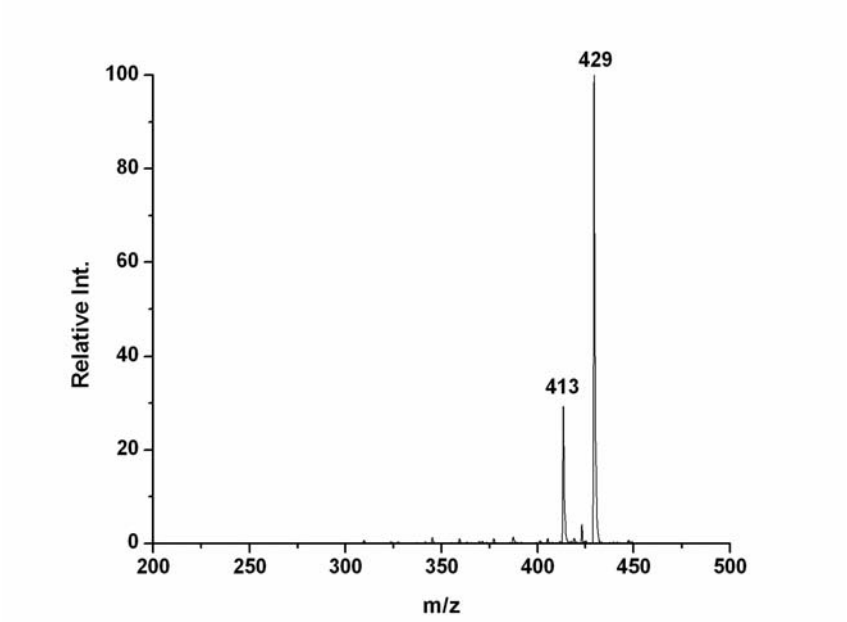

FIGURE 3.4. The precursor ion scan MS spectrum of PYD and DPD standard. Q1 is scanning to transmit all the ions formed at the ESI source, and Q3 is fixed at m/z = 267. N_2 is used as the collision gas, and the collision energy is 45 eV.

To find the best fingerprint fragment ion for detection of PYD and DPD, we also tested other peaks in precursor ion scan experiments: the smallest product ions of PYD and DPD that are m/z = 82 and m/z = 84, respectively (Figure 3.2). Another necessity to test the performance of the precursor ion scan of those two product ions lies in the fact those two ions are part of the lysine/hydroxylysine residue (Figure 3.2), so other cross-linked amino acids might also be able to generate those two product ions upon fragmentation. So those two peaks (m/z = 82 and 84) might be used as fingerprint peaks for identification of more cross-linked amino acids besides PYD and DPD.

The precursor ion scan MS spectra of m/z = 84 and 82 for the PYD and DPD standard are shown in Figure 3.5. In the precursor ion scan of m/z = 84 (Figure 3.5a), a strong peak appears at m/z = 413, meaning that DPD contributes most to the formation of the m/z = 84 peak. However, a group of peaks in the lower mass range (m/z = 180 ~ 240) also show a relatively strong intensity. And a small peak at m/z = 429 can be observed too, which implies that the method is not selective enough. The similar situation is true for the precursor ion scan of m/z = 82 (Figure 3.5b). Besides the strongest signal at m/z = 429 for PYD, other peaks can be also observed including a small peak at m/z = 413. The group of peaks in the lower mass range does not belong to any of the fragmentation peaks from PYD or DPD (Figure 3.5 and 3.3), which excludes the possibility of secondary fragmentation leading to the formation of m/z = 84 and 82 ions. The lower selectivity of the precursor ion scan of m/z = 84 or 82 than that of m/z = 267 can be explained as the fragmentation pathway of forming m/z = 84 or 82 ion is less unique; and there is more chance to form a smaller product ion than a bigger one just by probability. The precursor ion scans of m/z = 267, 84 and 82 illustrate that m/z = 267 is the best fingerprint peak to identify PYD and DPD.

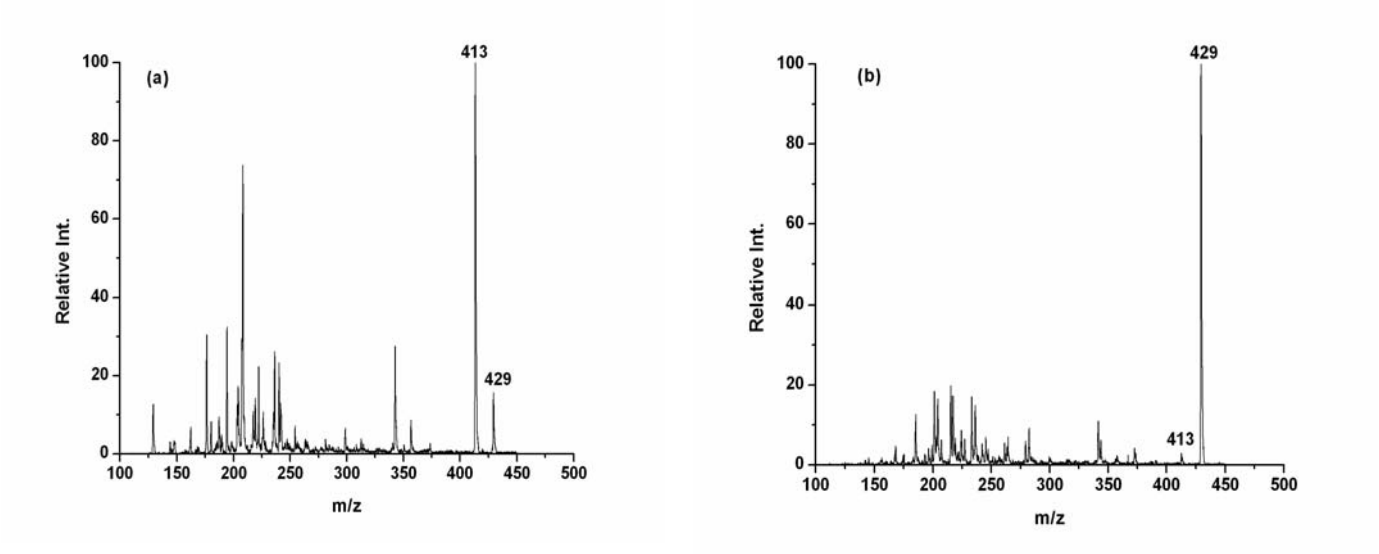

FIGURE 3.5. The precursor ion scan spectra of PYD and DPD standard. a) Q3 is fixed at m/z = 84; b) Q3 is fixed at m/z = 82. N_2 is used as the collision gas, and the collision energy is 45 eV.

3.3.3 MS Spectrum and Precursor Ion Scan for Hydrolyzed Mouse Ventricle Collagen

The hydrolyzed mouse ventricle collagen contains free amino acids and cross-linked amino acids and may contain other contaminants if the sample is not pure. The MS spectrum of the hydrolyzed collagen is shown in Figure 3.6. The MS spectrum is very noisy due to the extreme complexity of the sample. The expected peaks at m/z = 413 and 429 cannot be seen clearly (Figure 3.6a). It is noticed that there is a peak at m/z = 175 which matches the molecular ion of arginine. Compared with literature [29], the MS/MS spectrum of m/z = 175 confirms the identity of arginine (Figure 3.6b). The detection of arginine at least confirms that the sample is hydrolyzed protein, which is important because the extraction of collagen protein from a mouse ventricle is a very dedicated operation.

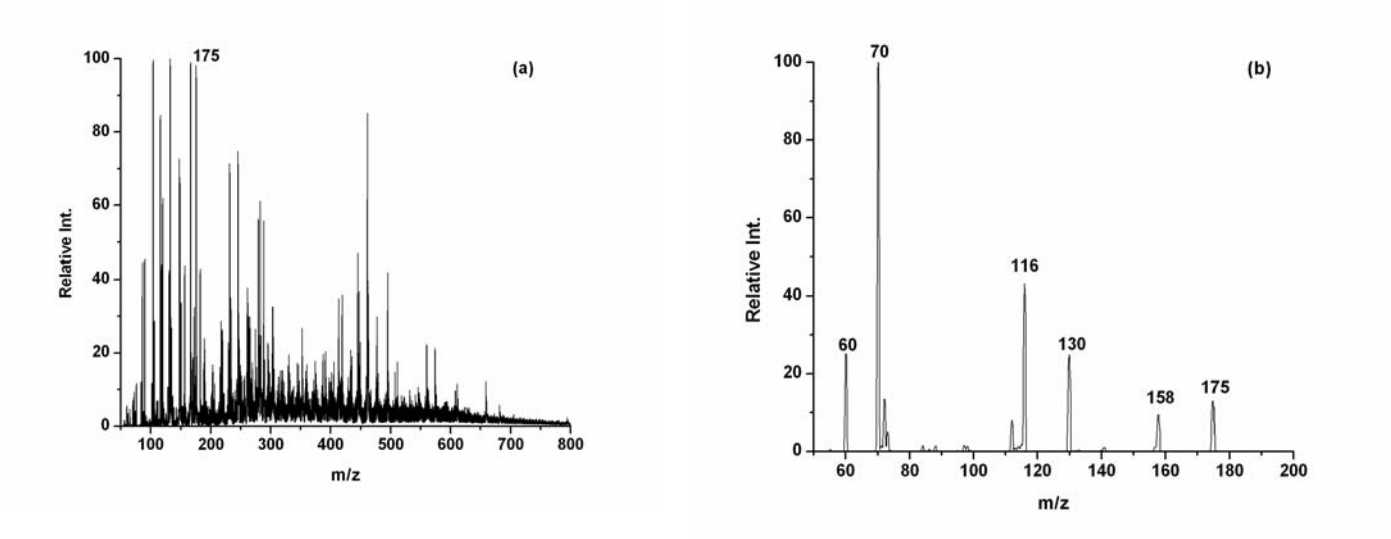

FIGURE 3.6. a) MS spectrum of hydrolyzed mouse ventricle collagen. b) MS/MS spectrum of the peak at m/z = 175 in Figure 3.6a. N_2 is used as the collision gas, and the collision energy is 25 eV.

The precursor ion scan MS spectrum of hydrolyzed mouse ventricle collagen is shown in Figure 3.7. The spectrum is not as clean as that of the PYD and DPD standard due to its complexity (Figure 3.4); nevertheless, the signal for DPD at m/z = 413 still can be observed. There is no PYD signal detected. It is not surprising that PYD cannot be detected, because PYD is found almost exclusively in bone collagen [26]. In the spectrum, there are many other peaks that can contribute to the formation of m/z = 267 ion. It is a positive sign that the signal at m/z = 413 is the highest among all peaks, which strengthens the conclusion that DPD is detected in the hydrolyzed mouse ventricle collagen.

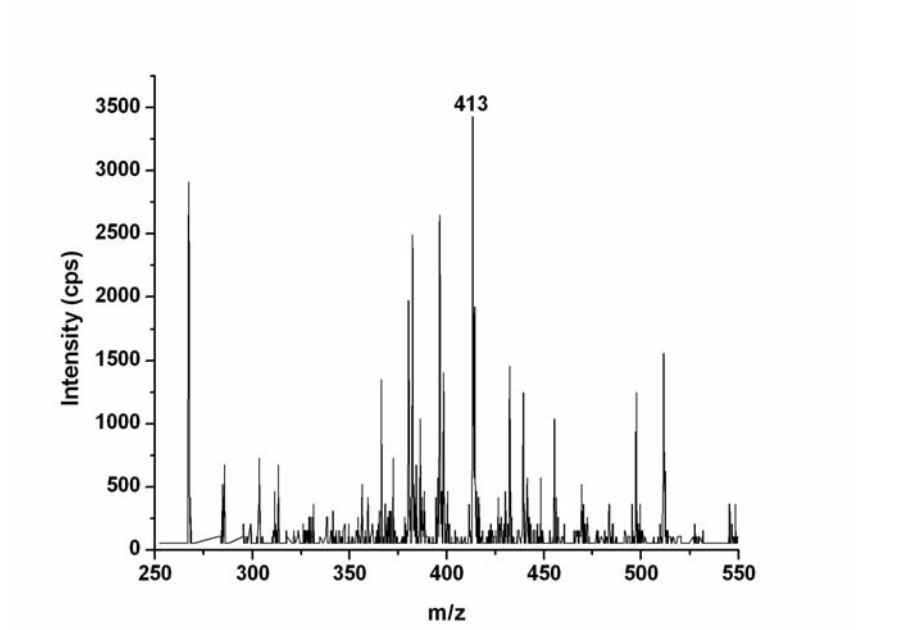

FIGURE 3.7. The precursor ion scan spectrum of hydrolyzed mouse ventricle collagen. Q3 is fixed at m/z = 267. N_2 is used as the collision gas, and the collision energy is 45 eV.

Because the DPD signal intensity is not very high (~ 3200 cps), it might be thought that the signal is mostly from noise or contaminants. To ensure the reproducible signal is from the hydrolyzed mouse ventricle sample, the hydrolyzed mouse ventricle sample is measured multiple times on different days, and the same result is obtained (data not shown). Additionally, the same precursor ion scan experiment is performed when only MeOH:H_2O (70:30 v/v) is sprayed into the mass spectrometer. The precursor ion scan MS spectrum of solvent shown in Figure 3.8. In the spectrum, no signal is present at m/z = 413, and more importantly, the signal intensity is only about 300 cps. The comparison between the hydrolyzed sample and solvent background further confirms that the signals detected, especially the DPD's response at m/z = 413 in Figure 3.7, are indeed from the hydrolyzed mouse ventricle sample.

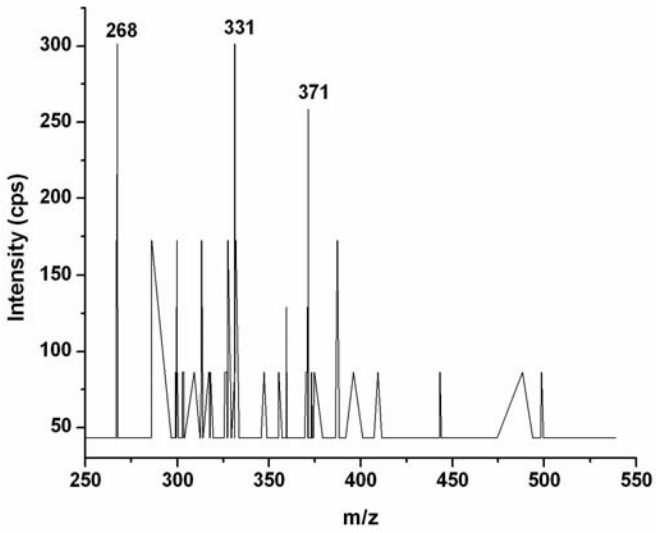

FIGURE 3.8. The precursor ion scan spectrum of solvent. Q3 is fixed at m/z = 267. N_2 is used as the collision gas, and the collision energy is 45 eV.

3.3.4 LC-MS Analysis of Intact Type I Rat Tail Collagen

One of the major objectives of the present research project is to study the structure and quantification of cross-linked amino acids in heart collagen. Besides examining the cross-linked amino acids PYD and DPD as discussed previously, we also tried to solve the problem by analyzing intact collagen protein, which could possibly also provide some useful information about the cross-linking in collagen protein. This section will focus on some LC-MS results obtained for Type I rat tail collagen, a model system for mouse ventricle collagen. Both rat tail collagen and mouse ventricle collagen are composed of three coiled α chains, two of which are identical called α(1), and the other is called α(2). Theoretically in an LC-MS experiment, the protein is denatured when eluting out the column with the mobile phase solvents, therefore the mass spectrometer is expected to detect the single α chains, as well as di-cross-linked dimers (β) and tri-cross-linked trimers (γ) with molecular weights expected to be roughly 100 kDa, 200 kDa and 300

kDa, respectively. The goal is to determine if these species can be well separated, and if so, the corresponding peak intensities can be used to reveal some quantitative information about the species present. This method can be used to characterize the extent of cross-linking of collagen, although it cannot provide the information about what cross-links are involved.

The chromatogram from an LC-MS run of rat tail collagen as shown in Figure 3.9a has several distinct peaks. By examining the mass spectrum under each chromatogram peak, we can get the molecular weight information of the corresponding species. The mass spectrum of peak 1 is shown in Figure 3.9b. The multiple charged peaks reveal that the molecular weight is about 95 kDa that matches the mass of one single α chain. However, when exploring the mass spectra under other chromatogram peaks, the MS spectra appear to be irresolvable, which is probably due to the fact that the complex mixture are not well separated by HPLC. At present, we think the mixtures contain dimers and trimers, but they cannot be well separated by HPLC. Previous studies [27] also demonstrated the difficulties of separating denatured collagen proteins by HPLC due to the similarity of the hydrophobicity of the dimer and trimer.

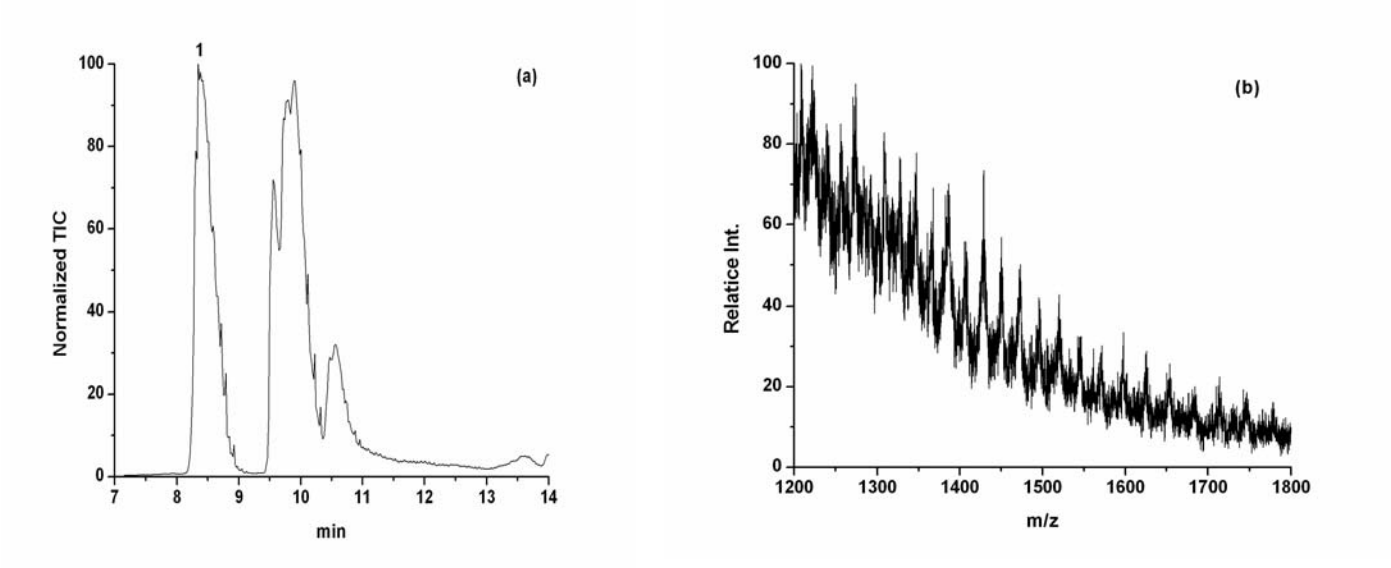

FIGURE 3.9. a) Liquid Chromatogram of rat tail collagen protein; b) Mass spectrum of peak 1 in Figure 3.9a.

The detection of single α chains suggests that the collagen protein has been denatured in HPLC run, to some extent. Literature [28] shows that heating would help completely denature the collagen protein. To test this, the heated rat tail collagen (60^0C, 1 hour) was also analyzed by LC-MS under the same condition as the unheated protein. The chromatogram is shown in Figure 3.10a. The chromatogram shows more peaks than that of unheated collagen proteins, which indicates that heating may further denature the protein and produce more species. However, only the MS spectrum of peak 1 is resolvable showing that the molecular weight is about 95 kDa corresponding to α chains (Figure 3.10b).

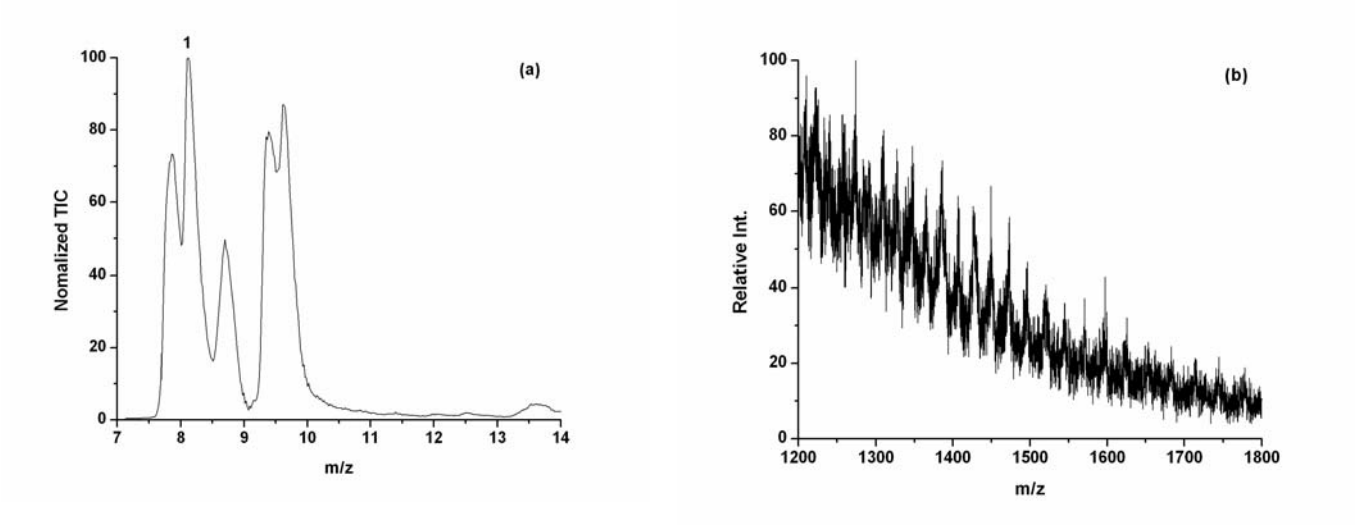

FIGURE 3.10. a) Liquid Chromatogram of heated rat tail collagen protein; b) Mass spectrum of peak 1 in Figure 3.10a.

We also tried to analyze the mouse ventricle collagen extracted from mouse heart by LC-MS method described above. However, the sample contains undissolvable white pieces even after heating, which is suspected to be mouse ventricle collagen, because it is known that mouse ventricle collagen may have lower water solubility than rat tail collagen due to its higher level of cross-linking. The supernatant of the sample does not show any protein or peptide signal in the LC-MS analysis. To examine whether the supernatant contains any protein and check the complexity of the rat tail collagen, 1D gel electrophoresis was used to analyze the protein samples (Figure 3.11). The blank lanes of 8 and 9 indicate that there is no detectable protein in the supernatant of the sample. This does not necessarily mean the extraction procedure had failed, because amino acids and DPD have been detected in the hydrolyzed mouse ventricle sample. Clearly, a way to introduce the undissolvable mouse ventricle collagen into solution phase in future LC-MS measurements must be determined. All the rat tail collagen protein samples show

many bands in a wide mass range, indicating complexity of the rat tail collagen protein samples, which makes it more difficult for HPLC to separate them efficiently.

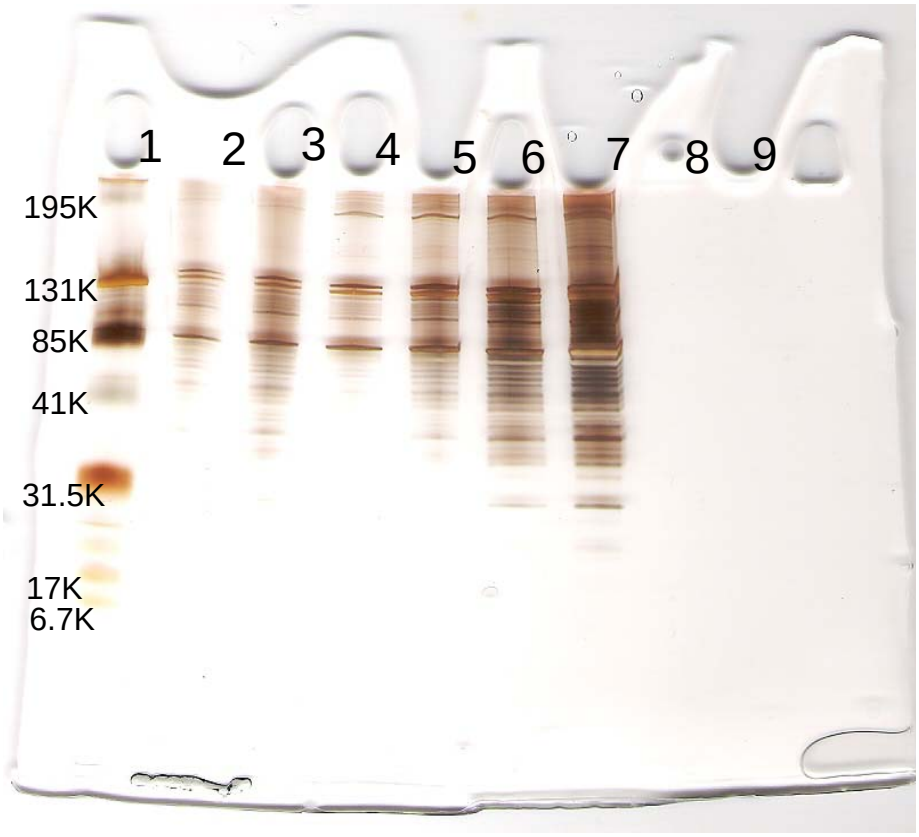

FIGURE 3.11. 1D gel electrophoresis of collagen proteins. Lane1 Standard 2 µL; Lane2 Rat Tail Collagen (powder) 10 µL;Lane3 Rat Tail Collagen (powder) 20 µL; Lane4 Rat Tail Collagen (solution) 10 µL; Lane5 Rat Tail Collagen (solution) 20 µL; Lane6 Heated (60^0C 1h)Rat Tail Collagen (solution) 10 µL; Lane7 Heated (60^0C 1h)Rat Tail Collagen (solution) 20 µL; Lane8 Mouse Ventricle 10 µL; Lane9 Mouse Ventricle 20 µL. * Powder means the sample was purchased as powder, and solution means the sample was purchased as solution.

3.4 Conclusions and Future Directions

The fragmentation patterns of pyridinoline (PYD) and deoxypyridinoline (DPD) are investigated in the study. Based on the MS/MS spectra of PYD and DPD, m/z = 267 ion is chosen to be the fingerprint peak for the identification of PYD and DPD. Precursor ion scan of m/z = 267 is applied to identify PYD and DPD from a mixture. This precursor ion scan mode shows high selectivity for PYD and DPD. We have successfully detected DPD

in the hydrolyzed mouse ventricle collagen, but PYD is not detected. LC-MS is applied to examine the intact collagen protein. The denatured rat tail collagen protein or subunits can be separated by HPLC into several subgroups, but only α chains can be identified by MS at this stage.

In the future, we need to figure out how to introduce the undissolvable mouse ventricle collagen into solution phase, and then we can employ LC-MS or other separation techniques to study the intact mouse ventricle collagen. Our group has started to digest the mouse ventricle collagen sample by various enzymes, and use an LC-MSMS method to analyze the peptides. Recent work has shown potential to be a plausible method to study the mouse ventricle collagen. Meanwhile, we would like to develop methods to detect more cross-linked amino acids besides PYD and DPD. More cross-linked amino acid standards are desired to study their fragmentation patterns and set up corresponding precursor ion scan modes for them. In general, a better extraction and enrichment method for mouse ventricle collagen is likely to considerably improve the ability to analyze the sample via mass spectrometric analyses.

REFERENCES

(1) Boot-Handford, R.P.; Tuckwell, D.S. Fibrillar collagen: the key to vertebrate evolution? A tale of molecular incest. *Bioessays* **2003**, *25*, 142-151.

(2) Dreisewerd, K.; Rohlfing, A.; Spottke, B.; Urkanke, C.; Henkel, W. Characterization of Whole Fibril-Forming Collagen Proteins of Type I, III and V from Fetal Calf Skin by Infrared Matrix-Assisted Laser Desorption Ionization Mass Spectrometry. *Anal. Chem.* **2004**, *76*, 3482-3491.

(3) Bornstein, P. Covalent Cross-links in Collagen: a Personal Account of Their Discovery. *Matrix Biol.* **2003**, *22*, 385-391.

(4) Veis, A. Characterization of Soluble Collagens by Physical Techniques. In: Cunningham, L.W.; Frederiken, D.F. editors. *Methods in Enzymology.* Academic Press, New York, 1982.

(5) Miller, E.J.; Matukas, V.J. Chick Cartilage Collagen: A New Type of 1 Chain Not Present in Bone or Skin of the Species. *Proc. Natl. Acad. Sci. USA.* **1969**, *64*, 1264-1268.

(6) Cheung, E.; Miller, E.J. Collagen Polymorphism, Characterization of Molecules with the Chain Composition [alpha-1(III)]$_3$ in Human Tissues. *Science* **1974**, *183*, 1200-1201.

(7) Epstein, E.H. Jr. [α-1(III)]$_3$ Human Skin Collagen. *J. Biol. Chem.* **1974**, *249*, 3225-3231.

(8) Miller, E.J. Collagen. In: Cunningham, L.W.; Frederiksen, D.F. editors. An Overview Method of Enzymology. Academic Press, New York, 1982.

(9) Benya, P.D. Two-dimensional CNBr Peptide Patterns of a Collagen Type I, II and III. *Coll. Res.* **1981**, *1*, 17-26.

(10) Bailey, A.J.; Paul, R.G.; Knott, L. Mechanisms of maturation and ageing of collagen. *Mech. Ageing Dev.* **1998**, *106*, 1-56.

(11) Eyre, D.R.; Paz, M.A.; Gallop, P.M. Cross-linking in Collagen and Elastin. *Annu. Rev. Biochem.* **1984**, *53*, 717-748.

(12) Robins, S.P. Fibrillogenesis and Maturation of Collagen. In: Seibel, M.J.; Robins, S.P.; Bilezikian, J.P. editors. *Dynamics of Bone and Cartilage Metabolism.* Academic Press, London, 1999.

(13) Deshmukh, A.; Deshmukh, K.; Nimni, M.E.; Synthesis of Aldehydes and Their Interactions during the in vitro Aging of Collagen. *Biochemistry*, **1971**, *10*, 2337.

(14) Eyre, D.R.; Wu, J.J. Collagen Cross-links. *Top Curr. Chem.* **2005**, *247*, 207-229.

(15) Watts, N.B. Clinical utility of biochemical markers of bone remodeling. *Clin. Chem.* **1999**, *45*, 1359-1368.

(16) Christenson, R.H. Biochemical markers of bone metabolism: An overview. *Clin. Biochem.* **1997**, *30*, 573-593.

(17) Delmas, P.D. Biochemical Markers of Bone Turnover. *J. Bone Miner. Res.* **1993**, *8*, S549-S555.

(18) Bank, R.A.; teKoppele, J.M.; Janus, G.J.; Wassen, M.H.; Pruijs, H.E.; Van der Sluijs, H.A.; Sakkers, R.J. Pyridinium cross-links in bone of patients with osteogenesis imperfecta: Evidence of a normal intrafibrillar collagen packing. *J. Bone. Miner. Res.* **2000**, *15*, 1330-1336.

(19) Lohmander, L.S.; Atley, L.M.; Pietka, T.A.; Eyre, D.R. The release of crosslinked peptides from type II collagen into human synovial fluid is increased soon after joint injury and in osteoarthritis. *Arthritiss Rheum* **2003**, *48*, 3130-3139.

(20) Weber, K.T. Cardiac Interstitium in Health and Disease: the Fibrillar Collagen Network. *J. Am. Coll. Cardiol.* **1989**, *13*, 1637-1652.

(21) Yu, Q.; Waston, R.R.; Marchalonis, J.J.; Larson, D.F. A Role for T Lymphocytes in Mediating Cardiac Diastolic Function. *Am. J. Physiol. Heart Circ. Physiol.* **2005**, *289*, H643-H651.

(22) Yu, Q; Horak, K.; Larson, D.F, Role of T Lymphocytes in Hypertension-induced Cardiac Extracellular Matrix Remodeling. *Hypertension* **2006**, *48*, 98-104.

(23) http://www.wrongdiagnosis.com/h/hypertension/stats.htm#death_and_mortality_stats Accessed on Jan 10th, 2008.

(24) Robins, S.P. Functional-properties of Collagen and Elastin. *Bailliere's Clin. Rheumatol.* **1988**, *2*, 1-36

(25) Black, D.; Duncan, A.; Robins, S.P. Quantitative-analysis of the Pyridinium Crosslinks of Collagen in Urine Using Iin-paired Reversed-Phase High Performance Liquid-Chromatography. *Anal. Biochem.* **1988**, *169*, 197-203.

(26) Rafferty, T.L.; Gallagher, R.T.; Derrick, P.J.; Heck, A.J.R.; Duncan, A.; Robins, S.P. Low- and High-energy Collision-induced Dissociation of Pyridinoline and Deoxypyridinoline Ions Using Fourier Transform Ion Cyclotron Resonance Electrospray and Liquid Secondary-ion Magnetic Sector Mass Spectrometry. *Int. J. Mass Spec. and Ion Proc.* **1997**, *160*, 377-386.

(27) Bateman, J.F.; Mascara, T.; Chan, D.; Cole, W.G. Rapid Fractionation of Collagen Chains and Peptides by High-performance Liquid-Chromatogrphy. *Anal. Biochem.* **1986**,*154*, 338-344.

(28) Kim, S.H.; Lee, J.H.; Yun, S.Y.; Yoo, J.S.; Jun, C.H.; Chung, K.Y.; Suh, H. Reaction monitoring of succinylation of collagen with matrix-assisted laser desorption/ionization mass spectrometry. *Rapid Commun. Mass Spectrom*. **2000**, *14*, 2125-2130.

(29) Shek, P.Y. I.; Zhao, J.; Ke, Y.; Siu, K.W.M.; Hopkinson, A.C. Fragmentations of Protonated Arginine, Lysine and Their Methylated Derivatives: Concomitant Losses of Carbon Monoxide or Carbon Dioxide and An Amine. *J. Phys. Chem. A* **2006**, *110*, 8282-8296.

Chapter 4

CONSTRUCTION OF A DESI SOURCE AND ITS APPLICATION IN PEPTIDES AND PROTEINS ANALYSIS

4.1 Introduction

The development of soft ionization such as electrospray (ESI) and matrix-assisted laser desorption/ionization (MALDI) has expanded the application of mass spectrometry into the analysis of large biomolecules (Section 1.2.1). However, time-consuming sample preparation is often required for ESI-MS or MALDI-MS, because they are not suitable for the analysis of samples directly under ambient conditions.

Novel ambient techniques that require minimal sample preparation include direct analysis in real time (DART) [1] and atmospheric solid analysis probe (ASAP) [2]. However, they are not capable of ionizing high molecular weight biomolecules. Recently, the desorption electrospray ionization (DESI) technique emerged to allow the analysis of samples including larger biomolecules directly from a surface under ambient conditions [3]. In DESI-MS, a fine spray of charged droplets formed under high electric field hits the surface of interest, where it extracts small organic molecules or large biomolecules, ionizes them, and delivers the ions into the mass spectrometer (Figure 4.1).

Since its introduction, the use of DESI-MS has been reported in many research fields. One is the analysis of explosives from surfaces that are common in possession of air passengers, like TNT [5]. Pharmaceuticals like drug tablets and soft creams have also been analyzed [6]. Metabolites have also been analyzed by DESI-MS because DESI has the ability to detect analytes from a complex matrix without losing time-sensitive

information during sample preparation [7]. In addition to being coupled with mass spectrometry, DESI has also been coupled with thin-layer chromatography (TLC) [8] and ion mobility spectrometry [9]. More recently, more attention has been paid to analysis of peptides, proteins, and protein complexes by DESI, because this is an important component of proteomic research, including protein identification, post-translational modification, etc. There are literature reports on the DESI analysis of peptides and proteins [10, 11], intact biological tissues [12] and enzyme-substrate complexes [13]. However, there are still problems for protein analysis by DESI, for example, it has not been successful to ionize very large proteins (> 100 kDa), and how to increase the signal-to-noise ratio is another challenge.

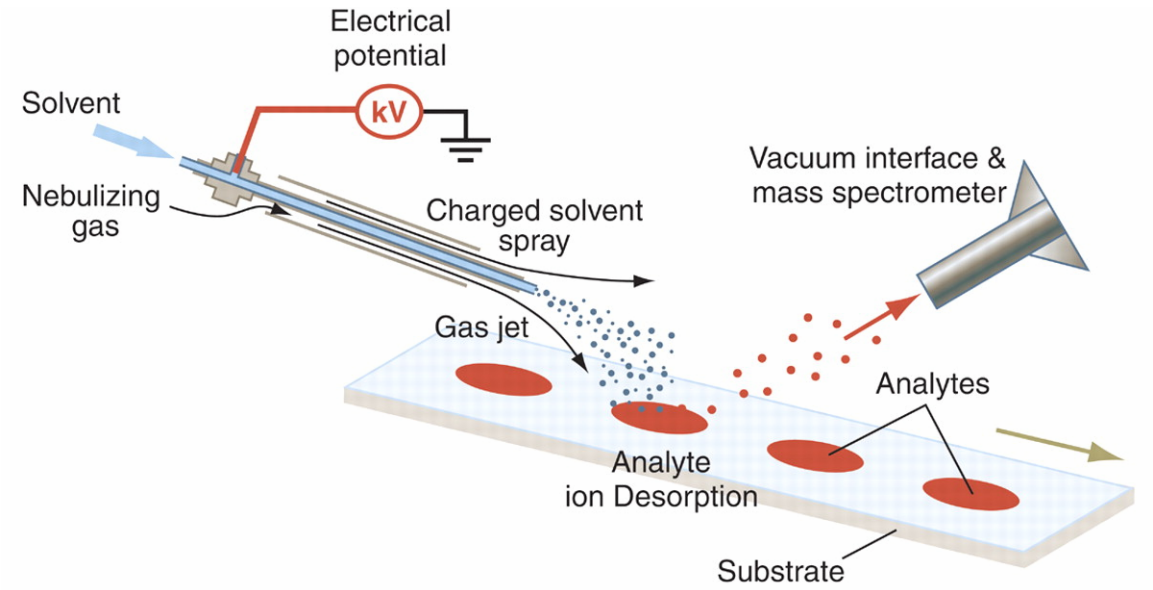

FIGURE 4.1. A diagram of desorption electrospray ionization source (Figure from reference [4] with permission).

As more and more applications of DESI have been developed, it is necessary to better understand the fundamental mechanism of the DESI process. Several mechanisms have been proposed. One is called “chemical sputtering”, which refers to charge and momentum transfer during reactive projectile/surface collisions. It hypothesizes that

compounds with a high vapor pressure may react with free ions above the surface or with the droplet close to the surface and become incorporated into the liquid droplet [14, 15]. Another model is referred to as the "droplet pick-up" model. It is believed that droplet pick-up occurs during the brief contact time when droplets collide with the sample surface and analytes are extracted into the leaving liquid droplets. After droplet pick-up, ionization happens through the common ESI process, i.e. charge residue model (CRM) or ion evaporation model (IEM) (Section 1.2.1) [15]. It is generally believed that ionization of peptides and proteins is accounted for by the "droplet pick-up" model, while low mass compounds may be ionized by "chemical sputtering". However, a more recent study shows that chemical sputtering cannot take place because the velocity of the droplet that is less than 200 m/s is not high enough to cause the chemical sputtering [16]. So far, there is not a perfect model available to describe the DESI process.

In the present study, we aimed to build a DESI source and couple it to a mass spectrometer. We used the home-built DESI source to successfully ionize several peptides and proteins. Then we planed to couple DESI-MS to a surface based separation technique to characterize the separated proteins in a timely fashion. We also investigated the surface effect on the signal intensity. Finally, we compared the MS spectra obtained by DESI and ESI to shed some light on the mechanism of DESI. In all, the present study tries to improve the fundamental understanding of DESI and its application in peptide and protein analysis.

4.2 Experimental

Materials

All peptide and protein standards were purchased from Sigma-Aldrich (St. Louis, MO) and used without further purification. Methanol, water, acetic acid (AcOH) were all HPLC grade. Poly(methyl methacrylate) (PMMA) plates were purchased from Professional Plastics (Fullerton, CA). C12F10 self assembled monolayer ($CF_3(CF_2)_9(CH_2)_2SH$) on gold substrate and C16 self assembled monolayer ($CH_3(CH_2)_{15}SH$) on gold substrates were prepared according to reference [17].

DESI Source Set-up and Mass Spectrometry

The set-up of our home-made DESI source is shown in Figure 4.2. The electrospray emitter is composed of a Swagelok T-piece and two coaxial sections of fused silica capillary tubing (Polymicro Tech LLC, Phoenix, AZ). The outer capillary has an outer diameter (OD) of 360 μm and an inner diameter (ID) of 250 μm. The internal capillary has an OD of 150 μm and an ID of 50 μm. Nebulizing gas (N_2) flows through the space between the internal and outer capillary tubing. The central leg of the T-piece is connected to the N_2 tank. The pressure of the gas tank can be varied from 0 psi to 200 psi. The internal capillary tubing is extended through the T-piece and connected to a syringe pump that supplies the spray solvent to the sprayer at a rate of ~2 μL/min. The emitter end of the internal capillary tubing is extended 0.5 mm beyond the outer capillary tubing. A potential between 4 kV and 5 kV is applied from the mass spectrometer to the stainless-steel needle of the syringe. The DESI source is installed on an LCQ Deca mass spectrometer or an LTQ mass spectrometer (Thermo-Finnigan, San Jose, CA).

FIGURE 4.2. The set-up of DESI source used in the present study.

In the following DESI-MS experiments, peptides and proteins were dissolved in water with a concentration of 50 μM. Protein solutions were deposited on surfaces and dried slowly. MeOH:H_2O:AcOH (49.5:49.5:1) was used as the spray solution. In the NanoESI-MS experiment, cytochrome c was dissolved in the spray solution to reach a concentration of 1 μM before being introduced into the mass spectrometer.

Optimum DESI-MS conditions

The positions and angles of the DESI spray were adjusted to get the strongest and long-lasting signal (Figure 4.3). The optimum conditions are listed below for a number of variables: the pressure of the gas tank is set at 140 psi; α (sprayer to surface angle) is between 50 and 60 degrees; and β (surface to MS inlet angle) is less than 10 degrees. The distance between the inner solvent capillary and the sample distance is about 1 mm; and the distance between the sample surface and the MS inlet is less than 1 mm.

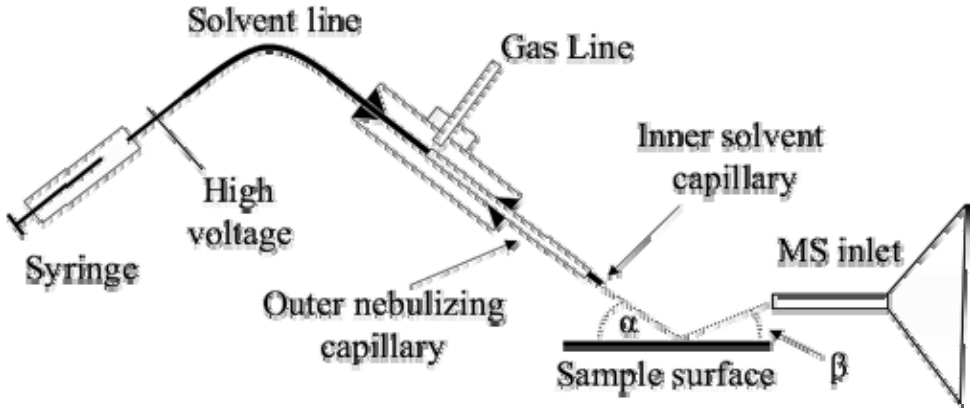

FIGURE 4.3. A diagram of DESI sprayer. (Figure from Reference [16] with permission)

4.3 Results and Discussion

4.3.1 Mass Spectra of Peptide and Proteins by DESI-MS

We evaluated the capacity of our DESI source for the detection of peptides and proteins with a series of standards ranging in molecular weight from 1 kDa to 66.4 kDa. Figure 4.4 shows the DESI mass spectra for those standards. Bradykinin (1.06 kDa), cytochrome c (12.3 kDa) and lysozyme (14.3 kDa) show well defined multiple charged patterns. (It should be noted that while bradykinin was run in he initial test, several other peptides have been tested with our DESI source, many of these are included below for the analysis of surface composition.) However, BSA (66.4 kDa) generates a poorly defined mass spectrum. The results indicated that there might be a molecular weight limitation of sample desorption and ion transfer for the current DESI design. The peak widths of those DESI-MS spectra are generally wider than normal MS spectra obtained by an ESI source. We suspect that the peak widening might be due to the solvent adducts that did not evaporate completely before the ions were delivered into the mass spectrometer.

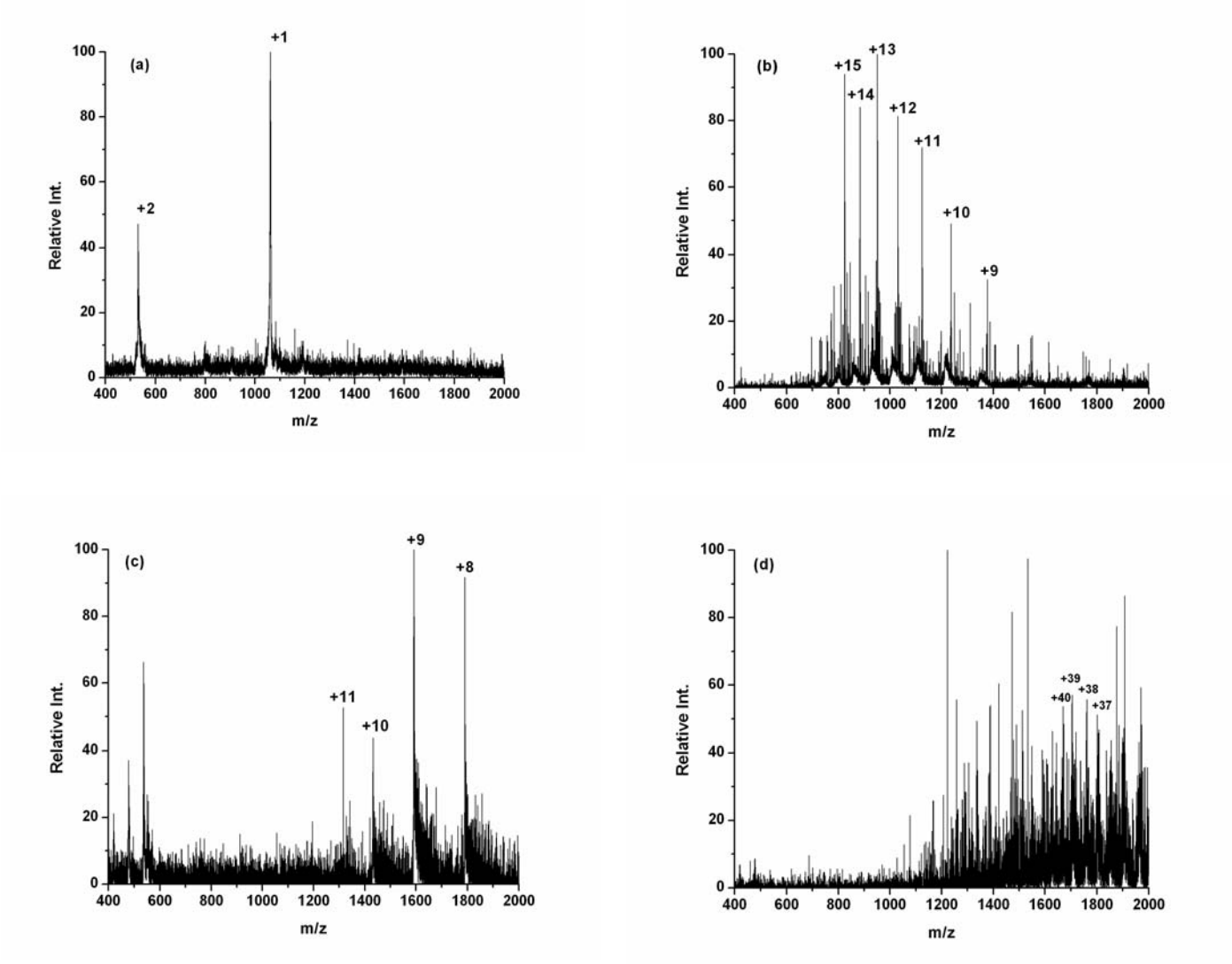

FIGURE 4.4. DESI mass spectra of intact peptide and protein standards under optimum conditions: a) bradykinin (1.06 kDa); b) cytochrome c (12.3 kDa); c) lysozyme (14.3 kDa) and BSA (66.4 kDa). The peptide and proteins (~ 1 μM) were deposited on a PMMA surface.

We also observed that the charge distribution and peak width of the DESI-MS spectra can easily change depending on the experimental conditions. Figure 4.5 illustrates how the distance between the sprayer and mass spectrometer inlet would affect the spectra quality. Figure 4.5a of cytochrome c was collected under the optimum conditions; and Figure 4.5b was collected with the sprayer and the sample surface much closer to the mass spectrometer inlet (due to the simple set-up of our DESI source, we were not able to

measure the exact distance). One significant difference is that when the sprayer and the sample surface get closer to the mass spectrometer inlet, the peak width becomes much wider. It might be because the solvent molecules did not have enough time to evaporate from the charged droplets as they entered the mass spectrometer. In addition, Figures 4.5b shows a greater abundance of lower charge state ions than Figure 4.5a. Based on ion evaporation model (IEM) of ESI (Section 1.2.1), this trend could be explained by the fact that the charge density of the droplets is lower if the droplet size is larger upon entering the MS capillary.

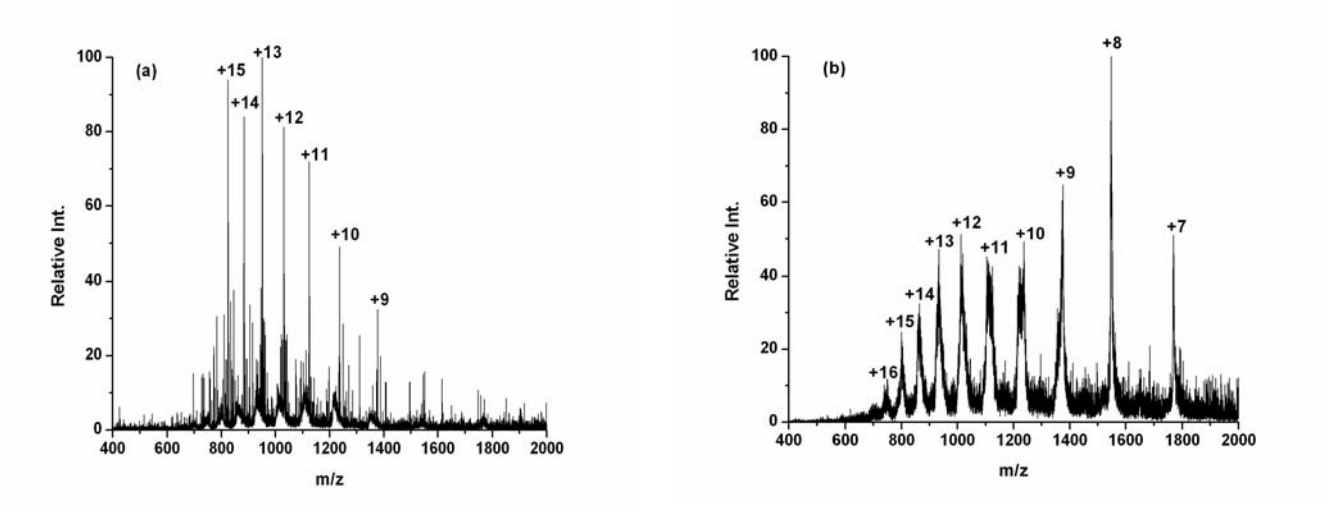

FIGURE 4.5. DESI mass spectra of cytochrome c: a) The spectrum was collected under optimum condition; b) the spectrum was collected when the sprayer and sample surface are much closer to the mass spectrometer inlet.

The differences between DESI-MS and ESI-MS were investigated by measuring cytochrome c with the two sources. Figure 4.6a and 4.6b show the DESI-MS spectrum and the NanoESI-MS spectrum of cytochrome c, respectively. It is clear that higher charged ions are dominant in the DESI-MS spectrum, and the charge distribution looks like a Gaussian distribution. However, lower charged ions are favored in the ESI-MS

spectrum, and the $[M+9H]^{9+}$ ion is dominant compared with other charged species. The comparison indicates that there might be differences in charge transfer and ion formation between DESI and ESI sources, which need further investigations.

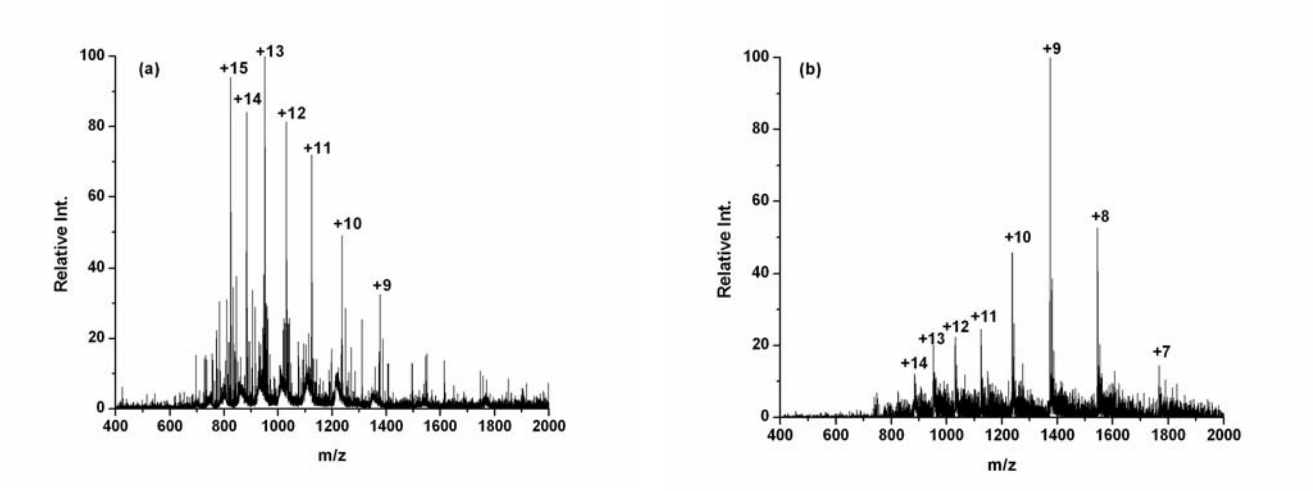

FIGURE 4.6. a) DESI mass spectrum of cytochrome c; b) NanoESI mass spectrum of cytochrome c. All mass spectrometry parameters remain the same for those two measurements.

4.3.2 Surface Effect on DESI-MS

DESI is a desorption ionization method, so the ionization process (desorption and charge transfer) can be affected by the properties of sample surfaces. We investigated the influence of surface composition on the spectra quality and ion signal in order to make the best choice of surface, as well as to improve our understanding of the mechanism of DESI ionization.

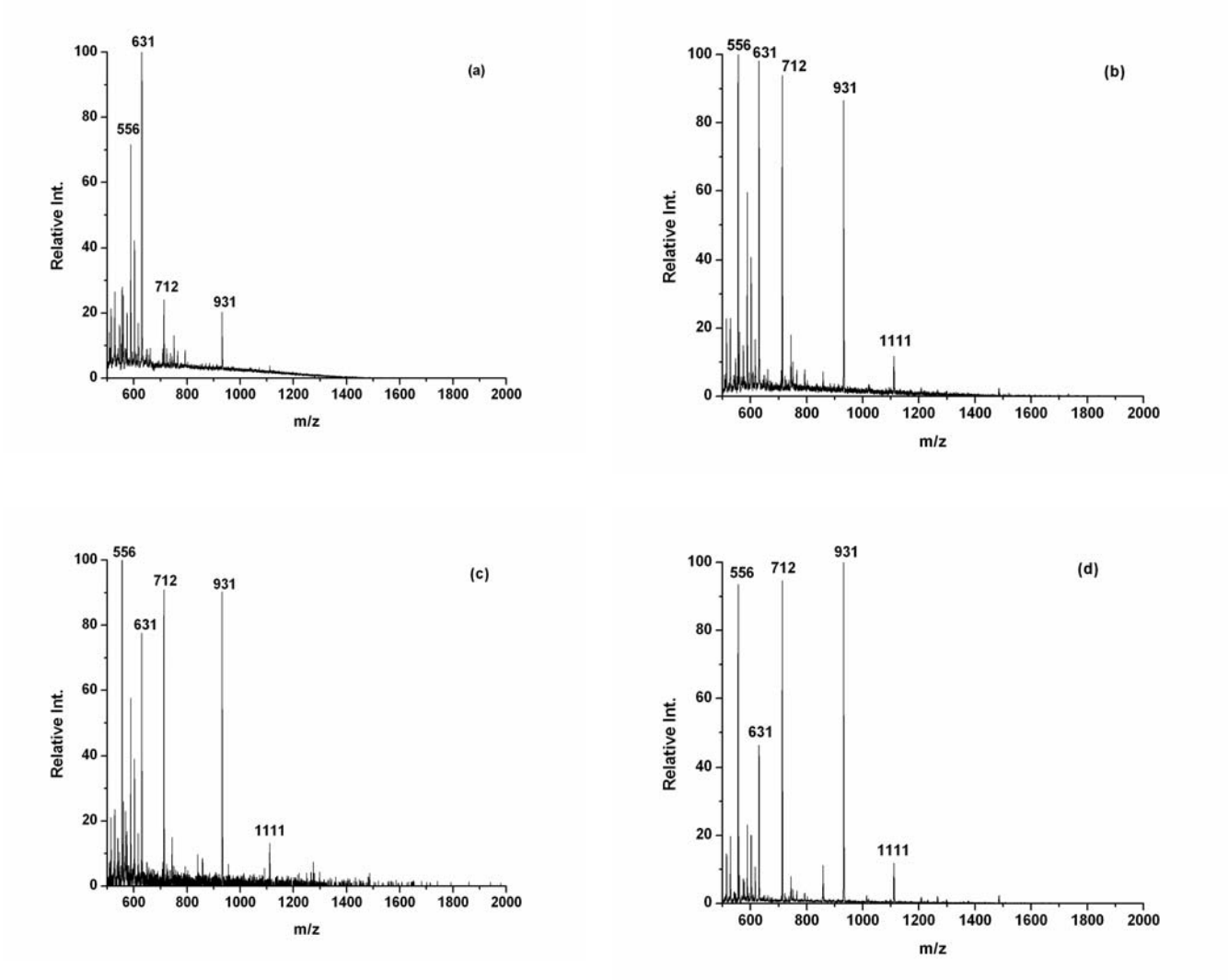

FIGURE 4.7. DESI-MS spectra of YGGFL, YGGFLR and angiotensin3 (RVYIHPF) mixture: a) bare gold; b) PMMA; c) C16 self assembled monolayer on gold; and d) C12F10 self assembled monolayer on gold.

Figure 4.7 shows the DESI-MS spectra of a peptide mixture of YGGFL (m/z =556, dimmer m/z = 1111), YGGFLR (m/z = 712) and angiotensin3 (RVYIHPF) (m/z = 931). The surfaces we used were bare gold, PMMA, a C16 self assembled monolayer (SAM) on gold and a C12F10 self assembled monolayer (SAM) on gold. All peptides can be detected from all of the four surfaces. Besides the peptide signals, we observed a peak at m/z = 631 in all cases, which is not from the sample. The m/z = 631 peak lasted during

the whole experiment and even when no sample was deposited on the surface, so we consider it as the contaminant inside the instrument that day. So we used the peak intensity ratio of YGGFLR (m/z = 712) and m/z = 631 to roughly represent the "S/N ratio" of the spectra. Figure 4.8 illustrates the ratio for the four surfaces. The "S/N ratio" increases in the order of bare gold surface, PMMA surface, C16 SAM surface and C12F10 SAM surface, implying that C12F10 SAM surface might be the better surface to assist peptide ionization in DESI-MS. The observed trend might be related to the electron transfer (neutralization) on the surface. It is believed that SAM films provide an insulating layer that reduces electron transfer from the gold surface, with the extent of electron transfer being lower for a fluorocarbon than a hydrocarbon one [17]. Thus more ions are believed to survive after impact with the FSAM surface. Another reason might be that the morphology on SAM surfaces may affect the sample distribution and crystallization on the surfaces.

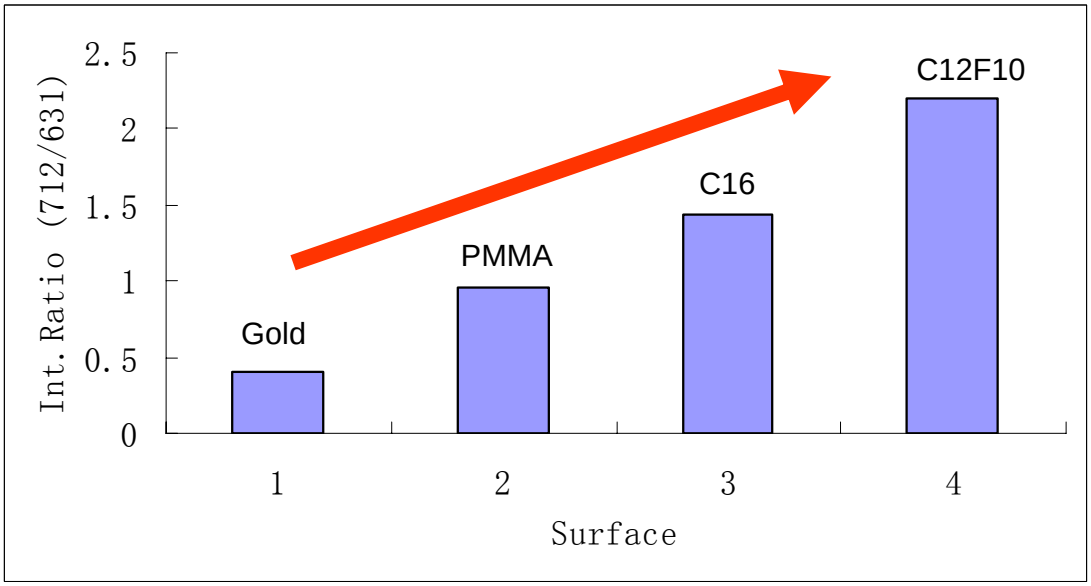

FIGURE 4.8. The peak intensity ratios between m/z = 712 (YGGFLR) and m/z = 631 for different surfaces used in DESI-MS.

4.4 Conclusions and Future Directions

We investigated the ionization capacity of our home-made DESI source for peptides and proteins. Peptides and small proteins (< 20 kDa) can be easily ionized and generate well-defined mass spectra. However, BSA (66.4 kDa) generates a poor defined mass spectrum, which indicates that there might be a molecular limitation for the current design of the DESI source. We discovered that the distance between the DESI sprayer and mass spectrometer inlet is critical, because the charge distribution, peak width and signal intensity can be significantly varied by changing the distance. In addition, the difference between the DESI-MS and ESI-MS spectra implies the differences in charge transfer and ion formation processes between those two ionization sources. Finally, we found that SAM surfaces may assist the ion formation in DESI, probably due to the decreased electron transfer on SAM surfaces.

In the future, we plan to couple the DESI source to a protein electroseparation technique based on silica colloid crystal developed by Dr. Wirth's group at the University of Arizona [18]. MALDI-MS has been employed to detect the separated proteins in the crystals, but DESI has the advantage of forming multiple charged ions and it does not suffer from matrix interference. Another direction of DESI would be molecular imaging. A DESI source with an automated surface stage capable of x, y translational motion has become a growing tool for 2D chemical imaging. There have been reports on forensic imaging [19] and tissue imaging [20], but it seems the sensitivity and resolution can be still improved.

REFERENCES

(1) Cody, R.B.; Laramee, J.A.; Durst, H.D. Versatile new ion source for the analysis of materials in open air under ambient conditions. *Anal. Chem.* **2005**, *77*, 2297-2302.

(2) McEwen, C.N.; Mckay, R.G.; Larsen, B.S. Analysis of Solids, Liquids, and Biological Tissues Using Solids Probe Introduction at Atmospheric Pressure on Commercial LC/MS Instruments. *Anal. Chem.* **2005**, *77*, 7826-7831.

(3) Takats, Z.; Wiseman, J.M.; Gologan, B.; Cooks, R.G. Mass Spectrometry Sampling under Ambient Conditions with Desorption Electrospray Ionization. *Science* **2004**, *306*, 471-473.

(4) Cooks, R.G.; Ouyang, Z.; Takats, Z.; Wiseman, J.M. Ambient Mass Spectrometry. *Science* **2006**, *311*, 1566-1570.

(5) Takats, Z.; Cotte-Rodriguez, I.; Talaty, N.; Chen, H.; Cooks, R.G. Direct, Trace Level Detection of Explosives on Ambient Surfaces by Desorption Electrospray Ionization Mass Spectrometry. *Chem. Commun.* **2005**, 1950-1952.

(6) Chen, H.; Talaty, N.; Takats, Z.; Cooks, R.G. Desorption Electrospray Ionization Mass Spectrometry for High-throughput Analysis of Pharmaceutical Samples in the Ambient Environment . *Anal. Chem.* **2005**, *77*, 6915-6927.

(7) Kauppila, T.J.; Wiseman, J.M.; Ketola, R.A.; Kotiaho, T.; Cooks, R.G.; Kostiainen, R. Desorption Electrospray Ionization Mass Spectrometry for the Analysis of Pharmaceuticals and Metabolites. *Rapid Commun. Mass Spectrom.* **2006**, *20*, 387-392.

(8) Van Berkel, G.J.; Ford, M.J.; Deibel, M.A. Thin-layer Chromatography and Mass Spectrometry Coupled Using Desorption Electrospray Ionization. *Anal.Chem.* **2005**, *77*, 1207-1215.

(9) Weston, D.J.; Bateman, R.; Wilson, I.D.; Wood, T.R.; Creaser, C.S. Direct Analysis of Pharmaceutical Drug Formulations Using Ion Mobility Spectrometry/Quadrupole-time-of-flight Mass Spectrometry Combined with Desorption Electrospray Ionization. *Anal. Chem.* **2005**, *77*, 7572-7580.

(10) Shin, Y.; Drolet, B.; Mayer, R.; Dolence, K.; Basile, F. Desorption Electrospray Ionization-Mass Spectrometry of Proteins. *Anal. Chem.* **2007**, *79*, 3514-3518.

(11) Bereman, M.S.; Nyadong, L.; Fernandez, F.M.; Muddiman, D.C.; Direct High-resolution Peptide and Protein Analysis by Desorption Electrospray Ionization Fourier Transform Ion Cyclotron Resonance Mass Spectrometry. *Rapid Commun. Mass Spectrom.* **2006**, *20*, 3409-3411.

(12) Wiseman, J.M.; Puolitaival, S.M.; Takats, Z.; Cooks, R.G.; Caprioli, R.M. Mass Spectrometric Profiling of Intact Biological Tissue by Using Desorption Electrospray Ionization. *Angew. Chem. Int. Ed.* **2005**, *44*, 7094-7097.

(13) Wiseman, J.M.; Takats, Z.; Gologan, B.; Davisson, V.J.; Cooks, R.G.; Direct Characterization of Enzyme-substrate Complexes by Using Electrosonic Spray Ionization Mass Spectrometry. *Angew. Chem. Int. Ed.* **2005**, *44*,913-916.

(14) Kasi, S.R.; Kang, H.; Sass, C.S.; Rabalais, J.W. Inelastic Processes in Low-energy Ion-Surface Collisions. *Surf. Sci. Rep.* **1989**, *10*, 1-104.

(15) Takats, Z; Wiseman, J.M.; Cooks, R.G. Ambient Mass Spectrometry Using Desorption Electrospray Ionization (DESI): Instrumentation, Mechanisms and Applications in Forensics, Chemistry, and Biology. *J. Mass Spectrom.* **2005**, *40*, 1261-1275.

(16) Venter, A.; Sojka, P.E.; Cooks, R.G.; Droplet Dynamics and Ionization Mechanisms in Desorption Electrospray Ionization Mass Spectrometry. *Anal. Chem.* **2006**, *78*, 8549-8555.

(17) Yang, X. Ph.D. Dissertation, University of Arizona, 2007.

(18) Zhang, S.P.; Ross, E.; Legg, M.A.; Wirth, M.J. High-speed electroseparations inside silica colloidal crystals. *J. Am. Chem. Soc.* **2006**, *128*, 9016-9017.

(19) Ifa, D.R.; Gumaelius, L.M.; Eberlin, L.S.; Manicke, N.E.; Cooks, R.G. Forensic analysis of inks by imaging desorption electrospray ionization (DESI) mass spectrometry. *Analyst* **2007**, *132*, 461-467.

(20) Wiseman, J.M.; Ifa, D.R.; Song, Q.; Cooks, R.G. Tissue imaging at atmospheric pressure using desorption electrospray ionization (DESI) mass spectrometry. *Angew. Chem. Int. Ed.* **2006**, *45*, 7188-7192.

(21) http://www.palaeos.com/Fungi/FPieces/CellWall.htmL. Accessed on Aug 18, 2008.

REFERENCES

References of Chapter 1

(1) Fenn, J.B.; Mann, M.; Meng, C.K.; Wong, S.F.; Whitehouse, C.M.; ESI for MS of Large Biomolecules. *Science* **1989**, *246*, 64-71.

(2) *Modern Mass Spectrometry;* Schalley, C.A., editor; Springer: New York 2003.

(3) *Mass Spectrometry in Drug Discovery;* Rossi, D.T.; Sinz, M.W., editors; Marcel Dekker; New York, 2002.

(4) Fenn, J.B.; Mann, M.; Meng, C.K.; Wong, S.F.; Electrospray Ionization – Principles and Practice. *Mass Spectrom. Rev.* **1990**, *9*, 37-70.

(5) *Electrospray Ionization Mass Spectrometry – Fundamentals, Instrumentation and Applications;* 1st ed.; Dole, R.B., editor; John Wiley & Sons: Chiechester 1997.

(6) www.bris.ac.uk/nerclsmsf/techniques/hplcms.htmL Accessed on December 1st, 2007.

(7) Winger, B.E.; Light-Wahl, K.J.; Ogorzalek Loo, R.R.; Udseth, H.R.; Smith, R.D.; Observation and Implications of High Mass-to-Charge Ratio Ions From ESI-MS. *J. Am. Soc. Mass Spectrom.* **1993**, *4*, 536-545.

(8) Mack, L.L.; Kralik P., Rheude, A.; Dole, M., Molecular Beams of Macroions. II. *J. Chem. Phys.* **1970**, *52*, 4977-4986.

(9) Filitsyn, N., Peschke, M., Kebarle, P., Origin and Number of Charges Observed on Multiply-protonated Native Proteins Produced by ESI. *Int. J. Mass Spectrom.* **2002**, *219*, 39-62.

(10) Iribarne, J.V.; Thomson, B.A. On the Evaporation of Small Ions from Charged Droplets. *J. Chem. Phys.* **1976**, *64*, 2287-2294.

(11) Thomson, B.A.; Iribarne J.V.; Field-induced Ion Evaporation from Liquid Surfaces at Atmospheric Pressure. *J. Chem. Phys.* **1979**, *71*, 4451-4463.

(12) Labowsky, M.; Fenn, J.B.; de la Mora, J.F. A Continuum Model for Ion Evaporation from a Drop: Effect of Curvature and Charge on Ion Solvation Energy. *Anal. Chim. Acta* **2000**, *406*, 105-118.

(13) *Mass Spectrometry of Proteins and Peptides;* Chapman, J.R., editor; Humana Press: Totowa, 2000.

(14) Phillips, J.J.; Yao, Z.P.; Zhang, W.; McLaughlin, S.; Laue, E.D.; Robinson, C.V.; Jackson, S.E. Conformational dynamics of the molecular chaperone Hsp90 in complexes with a co-chaperone and anticancer drugs. *J. Mol. Biol***. 2007,** *372* 1189-1203.

(15) Justin, L. P.; Benesch, B.T.; Ruotolo, D.A.; Simmons; Robinson, C.V. Protein Complexes in the Gas Phase: Technology for Structural Genomics and Proteomics *Chem. Rev.* **2007,** *10*, 3544 – 3567.

(16) Ardrey, R.E. *Liquid Chromatography – Mass Spectrometry – An Introduction;* John Wiley & Sons: Chichester, 2003

(17) Traeger, J.C.; ESI-MS of Organometallic Compounds. *Int. J. Mass Spectrom. Rev.* **1995**, *14*, 79-104

(18) Little, D.P.; Chorush, R.A.; Speir, J.P.; Senko, M.W.; Kelleher, N.L.; McLafferty, F.W. Rapid Sequencing of Oligonucleotides by High-Resolution-MS. *J. Am. Chem. Soc.* **1994**, 116,4893-4897.

(19) Karas, M.; Bahr, U.; Dulcks, T. Nano-ESI-MS: Addressing Analytical Problems Beyond Routine. *Fresenius J. Anal. Chem.* **2001**, 366, 669-676

(20) Smith, W.F.; Brooks, P. A critical evaluation of high performance liquid chromatography-electrospray ionization-mass spectrometry and capillary electrophoresis- electrospray-mass spectrometry for the detection and determination of small molecules of significance in clinical and forensic science. *Electrophoresis* **2004**, *25*, 1413-1446.

(21) http://www.chm.bris.ac.uk/ms/theory/maldi-ionisation.htmL Accessed on December 1st**,** 2007.

(22) *Mass Spectrometry;* Gross, J.H.; Springer: Berlin 2004

(23) Juhasz P.; Costello, C.E.; Biemann, K. MALDI-MS with 2-(4-Hydroxyphenylazo)benzoic Acid Matrix. *J. Am. Soc. Mass Spectrom.* **1993**, *4*, 399-409.

(24) Karas, M.; Gluckmann, M.; Schafer J. Ionization in MALDI: Singly Charged Molecular Ions Are the Lucky Survivors. *J. Mass Spectrom.* **2000**,

35, 1-12.

(25) *Mass Spectrometry of Polymers;* 1st ed.; Montaudo, G.; Lattimer, R.P., editor; CRC Press: Boca Raton, 2001

(26) Murgasova, R.; Hercules, D.M. Quantitative Characterization of a Polystyrene/Poly(α-methylstyrene) Blend by MALDI-MS and Size-exclusion chromatography. *Anal. Chem.* **2003**, *75*, 3744-3750.

(27) http://www.ivv.fraunhofer.de/ms/ms-analyzers.htmL Accessed on December 2nd, 2007.

(28) Dawson, P.H. Quadrupole Mass Analyzers: Performance, Design, and Some Recent Applications. *Mass Spectrom. Rev.* **1986**, *5*, 1-37.

(29) http://www.waters.com/WatersDivision/ContentD.asp?watersit=EGOO-66MNYR#quads Accessed on December 2nd, 2007.

(30) Garcia, B.A.; Shabanowitz, J.; Hunt, D.F. Characterization of histones and their post-translational modifications by mass spectrometry. *Curr. Opini. Chem. Biol.* **2007**, *11*, 66-73.

(31) *Quadrupole Storage Mass Spectrometry.* March, R.E.; Hughes, R.J. John Wiley & Sons: Chichester, 1989.

(32) Griffiths, I.W. Recent Advances in Ion-Trap Technology. *Rapid Commun. Mass Spectrom.* **1990**, 69-73

(33) http://www.ivv.fraunhofer.de/ms/ms-analyzers.htmL Accessed on December 2nd, 2007.

(34) Mao, D.; Douglas, D.J. H/D Exchange of Gas Phase Bradykinin Ions in a Linear Quadrupole Ion Trap. *J. Am. Soc. Mass Spectrom.* **2003**, *14*, 85-94.

(35) http://edoc.hu-berlin.de/dissertationen/xie-jing-2003-12-15/HTML/chapter2.htmL Accessed on December 7th, 2007.

(36) Loboda, A.V.; Ackloo, S.; Chernushevich, I.V. A high-performance matrix-assisted laser desorption/ionization orthogonal time-of-flight mass spectrometer with collisional cooling. *Rapid Commun. Mass Spectrom.* **2003**, *17*, 2508-2516.

(37) Whittal, R.M.; Li. L. High-Resolution MALDI in linear TOF-MS. *Anal. Chem.* **1995**, *67*, 1950-1954.

(38) Mamyrin, B.A. Laser Assisted Reflectron Time-of-Flight Mass Spectrometry. *Int. J. Mass Spectrom. Ion Proc.* **1994**, *131*, 1-19.

(39) http://edoc.hu-berlin.de/dissertationen/xie-jing-2003-12-15/HTML/chapter2.htmL Accessed on December 7th, 2007.

(40) Amster, I. J. Fourier Transform Mass Spectrometry. *J. Mass. Spectrom.* **1996**, *31*, 1325-1337.

(41) http://www.ivv.fraunhofer.de/ms/ms-analyzers.htmL Accessed on December 7th, 2007.

(42) Busch, K.L. The Electron Multiplier. *Spectroscopy* **2000**, *15*, 28-33.

(43) Laprade, B.N.; Labich, L.J.; Microchannel Plate-Based Detectors in Mass Spectrometry. *Spectroscopy* **1994**, *9*, 26-30.

(44) Futrell, J.H.; Development of Tandem MS. One Perspective. *Int. J. Mass Spectrom.* **2000**, *200*, 495-508.

(45) Glish, G.L.; Mcluckey, S.A.; Ridley, T.Y.; Cooks, R.G. A New "hybrid" Sector/Quadrupole Mass Spectrometer for MS/MS. *Int. J. Mass Spectrom. Ion Phys.* **1982**, *41*, 157-177.

(46) Bradley, C.D.; Curtis, J.M.; Derrick, P.J.; Wright, B. Tandem Mass Spectrometry of Peptides Using a Magnetic Sector/Quadrupole Hybrid-the Case for Higher Collision Energy and Higher Radio-Frequency Power. *Anal. Chem.* **1992**, *64*, 2628-2635.

(47) Schoen, A.E.; Amy, J.W.; Ciupek, J.D.; Cooks, R.G.; Dobberstein, P; Jung, G.A. Hybrid BEQQ Mass Spectrometer. *Int. J. Mass Spectrom. Ion Proc.* **1985**, *65*, 125-140.

(48) Yost, R.A.; Enke, C.G. Triple Quadrupole Mass Spectrometry for Direct Mixture Analysis and Structure Elucidation. *Anal. Chem.* **1979**, *51*, 1251-1261.

(49) Ehlers, M.; Schmidt, S.; Lee, B.J.; Grotemeyer, J. Design and Set-Up of an External Ion Source Coupled to a Quadrupol-Ion-Trap Reflectron-Time-of-Flight Hybrid Instrument. *Eur. J. Mass Spectrom.* **2000**, *6*, 377-385.

(50) Hager, J.W. A New Linear Ion Trap Mass Spectrometer. *Rapid Commun.*

Mass Spectrom. **2002**, *16*, 512-526.

(51) Guilhaus, M.; Selby, D.; Miynski, V. Orthogonal Acceleration TOF-MS. *Mass Spectrom. Rev.* **2000**, *19*, 65-107.

(52) McLuckey, S.A. Principles of Collisonal Activation in Analytical MS. *J. Am. Soc. Mass Spectrom.* **1992**, *3*, 599-614.

(53) Keseler, I.M.; Collado-Vides, J.; Gama-Castro, S.; Ingraham, J.; Paley, S.; Paulsen, I.T.; Peralta-Gill, M.; Karp, P.D. Ecocyc: a Comprehensive Database Resource for *Escherichia coli*. *Nucleic Acids Res.* **2005**, *33*, D334-D337.

(54) Mungur, R.; Glass, A.D.M.; Goodenow, D.B.; Lightfoot, D.A. Metabolite fingerprinting in transgenic Nicotina tabacum altered by the *Escherichia coli* glutamate dehydrogenase gene. *J. Biomed. Biotechnol.* **2005**, *2*, 198-214.

(55) Oldiges, M.; Lutz, S.; Pflug, S.; Schroer, K.; Stein, N.; Wiendahl, C. Metabolomics: Current State and Evolving Methodologies and Tools. *Appl. Microbiol. Biotechnol.* **2007**, *76*, 495-511.

(56) Fiehn, O. Metabolomics-the Link between Genotypes and Phenotypes. *Plant Mol. Biol.* **2002**, *48*, 155-171.

(57) De Graaf, A.A.; Striegel, K.; Wittig, R.M.; Laufer, B.; Schmits, G.; Wiechert, W.; Sprenger, G.A.; Sahm, H. Metabolic State of Zymononas Mobilis in Glucose-, Fructose, and Xylose-fed Continuous Cultures as Analyzed by C-13- and P-31-NMR Spectroscopy. *Arch. Microbiol.* **1999**, *171*, 371-385.

(58) Womersley, C. A Micromethod for the Extraction and Quantitative Analysis of Free Carbohydrates in Nematode Tissue. *Anal. Biochem.* **1981**, *112*, 182-189.

(59) Meyer, S.; Noiseommit-Rizzi, N.; Reuss, M.; Neubauer, P. Optimized Analysis of Intracellular Adenosine and Guanosine Phosphates in *Escherichia coli*. *Anal. Biochem.* **1999**, *271*, 43-52.

(60) Castrillo, J.I.; Hayes, A.; Mohammed, S.; Gaskell, S.J.; Oliver, S.G. An Optimized Protocol for Metabolome Analysis in Yeast Using Direct

Infusion Mass Spectrometry. *Phytochemistry* **2003**, *62*, 929-937.

(61) Dune, W.B.; Bailey, N.J.C.; Johnson, H.E. Measuring the Metabolome: Current Analytical Technologies. *Analyst* **2005**, *130*, 606-625.

(62) Annesley, T.M. Ion Suppression in Mass Spectrometry. *Clin. Chem.* **2003**, *49*, 1041-1044.

(63) Coulier, L.; Bas, R.; Jesperson, S.; Verheijm E.; van der Werf, M.J.; Hankemeier, T. Simultaneous Quantitative Analysis of Metabolites using Ion-pair Liquid Chromatography-Electrospray Ionization Mass Spectrometry. *Anal. Chem.* **2006**, *78*, 6573-6582.

(64) Luo, B.; Groenke, K.; Takors, R.; Wandrey, C.; Oldiges, M. Simultaneous Determination of Multiple Intracellular Metabolites in Glycolysis, Pentose Phosphate Pathway and Tricarboxylic Acid cycle by Liquid Chromatography-Mass Spectrometry. *J. Chromatogr. A* **2007**, *1147*, 153-264.

(65) Shellie, R.A.; Welthagen, W.; Zrostlikova, J.; Spranger, J.; Ristow, M.; Fiehn, O.; Zimmermann, R. Statistical Methods for Comparing Comprehensive Two-dimensional Gas Chromatography-Time-of-Flight Mass Spectrometry Results: Metabolomic Analysis of Mouse Tissue Extracts. *J. Chromatogr. A* **2005**, *1086*, 83-90.

(66) Noh, K.; Gronk, K.; Luo, B.; Takors, R.; Oldiges, M.; Wiechert, W. Metabolic Flux Analysis at Ultra Short Time Scale: Isotopically Non-stationary ^{13}C Labeling Experiments. *J. Biotechnol.* **2007**, *129*, 249-267.

(67) Van den Berg, R.A.; Hoefsloot, H.C.J.; Westerhuis, J.A.; Smilde, A.K.; van der Werf, M.J. Centering, Scaling, and Transformations: Improving the Biological Information Content of Metabolomics Data. *Bmc. Genomics* **2006**, *7*, 142.

(68) Katajamaa, M.; Miettinen, J.; Oresic, M. MZmine: Toolbox for Processing and Visualization of Mass Spectrometry Based Molecular Profile Data. *Bioinformatics* **2006**, *22*, 634-636.

References of Chapter 2

(1) http://www.mosquito.org Accessed on December 10, 2007.

(2) Price, N.P. Acylic sugar derivatives for GC/MS analysis of ^{13}C-enrichment during carbohydrate metabolism. *Anal Chem*. **2004**, *76*, 6566-6574.

(3) Ross, B.; Lin, A.; Harris, K.; Bhattacharya, P.; Schweinsburg, B. Clinical experience with ^{13}C MRS in vivo. *NMR Biomed.* **2003,** *16*, 358-369.

(4) Chace, D. H.; Millington, D. S.; Terada, N.; Kahler, S. G.; Roe, C. R.; Hofman, L. F. Rapid Diagnosis of Phenylketonuria by Quantitative Analysis for Phenylalanine and Tyrosine in Neonatal Blood Spots by Tandem Mass Spectrometry. *Clin. Chem.* **1993**, *39*, 66–71.

(5) Chace, D. H.; Hillman, S. L.; Millington, D. S.; Kahler, S. G.; Roe, C. R.; Naylor, E. W. Rapid Diagnosis of Maple Syrup Urine Disease in Blood Spots from Newborns by Tandem Mass Spectrometry. *Clin. Chem.* **1995**, *41*, 62–68.

(6) Chace, D. H.; Hillman, S. L.; Millington, D. S.; Kahler, S. G.; Adam, B. W.; Levy, H. L. Rapid Diagnosis of Homocystinuria and Other Hypermethioninemias from Newborns' Blood Spots by Tandem Mass Spectrometry. *Clin. Chem.* **1996**, *42*, 349–355.

(7) Chace, D. H.; Sherwin, J. E.; Hillman, S. L.; Lorey, F.; Cunningham, G. C. Use of Phenylalanine-to-tyrosine Ratio Determined by Tandem Mass Spectrometry to Improve Newborn Screening for Phenylketonuria of Early Discharge Sspecimens Collected in the First 24 Hours. *Clin. Chem.* **1998**, *44*, 2405–2409.

(8) Chace, D. H.; Kalas, T. A.; Naylor, W. The Application of Tandem Mass Spectrometry to Neonatal Screening for Inherited Disorders of Intermediary Metabolism. *Annu. Rev. GenomicsHum. Genet.* **2002,** *3,* 17–45.

(9) Chace, D. H.; Kalas, T. A.; Naylor, E. W. Use of Tandem Mass Spectrometry for Multianalyte Screening of Dried Blood Specimens from Newborns. *Clin. Chem.* **2003**, *49*, 1797–1817.

(10) Nagy, K.; Takats, Z.; Pollreisz, F.; Szabo, T.; Vekey, K. Direct tandem mass spectrometric analysis of amino acids in dried blood spots without

chemical derivatization for neonatal screening. *Rapid Commun. Mass Spectrom*. **2003**, *17*, 983–990.

(11) Scaraffia, P.Y.; Zhang, Q.; Wysocki, V.H.; Isoe, J.; Wells, M.A. Analysis of whole body ammonia metabolism in Aedes aegypti using [15N]-labeled compounds and mass spectrometry. *Insect Biochem Mol Biol*. **2006,** *36*, 614-22

(12) Luo, W.Y.; Kwon, Y.K.; Rabinowitz, J.D. Isotope Ratio-Based Profiling of Microbial Folates. *J. Am. Soc. Mass Spectrom*. **2007**, *18*, 898-909

(13) Honda, S.; Oked, J.; Iwanaga, H.; Kawakami, S.; Taga, A.; Suzuki, S.; Imai, K. Ultramicroanalysis of reducing carbohydrates by capillary electrophoresis with laser-induced fluorescence detection as 7-nitro-2,1,3-benzoxadiazole-tagged N-methylglycamine derivatives. *Anal Biochem.* **2000**, *286*, 99-111.

(14) Zhou, Z.R.; Ogden, S.; Leary, J.A. Linkage position determination in oligosaccharides - MS/MS study of lithium-cationized carbohydrates *J. Org. Chem.* **1990**, *55*, 5444-5446

(15) Staempfli, A.; Zhou, Z.R.; Leary, J.A. Gas-Phase dissociation mechanisms of dilithiated disaccharides- Tandem mass-spectrometry and semiempirical calculations. *J. Org. Chem.* **1992,** *57*, 3590-3594

(16) Hofmeister, G.E.; Zhou, Z.; Leary, J.A. Linkage position determination in lithium –cationized disaccharides- tandem mass-spectrometry and semiempirical calculations *J. Am. Chem. Soc.* **1991,** *113*, 5964-5970

(17) Harvey, D.J. Collision-induced fragmentation of underivatized N-linked carbohydrates ionized by electrospray *J. Mass Spectrom.* **2000**, *35*, 1178-1190

(18) Anbalagan, V.; Patel, J.N.; Niyakorn, G.; Stipdonk, M.J.V. Mclafferty-type Rearrangement on the collision-induced Dissociate of Li^+, Na^+ and Ag^+ Cationed Ester of N-Actetylated Peptides. *Rapid Commun. Mass Spectrom.* **2003**, *17*, 291-330

(19) Trinh, M.B.J.; Harrison, RJ.; Gerace, R.; Ranieri, E.; Fletcher, J.; Johnson, D.W. Quantification of Glutamine in Dried Blood Spots and Plasma by

Tandem Mass Spectrometry for the Biochemical Diagnosis and Monitoring of Ornithine Transcabamylase Deficiency. *Clin. Chem.* **2003**, 481-683.

(20) Zhang, Q.; Wysocki, V.H.; Scaraffia, P.Y.; Wells, M.A. Fragmentation pathway for glutamine identification: loss of 73 Da from dimethylformamidine isobutyl glutamine. *J. Am. Soc. Mass Spectrom*. **2005**, *16*, 1192–1203.

References of Chapter 3

(1) Boot-Handford, R.P.; Tuckwell, D.S. Fibrillar collagen: the key to vertebrate evolution? A tale of molecular incest. *Bioessays* **2003**, *25*, 142-151.

(2) Dreisewerd, K.; Rohlfing, A.; Spottke, B.; Urkanke, C.; Henkel, W. Characterization of Whole Fibril-Forming Collagen Proteins of Type I, III and V from Fetal Calf Skin by Infrared Matrix-Assisted Laser Desorption Ionization Mass Spectrometry. *Anal. Chem.* **2004**, *76*, 3482-3491.

(3) Bornstein, P. Covalent Cross-links in Collagen: a Personal Account of Their Discovery. *Matrix Biol.* **2003**, *22*, 385-391.

(4) Veis, A. Characterization of Soluble Collagens by Physical Techniques. In: Cunningham, L.W.; Frederiken, D.F. editors. *Methods in Enzymology.* Academic Press, New York, 1982.

(5) Miller, E.J.; Matukas, V.J. Chick Cartilage Collagen: A New Type of 1 Chain Not Present in Bone or Skin of the Species. *Proc. Natl. Acad. Sci. USA.* **1969**, *64*, 1264-1268.

(6) Cheung, E.; Miller, E.J. Collagen Polymorphism, Characterization of Molecules with the Chain Composition [alpha-1(III)]$_3$ in Human Tissues. *Science* **1974**, *183*, 1200-1201.

(7) Epstein, E.H. Jr. [α-1(III)]$_3$ Human Skin Collagen. *J. Biol. Chem.* **1974**, *249*, 3225-3231.

(8) Miller, E.J. Collagen. In: Cunningham, L.W.; Frederiksen, D.F. editors. An Overview Method of Enzymology. Academic Press, New York, 1982.

(9) Benya, P.D. Two-dimensional CNBr Peptide Patterns of a Collagen Type I, II and III. *Coll. Res.* **1981**, *1*, 17-26.

(10) Bailey, A.J.; Paul, R.G.; Knott, L. Mechanisms of maturation and ageing of collagen. *Mech. Ageing Dev.* **1998**, *106*, 1-56.

(11) Eyre, D.R.; Paz, M.A.; Gallop, P.M. Cross-linking in Collagen and Elastin. *Annu. Rev. Biochem.* **1984**, *53*, 717-748.

(12) Robins, S.P. Fibrillogenesis and Maturation of Collagen. In: Seibel, M.J.; Robins, S.P.; Bilezikian, J.P. editors. *Dynamics of Bone and Cartilage Metabolism.* Academic Press, London, 1999.

(13) Deshmukh, A.; Deshmukh, K.; Nimni, M.E.; Synthesis of Aldehydes and Their Interactions during the in vitro Aging of Collagen. *Biochemistry*, **1971**, *10*, 2337.

(14) Eyre, D.R.; Wu, J.J. Collagen Cross-links. *Top Curr. Chem.* **2005**, *247*, 207-229.

(15) Watts, N.B. Clinical utility of biochemical markers of bone remodeling. *Clin. Chem.* **1999**, *45*, 1359-1368.

(16) Christenson, R.H. Biochemical markers of bone metabolism: An overview. *Clin. Biochem.* **1997**, *30*, 573-593.

(17) Delmas, P.D. Biochemical Markers of Bone Turnover. *J. Bone Miner. Res.* **1993**, *8*, S549-S555.

(18) Bank, R.A.; teKoppele, J.M.; Janus, G.J.; Wassen, M.H.; Pruijs, H.E.; Van der Sluijs, H.A.; Sakkers, R.J. Pyridinium cross-links in bone of patients with osteogenesis imperfecta: Evidence of a normal intrafibrillar collagen packing. *J. Bone. Miner. Res.* **2000**, *15*, 1330-1336.

(19) Lohmander, L.S.; Atley, L.M.; Pietka, T.A.; Eyre, D.R. The release of crosslinked peptides from type II collagen into human synovial fluid is increased soon after joint injury and in osteoarthritis. *Arthritiss Rheum* **2003**, *48*, 3130-3139.

(20) Weber, K.T. Cardiac Interstitium in Health and Disease: the Fibrillar Collagen Network. *J. Am. Coll. Cardiol.* **1989**, *13*, 1637-1652.

(21) Yu, Q.; Waston, R.R.; Marchalonis, J.J.; Larson, D.F. A Role for T Lymphocytes in Mediating Cardiac Diastolic Function. *Am. J. Physiol. Heart Circ. Physiol.* **2005**, *289*, H643-H651.

(22) Yu, Q; Horak, K.; Larson, D.F, Role of T Lymphocytes in Hypertension-induced Cardiac Extracellular Matrix Remodeling. *Hypertension* **2006**, *48*, 98-104.

(23) http://www.wrongdiagnosis.com/h/hypertension/stats.htm#death_and_mortality_stats Accessed on Jan 10th, 2008.

(24) Robins, S.P. Functional-properties of Collagen and Elastin. *Bailliere's Clin. Rheumatol.* **1988**, *2*, 1-36

(25) Black, D.; Duncan, A.; Robins, S.P. Quantitative-analysis of the Pyridinium Crosslinks of Collagen in Urine Using Iin-paired Reversed-Phase High Performance Liquid-Chromatography. *Anal. Biochem.* **1988**, *169*, 197-203.

(26) Rafferty, T.L.; Gallagher, R.T.; Derrick, P.J.; Heck, A.J.R.; Duncan, A.; Robins, S.P. Low- and High-energy Collision-induced Dissociation of Pyridinoline and Deoxypyridinoline Ions Using Fourier Transform Ion Cyclotron Resonance Electrospray and Liquid Secondary-ion Magnetic Sector Mass Spectrometry. *Int. J. Mass Spec. and Ion Proc.* **1997**, *160*, 377-386.

(27) Bateman, J.F.; Mascara, T.; Chan, D.; Cole, W.G. Rapid Fractionation of Collagen Chains and Peptides by High-performance Liquid-Chromatogrphy. *Anal. Biochem.* **1986**,*154*, 338-344.

(28) Kim, S.H.; Lee, J.H.; Yun, S.Y.; Yoo, J.S.; Jun, C.H.; Chung, K.Y.; Suh, H. Reaction monitoring of succinylation of collagen with matrix-assisted laser desorption/ionization mass spectrometry. *Rapid Commun. Mass Spectrom*. **2000**, *14*, 2125-2130.

(29) Shek, P.Y. I.; Zhao, J.; Ke, Y.; Siu, K.W.M.; Hopkinson, A.C. Fragmentations of Protonated Arginine, Lysine and Their Methylated Derivatives: Concomitant Losses of Carbon Monoxide or Carbon Dioxide and An Amine. *J. Phys. Chem. A* **2006**, *110*, 8282-8296.

References of Chapter 4

(1) Cody, R.B.; Laramee, J.A.; Durst, H.D. Versatile new ion source for the analysis of materials in open air under ambient conditions. *Anal. Chem.* **2005**, *77*, 2297-2302.

(2) McEwen, C.N.; Mckay, R.G.; Larsen, B.S. Analysis of Solids, Liquids, and Biological Tissues Using Solids Probe Introduction at Atmospheric Pressure on Commercial LC/MS Instruments. *Anal. Chem.* **2005**, *77*, 7826-7831.

(3) Takats, Z.; Wiseman, J.M.; Gologan, B.; Cooks, R.G. Mass Spectrometry Sampling under Ambient Conditions with Desorption Electrospray Ionization. *Science* **2004**, *306*, 471-473.

(4) Cooks, R.G.; Ouyang, Z.; Takats, Z.; Wiseman, J.M. Ambient Mass Spectrometry. *Science* **2006**, *311*, 1566-1570.

(5) Takats, Z.; Cotte-Rodriguez, I.; Talaty, N.; Chen, H.; Cooks, R.G. Direct, Trace Level Detection of Explosives on Ambient Surfaces by Desorption Electrospray Ionization Mass Spectrometry. *Chem. Commun.* **2005**, 1950-1952.

(6) Chen, H.; Talaty, N.; Takats, Z.; Cooks, R.G. Desorption Electrospray Ionization Mass Spectrometry for High-throughput Analysis of Pharmaceutical Samples in the Ambient Environment . *Anal. Chem.* **2005**, *77*, 6915-6927.

(7) Kauppila, T.J.; Wiseman, J.M.; Ketola, R.A.; Kotiaho, T.; Cooks, R.G.; Kostiainen, R. Desorption Electrospray Ionization Mass Spectrometry for the Analysis of Pharmaceuticals and Metabolites. *Rapid Commun. Mass Spectrom.* **2006**, *20*, 387-392.

(8) Van Berkel, G.J.; Ford, M.J.; Deibel, M.A. Thin-layer Chromatography and Mass Spectrometry Coupled Using Desorption Electrospray Ionization. *Anal.Chem.* **2005**, *77*, 1207-1215.

(9) Weston, D.J.; Bateman, R.; Wilson, I.D.; Wood, T.R.; Creaser, C.S. Direct Analysis of Pharmaceutical Drug Formulations Using Ion Mobility Spectrometry/Quadrupole-time-of-flight Mass Spectrometry Combined with Desorption Electrospray Ionization. *Anal. Chem.* **2005**, *77*, 7572-7580.

(10) Shin, Y.; Drolet, B.; Mayer, R.; Dolence, K.; Basile, F. Desorption Electrospray Ionization-Mass Spectrometry of Proteins. *Anal. Chem.* **2007**, *79*, 3514-3518.

(11) Bereman, M.S.; Nyadong, L.; Fernandez, F.M.; Muddiman, D.C.; Direct High-resolution Peptide and Protein Analysis by Desorption Electrospray Ionization Fourier Transform Ion Cyclotron Resonance Mass Spectrometry. *Rapid Commun. Mass Spectrom.* **2006**, *20*, 3409-3411.

(12) Wiseman, J.M.; Puolitaival, S.M.; Takats, Z.; Cooks, R.G.; Caprioli, R.M. Mass Spectrometric Profiling of Intact Biological Tissue by Using Desorption Electrospray Ionization. *Angew. Chem. Int. Ed.* **2005**, *44*, 7094-7097.

(13) Wiseman, J.M.; Takats, Z.; Gologan, B.; Davisson, V.J.; Cooks, R.G.; Direct Characterization of Enzyme-substrate Complexes by Using Electrosonic Spray Ionization Mass Spectrometry. *Angew. Chem. Int. Ed.* **2005**, *44*,913-916.

(14) Kasi, S.R.; Kang, H.; Sass, C.S.; Rabalais, J.W. Inelastic Processes in Low-energy Ion-Surface Collisions. *Surf. Sci. Rep.* **1989**, *10*, 1-104.

(15) Takats, Z; Wiseman, J.M.; Cooks, R.G. Ambient Mass Spectrometry Using Desorption Electrospray Ionization (DESI): Instrumentation, Mechanisms and Applications in Forensics, Chemistry, and Biology. *J. Mass Spectrom.* **2005**, *40*, 1261-1275.

(16) Venter, A.; Sojka, P.E.; Cooks, R.G.; Droplet Dynamics and Ionization Mechanisms in Desorption Electrospray Ionization Mass Spectrometry. *Anal. Chem.* **2006**, *78*, 8549-8555.

(17) Yang, X. Ph.D. Dissertation, University of Arizona, 2007.

(18) Zhang, S.P.; Ross, E.; Legg, M.A.; Wirth, M.J. High-speed electroseparations inside silica colloidal crystals. *J. Am. Chem. Soc.* **2006**, *128*, 9016-9017.

(19) Ifa, D.R.; Gumaelius, L.M.; Eberlin, L.S.; Manicke, N.E.; Cooks, R.G. Forensic analysis of inks by imaging desorption electrospray ionization (DESI) mass spectrometry. *Analyst* **2007**, *132*, 461-467.

(20) Wiseman, J.M.; Ifa, D.R.; Song, Q.; Cooks, R.G. Tissue imaging at atmospheric pressure using desorption electrospray ionization (DESI) mass spectrometry. *Angew. Chem. Int. Ed.* **2006**, *45*, 7188-7192.

(21) http://www.palaeos.com/Fungi/FPieces/CellWall.htmL. Accessed on Aug 18, 2008.